Role of CD31 Binding Partners in Viable Leukocyte Detachment from Macrophages

Kim Wilkinson

A Thesis submitted for the degree Doctor of Philosophy

University of Edinburgh

2006

Table of Contents

Table of Figures

Table of Tables

List of Abbreviations

ABCA-1 (ATP binding cassette-1)

Akt (protein kinase B)

ANOVA (analysis of variance)

ATP (adenosine triphosphate)

BAEC (bovine aortic endothelial cells)

Bcl-2 (B cell lymphoma-2)

BCR (B cell receptor)

bEND (brain endothelial cells)

BMDM (bone marrow derived macrophages)

BTAM (biphosphotyrosyl activation motif)

C1q (complement 1 subcomponent q)

CD31KO (CD31 knockout)

CEACAM (carcinoembryonic antigen cell adhesion molecule)

CHO (Chinese hamster ovary)

CII (type II collagen)

CMV (cytomegalovirus)

Crk1 (cyclin-dependent kinase activating kinase)

CSK (C-terminal Src-kinase)

DC (dendritic cells)

DMEM (Dulbecco's Modified Eagle Medium)

Dok (downstream of tyrosine kinases)

dsDNA (double stranded DNA)

EAE (experimental autoimmune encephalitis)

ECL (enhanced chemiluminescence)

EDTA (ethylenediaminetetraacetic acid)

EIAV (equine infectious anaemia virus)

eIF3 (elongation initiation factor 3)

EOMA (endothelioma)

ERK (extracellular related kinase)

ES (embryonic stem cells)

F'ab (fragment antigen binding)

FACS (flow analysis cell sorter)

FAK (focal adhesion kinase)

FERM (4.1 ezrin radexin moesin)

FITC (Fluorescein isothiocyanate)

Gab1 (grb associated binder-1)

GFP (green fluorescent protein)

GOLO (greater lymphoid organ)

Grb2 (growth factor receptor binding protein 2)

GST (glutathione-S-transferase)

HEK (human embryonic kidney)

HEL (hen egg lysozyme)

HEPES (4-(2-hydroxyethyl)-1-piperazineethanesulfonic acid)

HERG (human ether related a go-go)

HIV-1 (Human immunodeficiency virus-1)

HMDM (human monocyte derived macrophages)

Hop (Hsp90 organising protein)

HRP (horseradish peroxidase)

Hsp90 (heat shock protein 90)

HUVEC (human umbilical cord venule endothelial cells)

IgSF (immunoglobulin superfamily)

IL-1β (interleukin-1β)

IMM (immunophilins)

IPA (isopropanol)

IPTG (isopropyl-beta-D-thiogalactopyranoside)

ITAM (immunoreceptor tyrosine based activation motif)

ITIM (immunoreceptor tyrosine based inhibitory motif)

JAK (janus kinase)

KIR (killer immunoglobulin like receptor)

Lac-Z (β glacatosidase)

LB (Luria Bertani)

LPS (lipopolysaccharide)

MALDI-TOF (matrix assisted laser desorption time of flight spectroscopy)

MAPK (mitogen activated protein kinase)

MBL (mannose binding lectin)

MDCK (m derby canine kidney cells)**

me/me (moth-eaten)

me^{v}/me^{v} (moth-eaten viable)

MHC-1 (major histocompatibility complex-1)

MM6 (monomac 6)

mRNA (messenger RNA)

NIH3T3 (mouse fibroblast cell line)

NK (natural killer)

PBS (phosphate buffered saline)

PC (phosphatidylcholine)

PCR (polymerase chain reaction)

PE (phosphatidylethanolamine)

PECAM-1 (platelet/endothelial cell adhesion molecule-1)

PH (pleckstrin homology)

PI3K (phosphatydl inositol 3 kinase)

PIKE (phosphatidylinositol-3' kinase enhancer)

PKC (protein kinase C)

PLC-γ1 (phospholipase-C)

PMA (phorbol -12 myristate 13-acetate)

PMN (polymorphonuclear cell)

PPP (platelet poor plasma)

PRP (platelet rich plasma)

PS (phosphotidylserine)

PSR (phosphatidlyserine receptor)

PTP1B (protein tyrosine phosphatase 1B)

PVA (polyvinyl acetate)

Rag (recombination activating gene)

RBL-2H3 (rat basophilic leukemia)

REN (endothelial cell line)

RISC (RNA-induced signalling complex)

RNAi (RNA interference)

RT-PCR (reverse transcriptase polymerase chain reaction)

SDF-1 (stromal derived factor-1)

SDS-PAGE (sodium dodecyl sulphate polyacrylamide gel electrophoresis)

SHIP (SH2 containing inositol 5-phosphatase)

SHP-1 (src homology containing phosphatase-1)

SHP-2 (src homology containing phosphatase-2)

shRNA (short-hairpin RNA)

SIC (spreading initiation centre)

siRNA (small interfering RNA)

SIRPα (signal regulatory protein α)

SK (sphingosine kinase)

SLE (systemic lupus erythromatosus)

SOCS (suppressors of cytokine signalling)

SOS (son of sevenless)

SR-B1 (scavenger receptor B-1)

STAT3 (signal transducers and activators of transcription)

TCR (T cell receptor)

TEMED (N,N,N',N'-Tetramethylethylenediamine)

THP-1 (acute monocytic leukemia)

TNC (thymic nursing cells)

TNFα (tumour necrosis factor α)

TPR (tetratricopeptide repeat)

TSP (thrombospondin)

U937 (chronic myeloid leukemic cell line)

VE (vascular endothelium)

VSV (vesicular stomatitis virus)

X-gal (5-bromo-4-chloro-3-indolyl-beta-D-galactopyranoside)

Declaration

I hereby declare that this thesis has been composed solely by myself and has not been accepted in any previous candidature for a higher degree. All work presented in this thesis was, unless acknowledged, initiated and executed by myself. All sources of information in the text have been acknowledged by reference.

Kim Wilkinson

Dedication

This work is dedicated to my parents, Bill and Jen Wilkinson, without their support I would never have made it this far.

Acknowledgements

I would like to thank the following people who have helped me during my PhD studies:

Dr Simon Brown my supervisor, for endless support, encouragement and positivity especially through the dark times.

Professor John Savill, for giving a Geordie girl a chance to prove herself.

Dr Elisabeth Vernon-Wilson for teaching me the mysteries of molecular biology, and for generating site-directed mutagenesis vectors.

Dr Jason King for assistance with siRNA constructs.

Dr Cheryl Hunter for help with the lentivirus system.

Dr Michael Douglas and Dr Ewan Ross (University of Birmingham) for generating stable Jurkat cell lines and plasmid vectors of CD31.

Dr David Critchley (Leicester University) for the talin construct.

Douglas Lamont (University of Dundee) for MALDI-TOF.

To all of the PIG Lab members past and present, I have learned so much from all of you, and have enjoyed your friendship.

Special thanks to Dr Ian Dransfield for proof-reading my thesis, beer, chocolate Amsterdam and horror movies.

To the MRC for funding my studentship.

And finally to my family who have stood by me through it all, and have always been on hand for a beer, a moan and moving furniture.

Abstract

CD31 mediates homophilic interactions between leukocytes and macrophages during inflammation, apoptotic cells remain attached and are engulfed whereas viable cells actively detach. We hypothesised that differential recruitment of signalling and adapter molecules to the cytoplasmic domain were responsible for the disengagement of the viable leukocyte from macrophages. Investigation with a static attachment assay using THP-1 as a macrophage model showed the ITIM of CD31 on the leukocyte was important for viable cell detachment. Our data also implicated a role for the recruitment of SHP-2 which we attempted to knock-down by siRNA delivered by lentivirus.

SHP-2, in addition to its phosphatase activity, also acts as a docking protein. To examine for potential interacting partners we fused the cytoplasmic domain of CD31 to GST which we used in pulldown assays from lysates of viable and apoptotic leukocytes. We demonstrated that the recruitment of SHP-1 and SHP-2 were dependent on an intact ITIM (immunoreceptor tyrosine-based inhibitory motif). Interestingly, apoptotic cell lysates promoted dephosphorylation of the *in vitro* phosphorylated GST-CD31, suggesting an increase in phosphatase activity in aged neutrophils. We were unable to demonstrate an interaction between the cytoplasmic domain of CD31 with putative binding partners β-catenin, src, RasGAPp120, RhoGAPp190, talin or calmodulin.

A proteomic approach by MALDI-TOF and MS/MS identified Hsp90 as a novel binding partner of CD31 irrespective of the phosphorylation state. In contrast, 14-3-

3ε bound to phosphorylated CD31, whereas eIF3 specifically bound to an ITIM double tyrosine mutant. The binding of Hsp90 to CD31 was proposed to occur via a TPR motif within the cytoplasmic domain of CD31 which comprises a surface fold of basic amino acids complexing a highly acidic carboxy tail of Hsp90. Truncation and site directed mutagenesis of the cytoplasmic domain revealed multiple binding sites for Hsp90; specifically two regions containing the sequences (KAFYLRKAKAK), previously shown to be the calmodulin binding region, and a novel area (SNNEKMSDMEANSHY) which has significant homology with other TPR-containing proteins. Systematic mutagenesis of the putative basic charged amino acids within the cytoplasmic domain of CD31 which may mediate the interaction with Hsp90 also supports the presence of a TPR motif.

The importance of Hsp90, 14-3-3ε and eIF3 is currently unknown, although it is interesting to note that CD31 was recently found within this laboratory to associate with the voltage-gated potassium channel HERG which also binds 14-3-3ε and Hsp90. eIF3 is an RNA helicase that may link CD31 and leukocyte motility to spreading initiation centres where motility can be viewed as a rapid turnover of focal adhesion complexes. Together, these studies have identified novel binding partners of CD31 may form a macromolecular complex to promote CD31-dependent leukocyte motility and detachment from macrophages.

1 Introduction

1.1 Leukocyte Migration

Leukocyte migration through the endothelium is an essential process allowing an efficient immune response to invasion by micro-organisms. The route by which leukocytes are able to reach the site of infection is controlled by various forms of adhesion and chemoattractants. The leukocyte initially mediates rolling adhesion along the endothelium via L-selectin on the leukocyte and E-selectin and P-selectin on the endothelial cell. This initial tethering gives way to firmer integrin-mediated adhesion and arrest of the leukocyte which is shear resistant. Integrins cycle between affinity states, leading to the activation of the immunoglobulin superfamily members. The leukocyte is then capable of diapedesis through the endothelium to the site of chemoattractant [1].

CD31 is intimately involved in the migration of leukocytes through vascular endothelium. CD31 has previously been shown to regulate β_1 and β_2 integrins during leukocyte adhesion to the endothelium, where an intact cytoplasmic domain was required, and the small GTPase Rap1 became activated [2]. Stromal derived factor-1 (SDF-1) induced transmigration of $CD34^+$ myeloid progenitor cells through IL-1β stimulated bone marrow endothelium was shown to require CD31 and β_1 and β_2 integrins, where CD31 may be transmitting signals leading to integrin activation and increased adhesion [3].

In T cells, CD31 was found to enhance β_1 and β_2 integrin-mediated adhesion, amplifying the adhesion of the T cell to the endothelium [4]. CD31 concentrated at the junctions of endothelial cells mediates adhesive interactions that activate β_2 integrins in an adhesion cascade [5]. CD31 regulates migration of T cells acting as an adhesion amplifier, upregulating β1 integrin adhesion of the T cell to the endothelium. This increases the adhesion of the T cell to a firm adhesion that facilitates transendothelial migration [4]. The recruitment of neutrophils to sites of inflammation is also mediated by CD31, where it upregulates α6β1 integrin surface expression. The upregulation allows the neutrophils to migrate through the perivascular basement membrane [6]. Ligation of CD31 on NK cells upregulates β2 integrins during extravasation into inflamed tissues [7].

Fab (fragment antigen binding) crosslinking of CD31 on neutrophils and macrophages lead to the activation of β_2 integrins showing CD31 participates in integrin activation in leukocyte migration [8]. Intravital microscopy experiments with the murine cremaster muscle demonstrated an *in vivo* role for homophilic CD31 interactions between leukocytes and endothelium. IL-1β induced migration of neutrophils showed the integrin $\alpha_6\beta_1$ was upregulated on the transmigrated cells, which could assist their migration through the basement membrane [6].

The integrin $\alpha_v\beta_3$ has previously been shown to be a ligand for CD31 [9]. During leukocyte migration in a model of transmigration through rat mesenteric venule endothelial cells, blocking antibodies against CD31 prevented IL-1β-induced migration through the basement membrane. However, antibodies blocking $\alpha_v\beta_3$

blocked transmigration in response to fMLP (formyl-methionyl-leucyl-phenylalanine), a synthetic peptide that induces integrin activation [10], a CD31-independent mechanism of migration, showed that although both CD31 and $\alpha_v\beta_3$ were involved in leukocyte transmigration, $\alpha_v\beta_3$ may not be acting as a ligand for CD31 *in vivo* [11]. Eosinophil adhesion to activated endothelium showed CD31 activated $\alpha_v\beta_3$ and increased the adhesion of $\alpha_4\beta_1$ to fibronectin. The increase in adhesion was shown to require the heterophilic CD31- $\alpha_v\beta_3$ interaction to upregulate β_1 integrin-mediated adhesion [12].

During monocyte migration, CD31 in the endothelial cell was recycled around the transmigrating monocyte in subjunctional reticulum, a membrane compartment found at the cell border beneath the membrane. The reticulum is a collection of vesicles connected to each other and the membrane, and CD31 cycles along the membrane as the monocyte migrates between the endothelial cells [13].

1.2 The Inhibitory Receptors of the Immunoglobulin Superfamily

The inhibitory receptors of the immunoglobulin superfamily are expressed on a variety of haematopoietic cells and serve to negatively regulate activating receptors such as the T cell receptor (TCR), and the B cell receptor, (BCR). TCR and BCR both contain an activation motif termed the ITAM (immunoreceptor tyrosine based activation motif). The ITAM corresponds to a particular sequence (YXXL/I [X_{6-8}] YXXL/I), where X is any amino acid. The phosphorylation of the ITAM allows SH2

domain containing proteins such as kinases to bind and transmit signals downstream leading to an activation response. The inhibitory receptors contain an ITIM (immunoreceptor tyrosine based inhibitory motif) sequence is ([I/V/L/S]-X-Y-XX-[L/V]). Once phosphorylated the ITIM bind SH2 domain containing phosphatases SHP-1 and SHP-2, and SHIP, a polyinositol 5′-phosphate phosphatase, these phosphatases signal downstream to inhibit activated signalling [14].

1.2.1 *SIRPα*

SIRPα (signal regulatory protein alpha) is an IgSF member, with three extracellular Ig-like domains, a single transmembrane spanning region and a cytoplasmic domain. The cytoplasmic domain contains four motifs that correspond to an ITIM configuration. SIRPα is expressed on haematopoietic and neuronal cells, and becomes phosphorylated on its ITIM after integrin-mediated cell adhesion, leading to association with SHP-1 and SHP-2, phosphatases. In fibroblasts expressing a cytoplasmic domain deficient SIRPα, SHP-2 was unable to associate and the cells had increased focal adhesions and actin stress fibres. Rho activity was also impaired, leading to defects in polarised migration [15].

From bone marrow derived macrophages (BMDM), SIRPα was found to associate with two other tyrosine phosphorylated proteins, pp55 and pp130. This association was independent of SHP-1 and tyrosine phosphorylation of SIRPα, signifying the ability of SIRPα to act as a scaffolding molecule to allow other proteins to bind and act as substrates for SHP-1 [16].

SIRPα engagement by its ligand CD47 on dendritic cells (DC) regulates their function by providing negative signals that result in the suppression of inflammatory cytokine release [17]. In human melanoma cells, SIRPα-CD47 interactions prevented cell migration by providing negative signals through the dissociation from SHP-2 [18].

1.2.2 *Killer Immunoglobulin-like Receptors*

The killer immunoglobulin-like receptors (KIR) are inhibitory receptors on the surface of natural killer (NK) cells, and inhibit NK activation following ligation by MHC I on target cells. Natural killer cells lyse cells that are infected with virus, or tumour cells where MHC I is typically downregulated. The KIR signal through ITIM motifs on the cytoplasmic domain, when the receptor binds ligand, the ITIM becomes phosphorylated and recruits SHP-1 [19]. The ITIM of KIR was shown to be essential in mediating the inhibitory signal as mutation of the tyrosines to phenylalanine abrogated the inhibitory effect of the receptor [20]. Specifically, the N-terminal ITIM was shown to be more effective in mediating the inhibitory signal [21].

SHP-1 binding to the KIR initiates a pathway that inhibits positive signalling through MHC I. Vav1 is a guanidine-nucleotide exchange factor of Rac that binds to the KIR/SHP-1 complex and may prevent the cytoskeletal rearrangement necessary for activating signalling [22]. SHP-2 is also recruited to the KIR cytoplasmic domain, and requires only the N-terminal ITIM, whereas SHP-1 requires both to be present, as studies with chimeric KIRs *in vivo* have shown [23]. SHP-2 recruited to the ITIM prevents NK cell cytotoxicity, and mutating the catalytic region of SHP-2 reverses this effect [24].

1.2.3 *FcγRIIb Receptor*

The FcγRIIb receptor on B cells also has an ITIM that inhibits activation via the B cell receptor (BCR). The phosphorylated ITIM binds SHIP (SH-2-containing inositol 5-phosphatase), which in turn binds Dok (downstream of tyrosine kinases), Dok is capable of binding RasGAP, which is an exchange factor for Ras [25]. This leads to the inhibition of calcium signalling in the B cell, and inhibition of its activation through coaggregation with the BCR[26-28].

Regulation of mast cell activation through coaggregation of FcγRIIb and FcεRI occurs through the phosphorylation of FcγRIIb by Lyn, and subsequent association of the inositol phosphatase SHIP. SHIP dephosphorylates phosphatidylinositol (3, 4, 5) triphosphate and prevents downstream calcium mobilisation [28].

FcγRIIb is also present in activated mature T cells. The receptor serves to regulate T cell activation through a similar mechanism to B cells, with tyrosine phosphorylation of SHIP upon coaggregation with the TCR (T cell receptor), and inhibition of downstream signalling [29].

1.2.4 *CD155*

Studies with CD155, a cell adhesion molecule expressed on fibroblasts with a similar structure to CD31, have shown it also has an ITIM motif in its cytoplasmic domain; this recruits SHP-2 upon ligand stimulation and subsequent phosphorylation. Cell

adhesion was reduced and cell migration enhanced, and these effects were prevented with the transfection of a point mutation of the ITIM [30].

1.3 The CD31 Molecule

1.3.1 *CD31 Expression*

Platelet-cell adhesion molecule-1 (PECAM-1) or CD31 is a 130kDa glycosylated protein found on the surface of endothelial cells, platelets, monocytes, neutrophils and a unique subset of T cells, with expression on naïve $CD4^+$ cells and memory $CD8^+$ cells [4]. The molecule is composed of six immunoglobulin-like extracellular domains, a single transmembrane spanning region and a 118 amino acid cytoplasmic domain. The inhibitory IgSF members are shown diagrammatically (Figure 1.3:1).

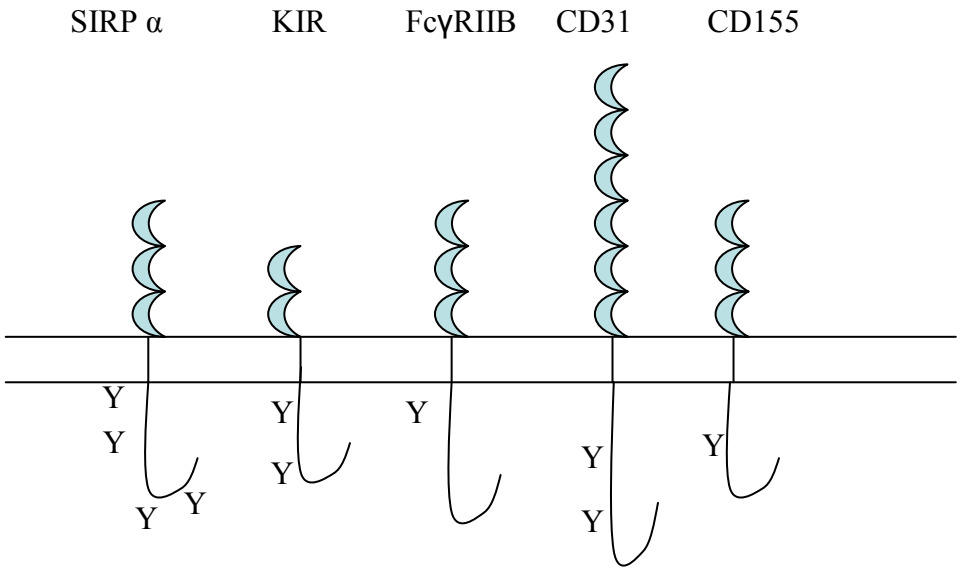

Figure 1.3:1. Cell adhesion molecules SIRPα, KIR, FcγRIIb , CD31 and CD155 showing the extracellular immunoglobulin-like domains, the transmembrane spanning region and the cytoplasmic domain with ITIM domains highlighted as Y.

1.3.2 *CD31 Gene Organisation*

The gene for CD31 is organised into sixteen exons, one for each of for the six extracellular domains, one for the transmembrane region, and unusually for a cell adhesion molecule, the cytoplasmic domain is encoded by seven individual exons. These exons are separated by long sequences of intron (Figure 1.3:2).

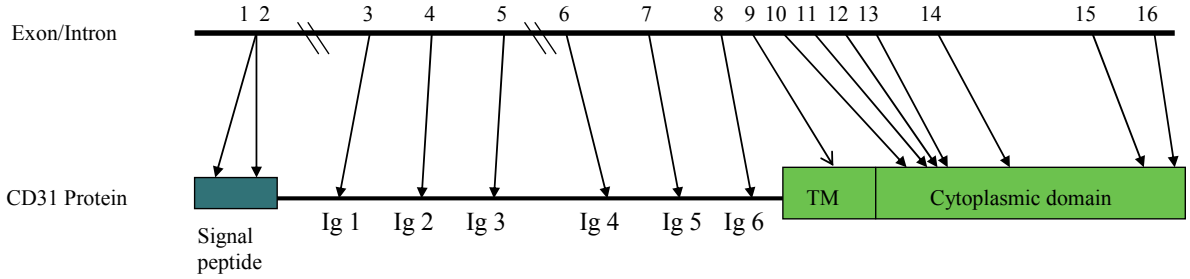

Figure 1.3:2. Exon/intron map of CD31 showing exons 1-6 encoding the extracellular domain and multiple exons 9-16 encoding the cytoplasmic domain [31].

From alternative splicing of the cytoplasmic exons, many variants of CD31 have been discovered. A soluble form exists from the alternative splicing and truncation of the genome at exon 9. Other cell adhesion molecules, including ICAM-1 also produce a soluble form. Both cells of the myeloid system and HUVECs have been shown to secrete the soluble form of CD31, and this form was also biologically active, capable of preventing aggregation of L cells. Interestingly, two isoforms of CD31 were observed in human plasma, a 90kDa and a 120kDa form. The 90kDa form is truncated at the transmembrane region and does not have the cytoplasmic domain, whereas the 120kDa form does have the cytoplasmic domain present [32].

In the developing embryo, CD31 isoforms have been detected during different stages of development, having functionally distinct features. The isoforms detected were (Δ12,15) and (Δ14,15). Both isoforms were able to form homophilic interactions upon transfection into L-cells, but differed in their sensitivity to antibodies against CD31. This suggested that the deletion of parts of the cytoplasmic domain affected the ability of CD31 to bind to ligands [33]. Cells switching between isoforms may provide a mechanism by which CD31 can modify adhesive contacts. Δ15 and Δ14/Δ15 expression modulates cadherin adhesion [34], and there is differential expression of these isoforms from the early stages of endothelial cell migration [35].

Of interest is the expression of Δ14 isoform, which does not have tyrosine 686, part of the ITIM that is required for SHP-2 binding and subsequent signalling. Switching isoform expression in murine embryonic stem cells (ES) and expression of Δ14

highlights the possibility that CD31 may have different roles in haematopoiesis and vasculogenesis during the process of development [36].

1.4 CD31 Knockout Mouse

CD31 knockout mice (CD31KO) were generated by disruption of exon 6-8, resulting in no protein expression on a C57BL/6 background, and have been shown to be viable and fertile. There were no differences observed in platelet, red blood cell or leukocyte counts between wild-type and knockout mice. Although there was no defect in the ability of leukocytes to migrate into areas of inflammation, CD31KO neutrophils were unable to migrate past the basement membrane. This defect was only observed when the cells were stimulated by IL-1β [37].

1.4.1 *CD31 Models of Inflammation*

CD31KO mice generated on a FVB/n background also have no difference in their total blood and leukocyte cell counts. However, their response to inflammation is markedly different compared with the original strain of knockout mice. Upon thioglycollate-induced peritonitis, the CD31KO FVB/n mice show reduced numbers of neutrophils, monocytes and macrophages, but the C57BL/6 does not. C57BL/6 mice have the unique ability to compensate for the lack of CD31, so perhaps further studies should be carried out in other strains of mice [38]. Chronic inflammatory lung disease leading to fibrosis was observed in CD31KO FVB/n mice, but not in CD31KO C57BL/C, also highlighting the effect of background strains in inflammatory responses [39].

Studies with different models of inflammation have elucidated a role for CD31 in leukocyte migration. A model of leukocyte transmigration with rat mesenteric venules showed treatment of the rat with anti-CD31 antibodies did not prevent IL-1β-induced transmigration through the junctions, but the leukocytes were prevented from migrating through the basement membrane [40]. Studies with the CD31KO mouse cremaster model of inflammation have shown CD31 and the integrin $\alpha_6\beta_1$ is required for the migration of leukocytes through the perivascular basement membrane [6].

Allergic responses involve mast cell degranulation, and existing therapy involves anti-inflammatory drugs, an alternative may be to activate molecules involved in the negative regulation of the immune response. Using both CD31KO and wild-type mice, it was shown Ig-E mediated anaphylaxis, and mast cell degranulation was enhanced in knockout mice. This suggests that CD31 may serve to dampen an allergic immune response by negatively regulating mast cell activation [41].

PVA sponges implanted into wild-type and CD31KO mice showed differences in their vascularisation. In the knockout animals, the amount of angiogenesis was reduced compared with wild-type. This may explain why in the CD31KO mouse, there is reduced leukocyte accumulation, as there are fewer vessels responsible for bringing the cells to the implants [42].

B cells deficient in CD31 show hyperproliferation upon IgM stimulation. However, the ability to produce antibody was not affected. During maturation of the B cell, absence of CD31 causes developmental defect in the transition from the immature to the mature cell. CD31 was found to negatively regulate the B cell receptor, and may do this by recruitment of signalling molecules to its cytoplasmic domain. By providing negative signals, CD31 may assist in the maintenance of tolerance, as CD31KO mice produced anti-dsDNA antibodies [43].

Although the CD31KO mouse is able to form endothelial junctions and adhesions in the absence of CD31, the response to LPS-induced endotoxic shock results in much reduced survival compared with wild-type. The CD31KO mice had increased vascular permeability, and increased apoptosis of spleen, liver and kidney, with elevated levels of inflammatory cytokines. Also reduced were the STAT3 (signal transducers and activators of transcription) levels. This suggested CD31 acts as a scaffold for STAT3 where it can be phosphorylated, and SHP-2 is able to bind and have its activity regulated. CD31 is also reported to bind tyrosine phosphorylated β-catenin, and is able to facilitate the dephosphorylation of β-catenin by also binding SHP-2. Dephosphorylated β-catenin was then released and was able to associate with VE-cadherin, reassembling the junctional adhesion complex and the integrity of the endothelium. In the absence of CD31, the regulation of these signalling molecules is impaired, leading to the increased permeability observed. CD31 is therefore thought again to be a functioning as a negative regulator of immune responses [44].

Murine experimental autoimmune encephalitis (EAE) is a model of human multiple sclerosis that studies demyelinating disease caused by inflammation in the CNS. This involves the induction of autoimmune T cells by administration of a myelin oligodendrocyte glycoprotein peptide [45], the migration of these cells across the blood-brain barrier, and the initiation and maintenance of inflammation in the CNS. Using CD31KO mice to stimulate this response, there was an early beginning of clinical symptoms, with increased migration of leukocytes across the blood-brain barrier, and a reduced ability to restore the endothelium. This increased permeability could explain the earlier onset of symptoms, and show CD31 to be essential for maintaining blood-brain barrier reliability [46].

A murine collagen-induced arthritis model highlighted the role of CD31 in negatively regulating immune responses to inflammation. Type-II collagen (CII) was administered, stimulating production of CII specific T cells, and antibody production by B cells. The second stage was where the T cells migrated to the joints and caused and maintained inflammation. CD31KO mice develop arthritis more quickly, with increased activation of T cells, and early production of anti-CII antibodies, there was also an increased number of infiltrating lymphocytes. In this model, CD31 was not required for leukocyte migration, but for the negative regulation of the immune response [47]. Studies on inflammation in the lung revealed CD31 dependent and independent responses. The CD31 responses were due to a defect in macrophage activation, with reduced Fcγ-mediated phagocytosis and release of TNFα [48].

1.5 CD31 Ligand

CD31 on endothelial cells localises to cell-cell junctions of confluent monolayers [49], where CD31 interacts with itself in homophilic binding to another CD31 molecule on the surface of the endothelial cell, this interaction is mediated by the first two immunoglobulin-like domains [50].

Other ligands for CD31 include CD38, a 45kDa glycoprotein expressed on endothelial cells and leukocytes with multiple functions including ADP-ribosyl cyclase activity, activating NK, B and T cells and as a selectin, mediating leukocyte tethering to endothelial cells. Inhibition of CD38-mediated adhesion by monoclonal antibody immunoprecipitation and reactivity with CD31-transfected cells suggested CD31 is capable of heterophilic interactions [51].

The integrin $a_v\beta_3$ is expressed on B, T, NK and mast cells amongst other cells types, and is comprised of two chains, alpha and beta. Integrins serve to mediate adhesive interactions during cell adhesion and migration, and $a_v\beta_3$ has been shown to act as a heterophilic ligand for CD31 during leukocyte adhesion to the endothelium *in vitro* [52]. Using CD31 recombinant proteins and the leukemic pro-monocyte cell line U937, the cells bound CD31 mostly in a heterotypic manner, with the binding site for $a_v\beta_3$ in domain 1 [9]. In T cells a 120kDa ligand for CD31 was discovered which when bound to CD31 decreased T cell activation after T cell receptor-ligand interactions [53].

1.5.1 *Tyrosine Phosphorylation of CD31 Cytoplasmic Domain*

Src family kinases have been implicated in phosphorylating the cytoplasmic domain of CD31. Co-precipitation studies showed CD31 is phosphorylated by c-src, particularly on Y663 and Y686, this association is mediated by the SH2 domains of c-src [54]. As inhibitors of src family kinases did not block the phosphorylation of CD31 in stimulated endothelial cells, other kinases may be involved in this particular signalling pathway. Fer is a ubiquitously expressed tyrosine kinase which phosphorylates p120-catenin and β-catenin in the adherens junction of endothelial cells. CD31 present at these junctions are tyrosine phosphorylated by Fer, which localises to microtubules in migrating cells [55]. Studies with murine CD31 showed that CD31 is phosphorylated by src and csk kinases, and only on tyrosine 686, there was no phosphorylation of tyrosine 663. csk substrates are usually the C-terminal tyrosine residue of src kinases [56].

Tyrosine phosphorylation of the cytoplasmic domain of CD31 allows the SH-2 domain containing phosphatases SHP-1 and SHP-2 to bind via its SH-2 domains, at tyrosine residues Y663 and Y686, part of the ITIM motif [57]. In T cells, CD31 becomes tyrosine phosphorylated after cross-linking to the T cell receptor or to itself, and recruits SHP-2. This prevented intracellular calcium release and activation of the cell [58].

1.5.2 *Role of the ITIM of CD31*

The role of the ITIM of CD31 in cell migration has been controversial. Transfecting REN (endothelial-like cell line) cells with wild-type CD31 or with Y663F/Y686F

CD31 demonstrated the ITIM of CD31 was required for the cells to migrate. The study postulated that tyrosine phosphorylation of CD31 acted to negatively regulate migration and required the recruitment of SHP-2 to these tyrosines to remove the inhibition [59]. Another study exploring the role of the ITIM in endothelial cell migration showed that transfection with Y686F CD31, cells had increased migration, which implied the ITIM acted as a brake to regulate migration. During endothelial cell migration, homophilic interactions between CD31 are lost, with a subsequent loss of tyrosine phosphorylation, and no recruitment of SHP-2 [60]. A study by the same group measuring wound healing migration with transfected REN cells showed there was no difference in migration with cells transfected with either Y663F/Y686F or wild-type CD31; but that transfection of these constructs was enough to restore the migration defect when compared with knock-out cells. The defect in knock-out cell migration was attributed to an imbalance of Rac and Rho, with less RhoGTP present in knock-out cells [61].

1.6 CD31-Mediated Signalling

CD31 has no intrinsic enzymatic activity and must associate with other proteins via its cytoplasmic domain to participate in intracellular signalling. The protein tyrosine phosphatases SHP-1 [57] and SHP-2 [62] have been shown to bind CD31. A study with a mesothelioma cell line expressing a Y663F/Y686F mutant CD31, which could not bind SHP-2 showed impaired migration when compared with cells expressing wild-type CD31. SHP-1 has been shown to require the ITIM of CD31 intact to bind, whereas SHP-2 requires only Y663 [63].

Tyrosine phosphorylated β-catenin has been shown to bind endothelial cell CD31 [64], and is thought to sequester β-catenin away from cadherins in the cell junction, allowing SHP-2 to bind and dephosphorylate β-catenin, which then dissociates from CD31 and can return to the adherens junction, thus leading to the loosening of the cell-cell contacts to facilitate migration [65]. γ-catenin is a molecule that participates in adherens junctions, and binds to CD31 cytoplasmic domain in EOMA cells. The association is regulated by PKC, where an increase of PKC serine/threonine phosphorylation decreased the amount of γ-catenin binding. The association is much lower than that observed for β-catenin [66].

The inositol phosphatase SHIP has been shown to bind to the cytoplasmic domain of CD31 in chicken DT40 B cells independently of tyrosine phosphorylation, and regulate the activation of the B cell receptor through a different pathway from the recruitment of SHP-1 and SHP-2 [62]. A GST fusion protein of the cytoplasmic domain also found SHIP capable of binding to CD31, however, this study showed that tyrosine 686 was required for binding [63]. Therefore, there is some controversy over the residues of CD31 required to recruit SHIP. SHIP has been shown to bind to the ITIM, and another downstream tyrosine residue of the FcγRIIb receptor on B cells and negatively regulate B cell activation. SHIP can also function as a docking protein by recruiting RasGAP, which converts the active GTP-bound form of Ras to the inactive GDP-bound form [67]. CD31 could conceivably be participating in this signalling pathway in B cells.

Signal transducer and activation of transcription 5 (STAT 5) has been shown to bind to the cytoplasmic domain of CD31 *in vivo* during murine development, and require tyrosine 701 [68]. STAT5 participates in receptor activated JAK (Janus kinase) signalling, and becomes phosphorylated where it translocates to the nucleus and binds to STAT5 recognition sequences and regulates transcription. STAT5 activation is regulated by SOCS (suppressors of cytokines signalling), and SHP-1 and SHP-2 phosphatases [69]. CD31 may be capable of influencing intracellular signalling through this pathway.

The SH2 domain containing signalling protein Grb2 has recently been shown to associate with crosslinked tyrosine phosphorylated CD31 on bEND cells (murine brain endothelial cells). Grb2, along with CrkI and Shc are then thought to activate the MAPK (mitogen activation protein kinase) and ERK (extracellular related kinase) pathway. This leads to the activation of the small GTPase Ras, which could impact upon cell migration [70].

Gab1 (Grb-associated binder 1) bound to tyrosine phosphorylated CD31 on mechanically stressed endothelial cells. Gab1 has plecstrin homology domains, an SH3 domain and a BTAM (biphosphotyrosyl activation motif) that recruits SHP-2 [71]. This leads to the phosphorylation of ERK [72].

The SH2 domain of Phospholipase C-γ (PLC-γ) has also been shown to bind to the cytoplasmic domain of CD31 in a study using BIAcore analysis. PLC-γ bound preferentially to tyrosine 663 [63], and the SH3 domain of PLC-γ has more recently been shown to act as a guanidine exchange factor for the GTPase PIKE (phosphatidylinositol-3' kinase [PI3K] enhancer). PIKE stimulates nuclear PI3K activity [73]. PI3K has also been shown to bind to the cytoplasmic domain of CD31. Ligation of CD31 on human neutrophils induced PI3K association and upregulation of β_1 integrins [74].

Talin is a 270kDa protein composed of a globular head, and rod domain. The head domain contains a FERM (4.1-ezrin, radexin, moesin) motif. Talin binds to β-integrin cytoplasmic domains [75] and links integrins and the extracellular matrix [76] or the adhesive contacts between cells [77]. CD31 has also been shown to activate β_1 integrins, and may be associating with talin for this integrin activation (Dr David Critchley, Leicester University, UK, personal communication).

When integrins are activated, src family kinases and FAK (focal adhesion kinase) and phosphatases become switched on, allowing rapid phosphorylation and dephosphorylation of proteins involved in focal adhesions [78]. Talin is in a folded conformation when inactive, and binding sites for integrin cytoplasmic domains are exposed [79] following activation by cleavage by calpain [80] or upon binding of the phosphoinositide $PI4,5P_2$

In a study where talin was knocked out in ES cells, the cells were unable to spread on gelatin, clearly demonstrating the role that talin plays in focal adhesion assembly [77].

In *C. elegans,* talin was found to co-localise in focal-adhesion structures in a complex with integrins, vinculin and actin [81]. Using RNAi to knock down talin in *C. elegans*, there were defects in migration in gonadal tissues, and uncoordination and paralysis, showing the essential role that talin plays in coordinating cell migration [82].

The known and postulated binding partners of CD31 are summarised (Table 1.6:1), with the cell type in which the discovery was made.

Protein	Cell Type
SHP-1	Platelets THP-1 T cells B cells
SHP-2	Platelets T cells B cells
PLC-γ	BAECS THP-1
ERK	bEND
MAPK	bEND
SHIP	THP-1 B cells
Gab1	BAECS
Grb2	RBL-2H3
STAT5	HEK 293T HUVEC
β-catenin	Endothelial cells SW40
γ-catenin	HUVEC EOMA
PI3K	PMN BAECS
Fyn	BAECS
Src	BAECS
Talin	NIH3T3

Table 1.6:1. Summary table of known and postulated CD31-binding proteins [70,83].

1.7 CD31 and Apoptosis

CD31 expressed on viable human neutrophils when ligated homophilically with CD31 upon macrophages promoted leukocyte detachment. The detachment signal led to the movement of the neutrophil away from the macrophage, whereas CD31 engagement on apoptotic leukocytes allowed firm tethering and subsequent engulfment of the apoptotic cell. Dissection of the signalling pathway showed SHP-1 did not associate with CD31, and SHP-2 was cleaved by caspases in apoptotic cells [84]. Apoptotic B cell lines have also been shown to interact with CD31 on macrophages, when CD31 was blocked with antibodies, phagocytosis of apoptotic cells was reduced. 70% of the apoptotic population expressed CD31, which suggested CD31 was upregulated on dying cells to afford clearance [85].

Neutrophils express CD47, the ligand for the immunoglobulin superfamily member SIRPα. This interaction in viable neutrophils was reported to lead to 'don't eat me' signals, when this interaction was blocked by Fab fragments, the cells were engulfed. CD47 was found to be distributed away from the cellular uptake receptors calreticulin and PS [86].

1.7.1 *CD31 and Cell Survival*

Transmigrated $CD14^+/CD34^+$/CD31 expressing mononuclear cells were protected from apoptosis by CD31 engagement on endothelial cells during transmigration. CD31 was found to deliver anti-apoptotic signals to the transmigrated cells. The signals were in the form of CD31 inducing PI3K activation of Akt, which lead to increased Bcl-2 and Bcl-X protein expression; these proteins were able to prevent the

cell undergoing apoptosis [87]. CD31 requires its cytoplasmic domain intact, and prevents the release of cytochrome C, caspase activation and nuclear condensation which is indicative of Bax-induced apoptosis, thus protecting leukocytes from programmed cell death[88]. Monocytes protected endothelial cells from apoptosis by engaging CD31 on the surface of the cell. When CD31 interactions were blocked by a monoclonal antibody, the protective effect was lost [89].

Endothelial cell serum-starvation and subsequent apoptosis was found to be inhibited by CD31 homophillic engagement, and may require intracellular signalling molecules associated with the cytoplasmic domain of CD31 [90]. Sphingosine kinase (SK) has been shown to signal through CD31 to prevent endothelial cell apoptosis, by activating PI3K/Akt pathway [91].

During apoptosis of endothelial cells, CD31 was cleaved into a soluble 100kDa fragment composed of the extracellular domain which was shed into the culture medium; and a 28kDa truncated form comprising of a small extracellular region, the transmembrane section and the cytoplasmic domain. The truncated form was shown to differentially recruit β-catenin, γ-catenin and SHP-2 when compared with full-length CD31. Expression of the truncated form only within SW480 cells demonstrated a decrease in viable cell number and an increase in apoptosis. The increase in apoptosis correlated with the activation of p38/JNK. The truncated form of CD31 may be taking on a conformation similar to that of the phosphorylated form, and thus differentially recruit signalling molecules during apoptosis [92]. In apoptotic

neutrophils, CD31 was found to be slightly downregulated [93], which may provide evidence in haemopoetic cells that cleavage of CD31 occurs.

1.8 SHP-1 and SHP-2 Knock-Out Mouse

The moth-eaten mouse is deficient in the protein tyrosine phosphatase SHP-1. The phenotype exists as the moth-eaten (*me/me*), and moth-eaten viable (me^v/me^v). *me/me* mice have no SHP-1 protein and live for about three weeks, during which they develop severe autoimmunity, characterised by reduced proliferation of B, T and NK cells, and hyperglobulinemia autoantibody expression, inflammatory lesions and pneumonitis. The me^v/me^v mouse lives for about nine weeks, and exhibits a more chronic immunological phenotype. me^v/me^v mice have a catalytically inactive SHP-1 and develop an overgrowth of macrophages in the skin and lungs, which causes fatal pneumonitis [94].

Studies with the me^v/me^v mouse showed SHP-1 was required for the detachment of macrophages from $\alpha m\beta_2$ integrin, and the detachment required membrane-associated PI3K regulation by SHP-1. The phenotype of the me^v/me^v mouse may be due to failure of macrophages to de-adhere normally in the tissues [95]. A study with me^v/me^v B cells transduced with hen-egg lysozyme (HEL) showed an increase in calcium release in response to HEL binding and a reduced threshold for elimination which implicates SHP-1 in negative regulation of B cell development [96].

SHP-2 knockout mice were shown to be embryonic lethal with major developmental abnormalities, particularly in haematopoiesis, where no progenitors of myeloid or

erythroid cells were found in SHP-2 KO embryos [97]. Specifically, SHP-2 was found to be required for lymphopoiesis, where chimeric ES cells (of SHP-2 and Rag-2 which are unable to rearrange V, D and J chains and thus any lymphopoiesis must have been from the SHP-2 cells) were unable to produce functional T or B cells [98]. A targeted deletion of exon 3, which resulted in a disruption of the N-terminal of SHP-2 [99] showed major defects in development and haematopoiesis.

1.9 Apoptotic Cell Clearance Mechanisms

Apoptotic cells must be cleared from the system to potentially avoid secondary necrosis and leakage of intracellular contents, which could have harmful consequences to the body with the development of autoantigens and disease, such as SLE (systemic lupus erythematosus). The apoptotic cell is recognised by macrophages engaging cellular receptors, which mediate the tethering and eventual engulfment of the apoptotic cell [100].

CD14 originally identified as the LPS receptor [101], is involved in the recognition of apoptotic cells by macrophages. This molecular interaction stimulates the production of the inflammatory cytokine TNFα. The interaction of apoptotic leukocytes with macrophages mediated by CD14 does not stimulate an inflammatory response [102]. A study with CD14KO mice revealed the persistence of apoptotic cells, and a decreased interaction between the leukocyte and the macrophage when compared with wild type cells. There was no autoantibody generation due to the presence of uncleared

apoptotic cells, which suggested CD14 does not contribute to autoimmunity, but is required for the efficient clearance of apoptotic leukocytes [103].

Other apoptotic cell recognition molecules include CD36 binding to thrombospondin (TSP) which acts as a 'molecular bridge' between CD36 and $\alpha_v\beta_3$ integrin on the macrophage, and the receptor on the apoptotic leukocyte [104]. A study with apoptotic fibroblasts showed TSP was released from the apoptotic cell and acted as a chemoattractant to macrophages, and was also capable of binding to CD36 on the apoptotic cell. This complex was recognised by the CD36/$\alpha_v\beta_3$/TSP on the macrophage, which led to the clearance of the apoptotic fibroblast [105].

Complement also plays a role in the clearance of apoptotic cells, specifically the C1q component. Studies with C1qKO mice demonstrate impaired clearance of apoptotic cells in a model of SLE. HMDM from C1q-deficient individuals also showed impaired phagocytic clearance [106]. Mannose-binding lectin (MBL) was also shown to bind to apoptotic cells, and with Clq bind to calreticulin on the macrophage. Calreticulin associates with CD91 to mediate uptake of apoptotic cells [107].

Stable phosphatidylserine (PS) exposure on the surface of apoptotic cells has been shown to mediate cellular uptake by macrophages [108]. On the surface of viable cells, the zwitterionic phospholipids phosphatidylcholine (PC) and sphingomyelin are normally expressed. In the inner leaflet the aminophospholipids PS and

phosphatidylethanolamine (PE) are expressed. The 'flip-flop' of PS from the outer membrane to the inner leaflet is maintained by aminophospholipids translocase [109]. When the cell undergoes apoptosis, this enzyme is inactivated, whereas a scramblase is activated resulting in stable expression of PS upon the cell surface [110]. Tethering of apoptotic cells to macrophages by receptor ligation has been shown to require PS-receptor interaction for engulfment [111]. A protein secreted by activated thioglycollate-elicited macrophages, milk fat globule epidermal growth factor-8 (MFG-E8) has been shown to bind to PS on the surface of apoptotic cells and enhance their uptake [112].

There is some controversy surrounding the receptor for PS (PSR), which was initially cloned in 2000 [113] suggesting PSR on macrophages recognises PS exposure on the surface of apoptotic cells. Generation of a PSRKO mouse was embryonic lethal and demonstrated uncleared apoptotic cell corpses in a variety of tissues. PSR-deficient macrophages also showed impaired phagocytosis of apoptotic cells [114]. However, although recent data has shown that ablating PSR in mice lead to development defects and embryonic lethality, the mutation had no defect in apoptotic cell clearance. PSRKO macrophages were able to phagocytose apoptotic cells in a variety of tissues, which suggested PSR is not involved in apoptotic cell clearance during development [115].

ABCA1 (ATP-binding cassette 1) expression was found in the developing murine embryo localised in areas of apoptotic cell death. ABCA1 is a molecule expressed on macrophages and a major function is to mediate the engulfment of apoptotic cells

[116]. ABCA1KO mice developed immune-complex induced glomerulonephritis, which was due to a defect in apoptotic cell clearance [117].

The scavenger receptor B1 (SR-B1) has a similar ligand binding affinity to CD36 for high density lipoprotein, and was shown to be a receptor for apoptotic thymocytes [118]. SR-B1 was shown to be the receptor for PS on non-professional phagocytes, in a study of the clearance of thymocytes by thymic nursing cells (TNC), SR-B1 was found to mediate the uptake of apoptotic thymocytes into the TNC [119]. Sertoli cells in murine testicles phagocytose apoptotic spermatozoa via SR-B1 binding to PS, and provide another mechanism by which 'amateur' phagocytes engulf apoptotic cells [120].

1.10 Hypothesis and Aims

The hypothesis underlying the work presented in this thesis is; the differential recruitment of signalling and adapter molecules to the cytoplasmic domain of CD31 in viable and apoptotic leukocytes, results in the tethering of apoptotic cells and the escape of viable cells. A difference in recruitment of signalling and adapter molecules may mediate the detachment of the viable cell from macrophages, and cause the apoptotic cell to remain attached, thus facilitating engulfment.

This work attempts to dissect the mechanism by which CD31 signals in viable and apoptotic leukocytes by signalling molecule association with the cytoplasmic domain.

2 Attachment Assay

2.1 Introduction

2.1.1 *CD31 and Diapedesis*

It is well established that CD31 has a critical role in the migration of leukocytes during diapedesis [5]. Recently, CD31 has been shown to localise to sub-cellular compartments in the endothelial cell membrane during leukocyte migration. As the leukocyte transmigrates, CD31 is recycled along the endothelial barrier, with high levels of expression of CD31 juxtaposed to the leukocyte, right through the process of migration [13]. Studies with human neutrophils migrating through a HUVEC monolayer showed that CD31 aligned migration in the direction of fluid flow, and that migration was accelerated through the endothelial cell layer, suggesting that CD31 plays a critical role in mediating the direction and velocity of leukocyte migration [121].

2.1.2 *Integrin Activation and CD31*

CD31 contributes to the process of migration of T cells acting as an adhesion amplifier, upregulating β1 integrins during adhesion of the T cell to the endothelium. Homophilic CD31 interactions thus increase the adhesion of the T cell by promoting firm adhesion that facilitates transendothelial migration [4]. Ligation of CD31 on NK cells has also been shown to upregulate β2 integrins during extravasation into inflamed tissues [7]. The recruitment of neutrophils to sites of inflammation is also facilitated by CD31, principally via the upregulation of α6β1 integrin surface expression, allowing rapid neutrophil migration through the perivascular basement

membrane [6]. Thus, CD31 works in concert with integrins during the process of leukocyte transmigration to sites of inflammation.

2.1.3 *CD31 and Cell Migration*

Endothelial CD31 also has a critical role in the process of angiogenesis, the growth of new blood vessels. Angiogenesis is a complex process involving capillary endothelial cells detaching, migrating to the new site, reforming cell-cell contacts and proliferating to form new endothelial layers. CD31 participates in the later stages of this process by forming tight cell-cell contacts giving rise to a cobblestone cell monolayer appearance. Furthermore, in an *in vitro* three-dimensional model of murine angiogenesis, tube formation was reduced by the addition of monoclonal antibodies against CD31 [122].

A regulatory function for CD31 was also found in wound healing migration experiments where cell monolayers were physically disrupted and cell migration into the wound was then quantified. NIH/3T3 cells normally null for CD31 expression, were transfected with full length, or CD31 missing the cytoplasmic domain and wound healing migration was then assayed. Migration was found to be impaired in the cells transfected with full length CD31 when compared with those transfected with only the extracellular domain, implying a role for the cytoplasmic domain in inhibitory signalling[123].

2.1.4 *Role of the ITIM in Migration-For or Against?*

Consistent with the evidence that CD31 is intimately involved in endothelial cell migration, wound-induced migration was impaired in REN (mesothelioma) cells transfected with CD31 missing the ITIM tyrosines, compared with REN cells transfected with full length CD31. SHP-2 requires intact ITIM tyrosines to bind to CD31, and the loss of these tyrosines, and consequently of SHP-2 binding resulted in decreased cell migration. SHP-2 is thought to be brought closer to the membrane in order to facilitate focal adhesion turnover, or be sequestered away to allow FAK to act in the later stages of focal adhesion maturation [59]. However, there is some conflicting evidence as to the role of the ITIM in CD31 migration and motility.

Wild-type CD31 was also found to be essential for mediating endothelioma cell migration; however in contrast to the findings with REN cells, the ITIM was found to act as a constraint to negatively regulate migration. Transfection with an ITIM mutant resulted in an increase in β-catenin phosphorylation, which could potentially loosen adherens junctions; and an increase in FAK phosphorylation, which is important for regulation of focal adhesion turnovers. In this system, an imbalance between Rac and Rho was found in CD31 knock-out cells, which increased single cell motility, but impaired co-ordinated wound healing motility [60]. Although this finding contrasts those for REN cells, CD31 clearly has the potential to regulate cellular adhesion and migration.

2.1.5 *CD31 and Cellular Detachment*

Macrophage recognition and ingestion of dying cells *in vivo*, is essential to protect from the potentially deleterious effects of toxic intracellular contents. Results from *in vitro* studies have shown that many different molecular pathways may contribute to interaction of macrophages with apoptotic cells[124]. Whilst a role for homotypic CD31 interaction in macrophages binding to both viable and apoptotic leukocytes might be expected, previous work from this laboratory demonstrated a novel role for CD31 in active viable leukocyte detachment from the macrophage surface. The experimental system exploited temperature-dependent differences in cell adhesion. Viable or apoptotic cells bound to macrophages at 20˚C were subsequently allowed to detach under flow at either 20˚C or 37˚C. In contrast to viable cells, which exhibited temperature dependent detachment at 37˚C, apoptotic cells remained attached. It was postulated that viable cells were able to transmit signals via CD31 to engage the cell's motor machinery and escape, whilst in the apoptotic cell signalling was disabled, and the cells were incapable of detaching [84].

2.1.6 *Experimental Aims*

An *in vitro* static detachment assay was developed as a model of leukocyte-macrophage interactions based on preliminary experiments (Dr Simon Brown, University of Edinburgh UK, personal communication). The myelomonocytic cell line THP-1 was used following differentiation into a 'macrophage-like' phenotype with PMA (phorbol 12 myristate 13-acetate). Undifferentiated cells grow in suspension, upon differentiation; the cells become adherent and show similar morphology to macrophages. THP-1 cells differentiated in this manner have been

used for studies involving macrophage models of disease such as atherosclerosis [125]. The differentiated THP-1, hence termed THP-1, were plated into 8 well glass chamber slides to allow ease of handling, and differentiation into a monolayer was observed after 5 days culture. Seven wells of cells were stained with cell tracker orange under serum-free conditions at room temperature. One well of cells was left unstained to act as a negative control during flow cytometry analysis. Excess stain was then well washed off with media containing serum and replaced with fresh complete media. Simultaneously, the test leukocytes were stained with cell tracker green also under serum free conditions, with a population from the same flask left unstained as a negative control. Excess stain was washed off with complete media and replaced with fresh. The populations of leukocytes used were at 75% or above viability, as confirmed by annexin V and propidium iodide staining under flow cytometric analysis.

One million of the test stained leukocytes were added to the THP-1 in 6 of the wells and allowed to settle for 15 minutes at room temperature. Room temperature was chosen to allow initial tethering to occur at a temperature where cytoskeletal reorganisation was inhibited[84]. The chamber slide was then placed into a media bath either at room temperature, or at 37˚C, and inverted for 30 minutes. The chamber slide was then turned right side up and removed from the media bath. The media was then gently removed and trypsin/EDTA was added for 15 minutes to remove the cells. The cells were then resuspended in FACS buffer for flow cytometric analysis. Results are expressed as the number of leukocytes still attached after inversion per 100 THP-1 cells counted.

The aim of the experiments shown in this chapter was to investigate the role of CD31 in viable leukocyte detachment from macrophages. A number of CD31-expressing cell lines were used initially to determine whether CD31 mediated detachment of viable cells represented a general phenomenon. The suspension T cell line Jurkats were used with stable transfection of CD31 with altered ITIM motifs to assess the contribution of cytoplasmic sequences within CD31 in regulating viable cell detachment.

Experiments were performed in triplicate and shown as the mean ±SD. Statistical tests used were t-test (two samples) or one way ANOVA (three or more samples) with appropriate post-hoc tests.

2.2 Results

2.2.1 *CD31 Positive and CD31 Negative Jurkat Attachment*

The attachment assay (Figure 2.2:1) with settling at room temperature and inversion at 37˚C was performed with CD31 negative and CD31 positive Jurkats, stably transfected to express CD31. A representative FACS dot plot shows two cell populations from a well by forward and side scatter (Figure 2.2:2 panel A). The Jurkats were then gated on their fluorescence as measured through the FL-1 channel (B), and the THP-1 gated on their fluorescence as measured through FL-2 (C).

More CD31 negative Jurkats remained attached to the THP-1 than CD31 positive Jurkats (Figure 2.2:3) (n=3, p=0.117), showing that CD31 mediates the detachment of viable CD31 positive Jurkats, validating the assay and thus supporting previous work where CD31 mediated the detachment of viable Jurkats from macrophages [84].

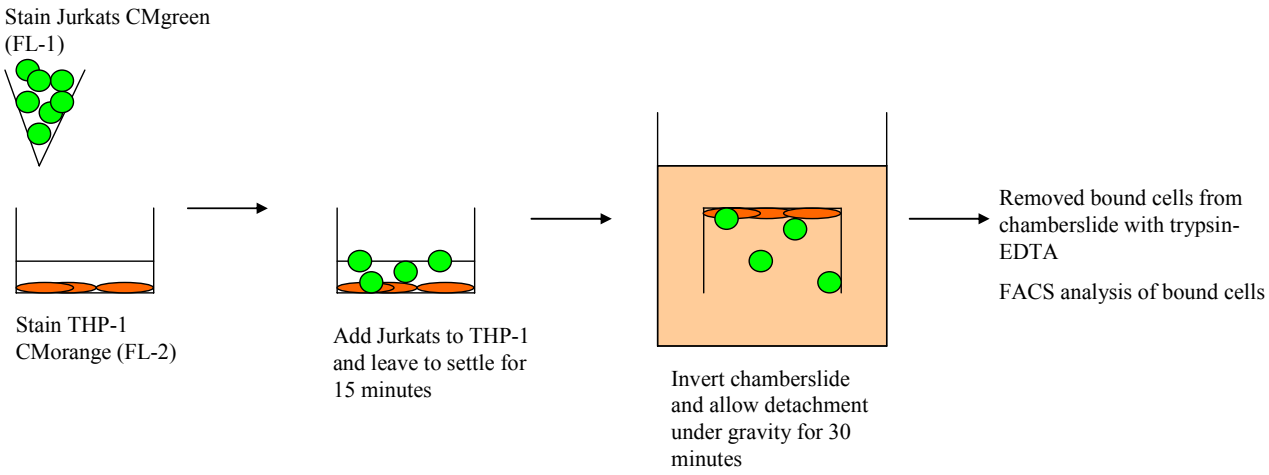

Figure 2.2:1. Model of leukocyte-macrophage interactions was developed. THP-1 are differentiated with PMA over 5 days onto 8 well chamber slides and stained with cell tracker orange. Leukocytes were stained with cell tracker green, and added to the THP-1 monolayer. After a 15 minute settling period, the chamber slide was immersed in a media bath and viable cells were allowed to detach under gravity for 30 minutes. The chamber slide was treated with trypsin-EDTA and the cells were analysed by flow cytometry. The results are expressed at number of leukocytes remaining bound per 100 THP-1 cells counted. Jurkats were assayed for viability by annexin V and propidium iodide staining (See materials and methods for a full description).

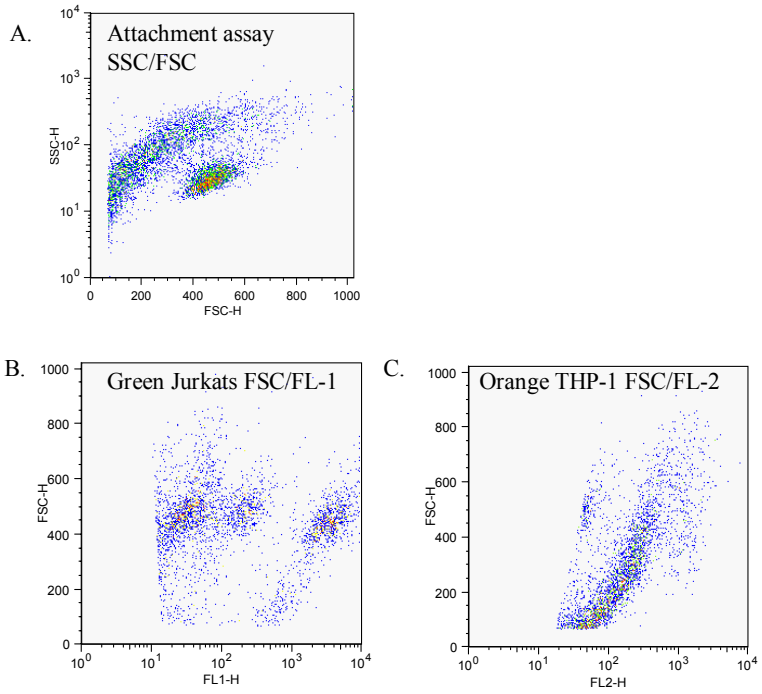

Figure 2.2:2. Representative FACS dot plot showing the end point of the attachment assay. Jurkats stained cell tracker green appear in the FL-1 channel, and the THP-1 stained orange appear in the FL-2 channel. The cells were gated on the percentage stained positive.

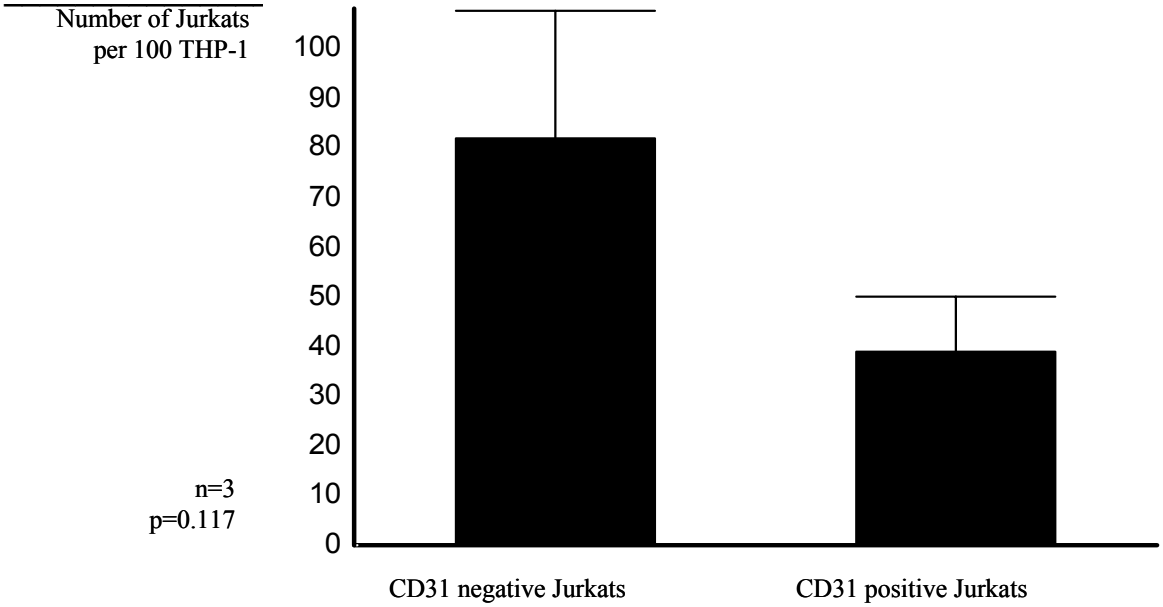

Figure 2.2:3. More CD31 negative Jurkats remain attached to the THP-1 than CD31 positive Jurkats under standard assay conditions (p=0.117, n=3).

2.2.2 *Leukaemic Cell Line Attachment Assay*

To determine if the CD31-dependent detachment from THP-1 was particular to stably transfected Jurkats, the standard attachment assay (with settling at room temperature and inversion at 37˚C) was utilised to assess a panel of leukemic cell lines. This included CD31 negative Jurkat T cells, CD31 positive Jurkats, U937, KG-1 and MM6 which all grow as a non-adherent suspension culture.

The Jurkats have been previously stably transfected with CD31 wild-type [2]. U937 are a monocytic leukaemia with CEACAM (CD66) surface expression [126,127]. MM6 (mono-mac 6) cells are a monocytic-like cells that express CD13, CD15, CD34, CD68 and HLA-DR and are negative for CD3, CD4, CD14, CD19 and CD33 [128]. KG-1 cells were established as an acute myelogenous leukaemia, of granulocytic phenotype that grows in suspension and expresses HLA-A30 and HLA-B35 [129]. Importantly, KG-1 cells do not express the SH2 domain containing phosphatase SHP-1 (Dr Isabelle Heinisch, University of Edinburgh, UK, personal communication).

Examination of CD31 surface expression by flow cytometry revealed all cell lines express CD31 (Figure 2.2:4), KG-1 and MM6 exhibited greater fluorescence as compared with isotype controls, suggesting higher overall CD31 surface expression. The standard attachment assay showed that the U937 cells exhibited greatest attachment to the THP-1 compared with CD31 positive Jurkats, KG-1 and MM6 cells (Figure 2.2:5) (n=3, p=0.001). The KG-1 and MM6 cell line showed attachment levels similar to CD31 positive Jurkats.

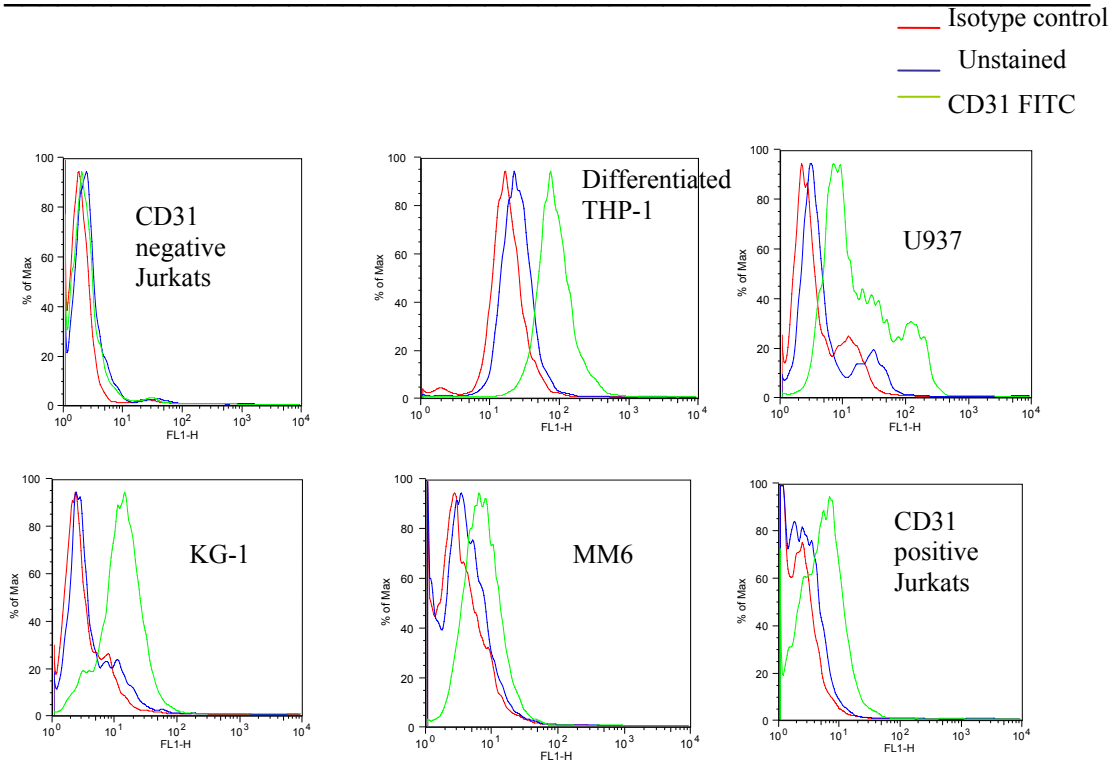

Figure 2.2:4. Expression of CD31 on different cell lines. FITC conjugated CD31 mouse anti-human was used to label the different leukemic cells lines and binding assessed by flow cytometry. Controls included unstained cells and an isotype control of mouse IgG_1-FITC. All cell lines, with the exception of CD31 negative Jurkats, express CD31 on their surface relative to isotype control IgG1 binding.

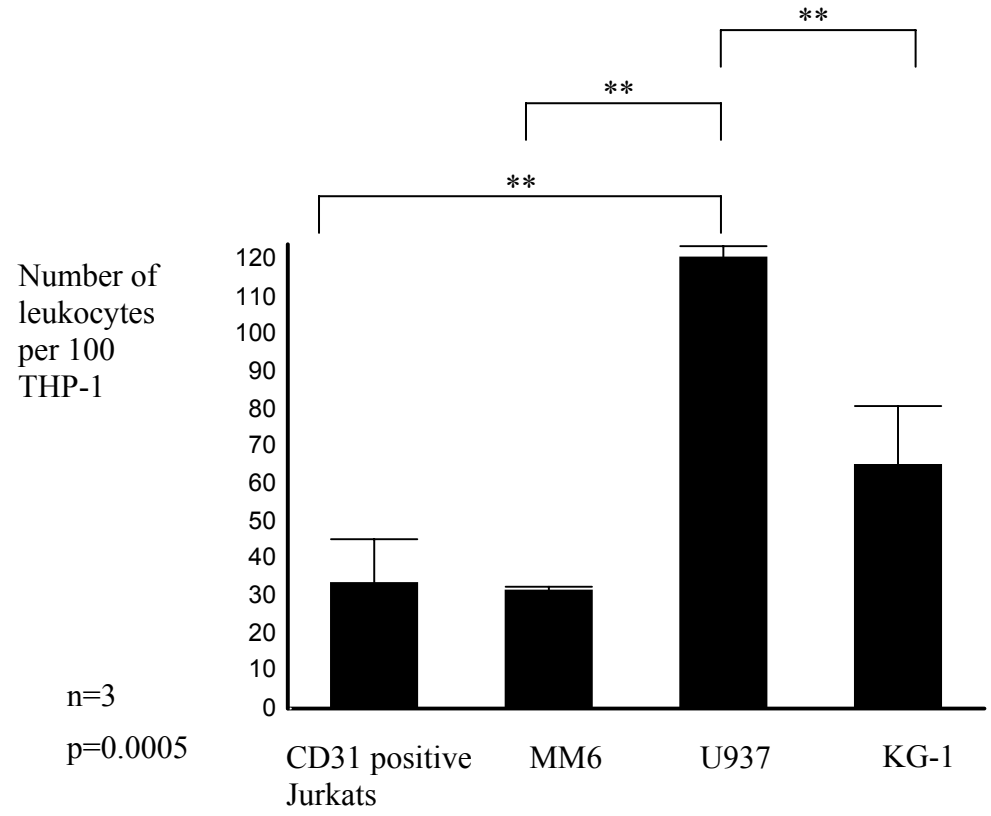

Figure 2.2:5. U937 exhibit the most attachment to the THP-1 than CD31 positive Jurkats, MM6 and KG-1 under standard assay conditions (p=0.0005, n=3).

2.2.3 *Leukaemic Cell Line Room Temperature Detachment Assay*

Although the initial experiments show the leukemic cell lines capable of interacting with the THP-1, and of note the dependence of the Jurkats on CD31 to mediate this interaction, the initial numbers of cells tethered at room temperature was not measured. The number of cells binding at the room temperature settling step provides information relating to the ability of the leukemic cell to interact with the THP-1, and therefore to detach at 37˚C. To overcome this and provide an indication of the initial interaction between the leukocyte and the THP-1, the detachment assay was carried out with all steps at 20˚C, including the inversion step where gravity provides the detaching force.

Comparison between the standard assay and the room temperature assay showed U937 exhibited low levels of attachment at 20˚C and increased attachment at 37˚C, (Figure 2.2:6) (n=3, p=0.093) suggesting that raising the temperature promotes the adhesion of the cells to the THP-1. However, the standard and room temperature assay revealed similar levels of attachment of MM6 cells under both conditions (Figure 2.2:7) (n=3, p=0.574). KG-1 cells also show similar levels of attachment with the standard and room temperature assay (Figure 2.2:8) (n=3, p=0.2951), suggesting that the temperature of the assay does not affect the ability of the leukocyte to adhere to the THP-1.

The initial tethering at room temperature of CD31 positive Jurkats was compared with the standard assay (Figure 2.2:9). The CD31 positive Jurkats were found to exhibit temperature-dependent attachment as shown in previous work (n=3, p=0.037)

[84]. CD31 negative Jurkats do not exhibit this temperature-dependent effect (Figure 2.2:10), implying the alternative attachment mechanisms allowing adhesion of the CD31 negative Jurkat to the THP-1 are not dependent on the temperature.

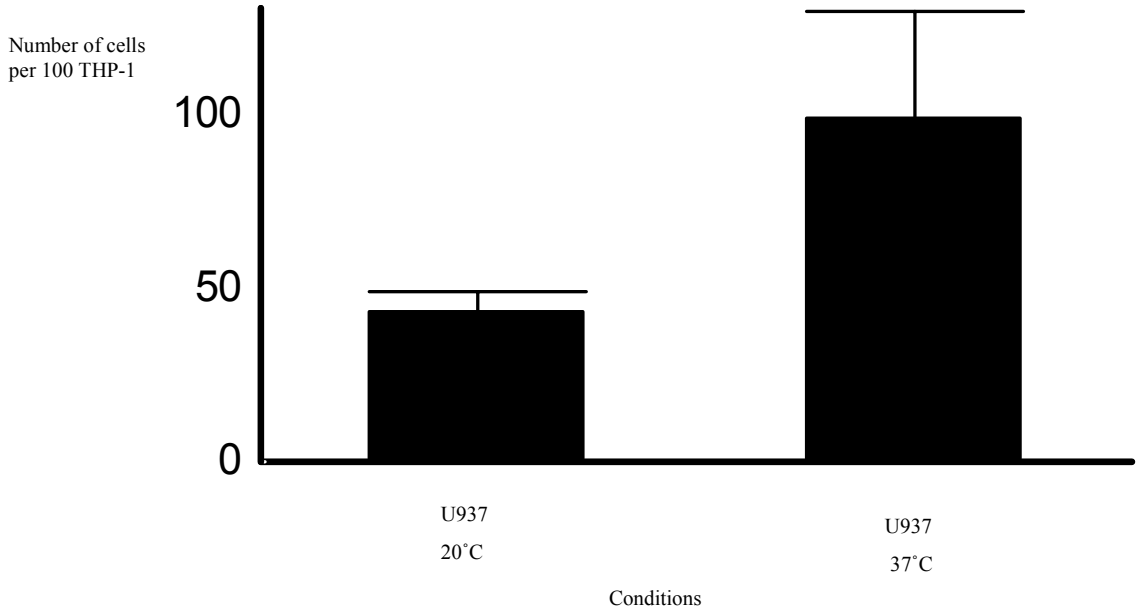

Figure 2.2:6. U937 exhibit lower levels of attachment at room temperature, compared with increased amount of attachment under standard conditions, (p=0.0931, n=3).

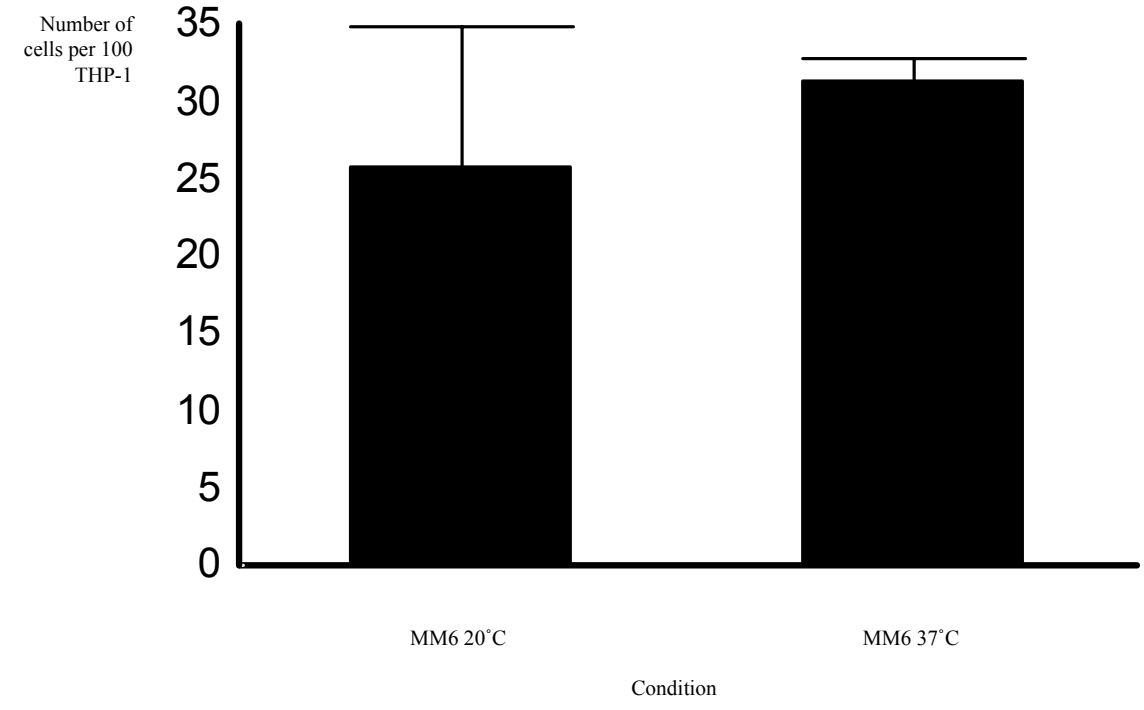

Figure 2.2:7. MM6 show similar levels of attachment at room temperature and under standard conditions, (p=0.5474, n=3).

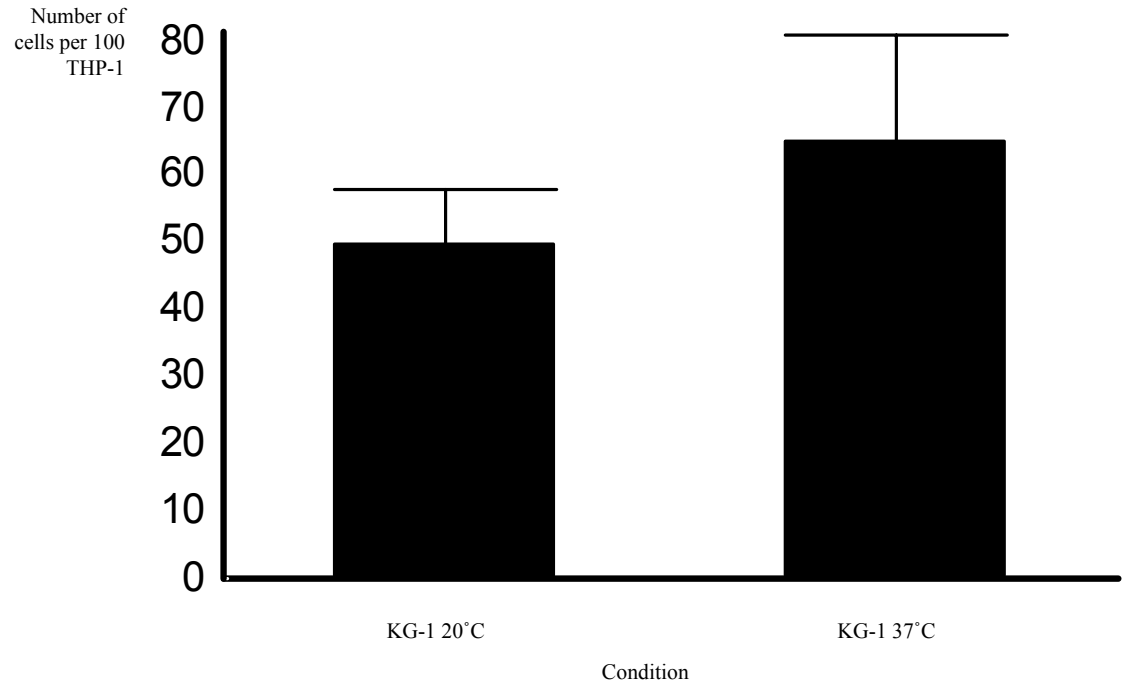

Figure 2.2:8. KG-1 show similar levels of attachment at room temperature and under standard conditions, (p=0.2951, n=3).

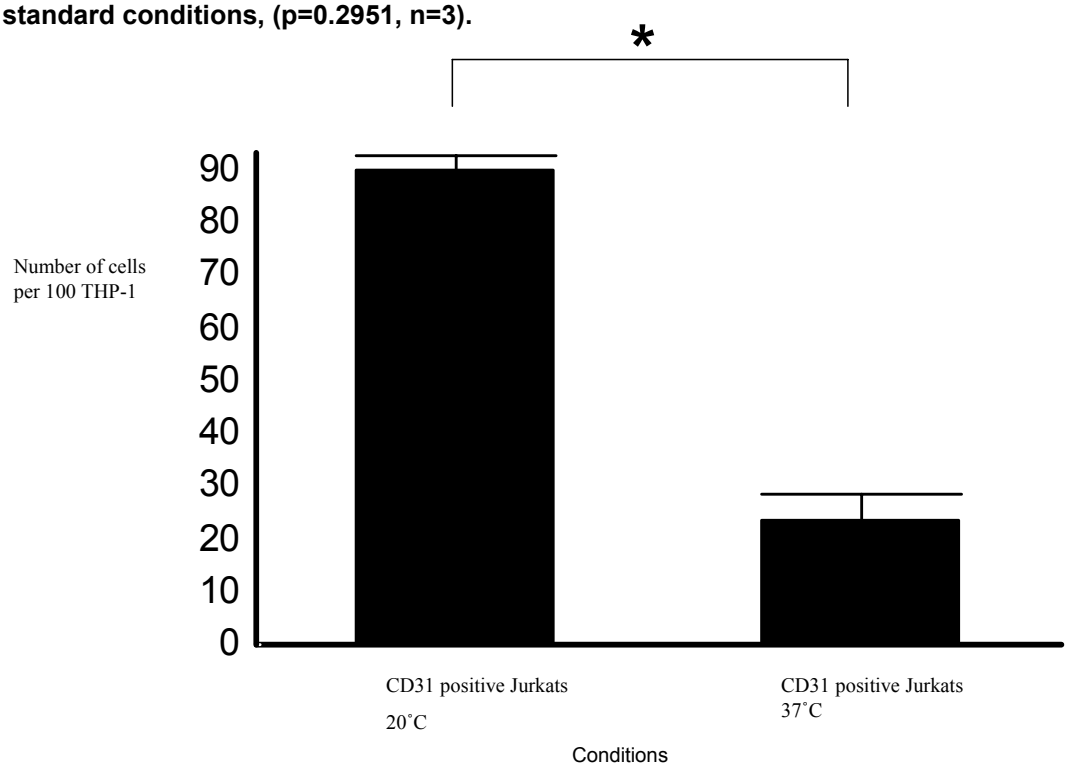

Figure 2.2:9. Attachment of CD31 positive Jurkats is increased at room temperature compared with lower attachment under standard conditions (p=0.0367, n=3).

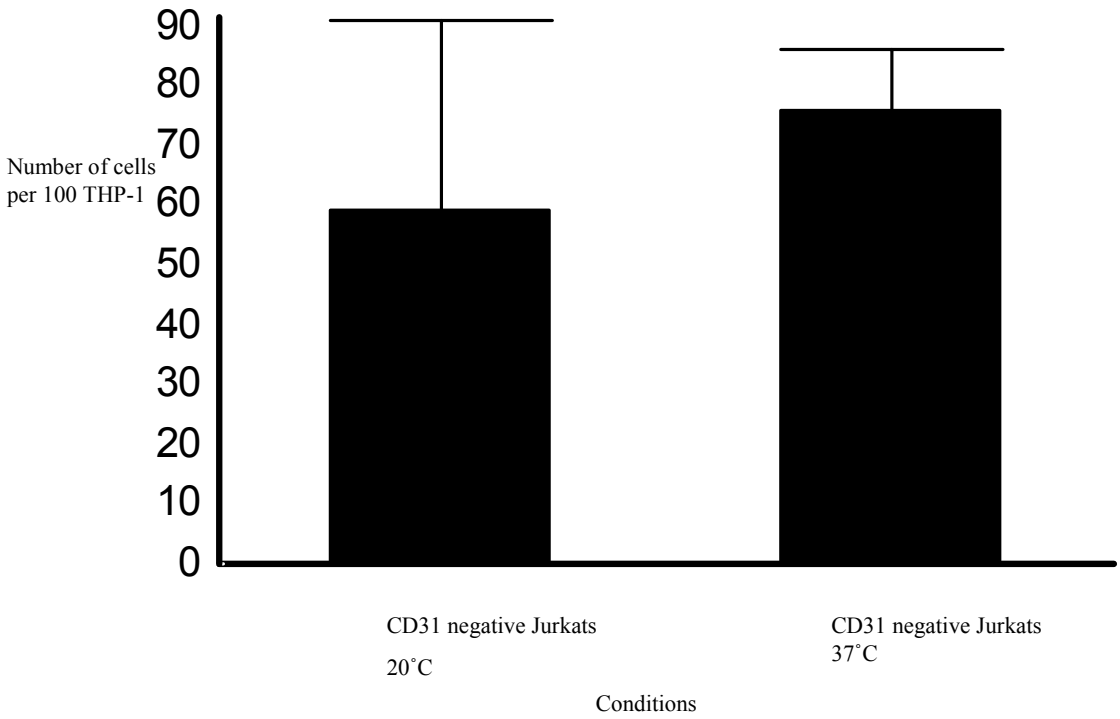

Figure 2.2:10. Attachment of CD31 negative Jurkats at room temperature is similar to attachment under standard conditions, (p=0.611, n=3).

2.2.4 *ITIM Mutant Jurkat Attachment*

Stable cell lines of CD31 transfected Jurkats with mutations in the cytoplasmic domain at ITIM tyrosines 663 (Y663F), 686 (Y686F) and both 663 and 686 (Y663F/Y686F)[2] were also used as the target leukocyte to examine the potential effect of tyrosine phosphorylation of the cytoplasmic domain of CD31 in mediating detachment signals (Figure 2.2:11) (n=3, p=0.0431). Using the standard assay, Y663F Jurkats showed similar levels of attachment to THP-1 as the wild-type CD31 positive Jurkats. Tyrosine 663 has previously been shown to be important for SHP-2 activation, whereas tyrosine 686 is important for binding of SHP-2, so with the Y663F point mutant, SHP-2 was still able to bind, and potentially bind downstream effectors participating in downstream signalling. Y686F Jurkats exhibited slightly more attachment to the THP-1 than wild-type or Y663F Jurkats. However, the greatest effect was observed with the Y663F/Y686F double mutant, which showed the greatest attachment. This finding therefore demonstrates the ITIM is essential for mediating detachment of viable leukocytes from macrophages, as without the ITIM, the cells remain pro-adhesive to the THP-1.

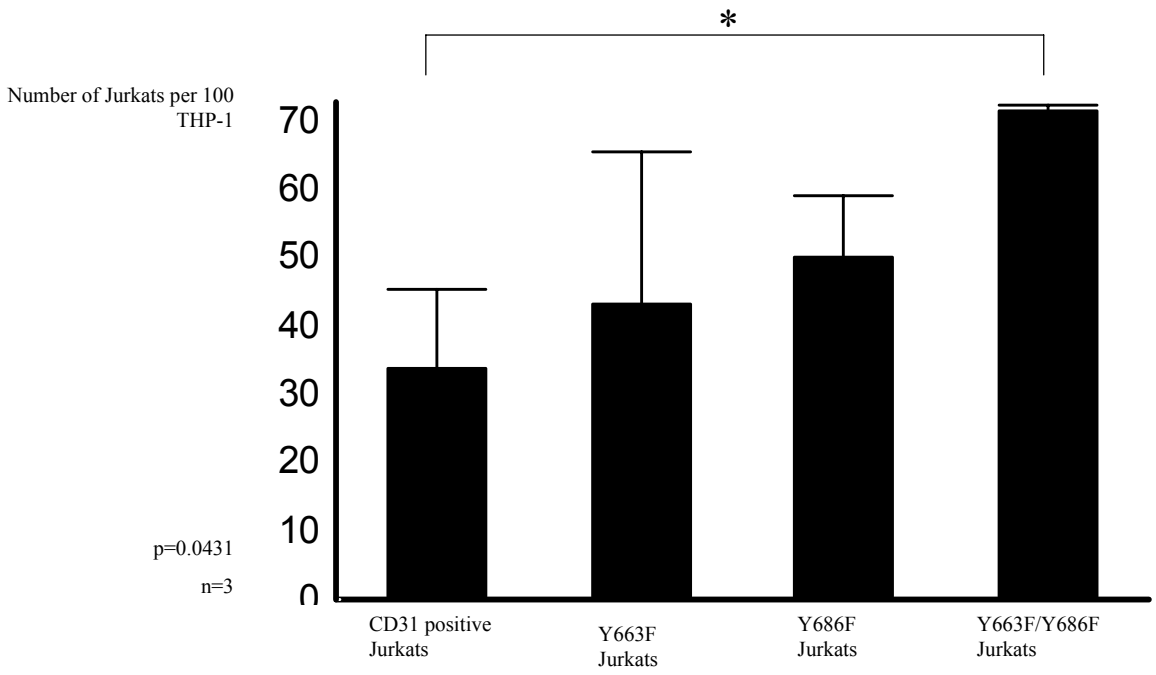

Figure 2.2:11. Y663F/Y686F Jurkats exhibited the greatest level of attachment to the THP-1 compared with the CD31 wild type Jurkats using the standard assay, (p=0.0431, n=3).

2.2.5 *Temperature Dependent ITIM Mutant Jurkat Attachment Assay*

As a temperature dependent attachment was demonstrated by CD31 positive wild-type expressing Jurkats, performing the assay with ITIM mutant Jurkats and all steps at room temperature may dissect the downstream signalling pathway involved in maintaining cellular attachment.

A temperature dependent effect was observed with Y663F mutant Jurkats, similar to the effect observed with wild type CD31 expressing Jurkats. With the room temperature assay, more cells bound to the THP-1 monolayer when compared with the standard assay. This observation demonstrated that subsequent detachment under gravity was likely to be independent of SHP-1 binding to CD31, as SHP-1 binding to CD31 requires the presence of both ITIM tyrosines (Figure 2.2:12) (n=3, p=0.021). With Y686F mutant Jurkats, there was little difference in attachment between the room temperature and standard assay (Figure 2.2:13) (n=3, p=0.516), which implies Jurkat detachment requires SHP-2 binding to CD31, as SHP-2 binding is dependent on intact tyrosine 686. Attachment of Y663F/Y686F mutant Jurkats was also similar between the room temperature and standard assay (Figure 2.2:14) (n=3, p=0.875), supporting the notion that the ITIM tyrosines and binding partners are required as part of the downstream signalling pathway leading to detachment of the viable cell.

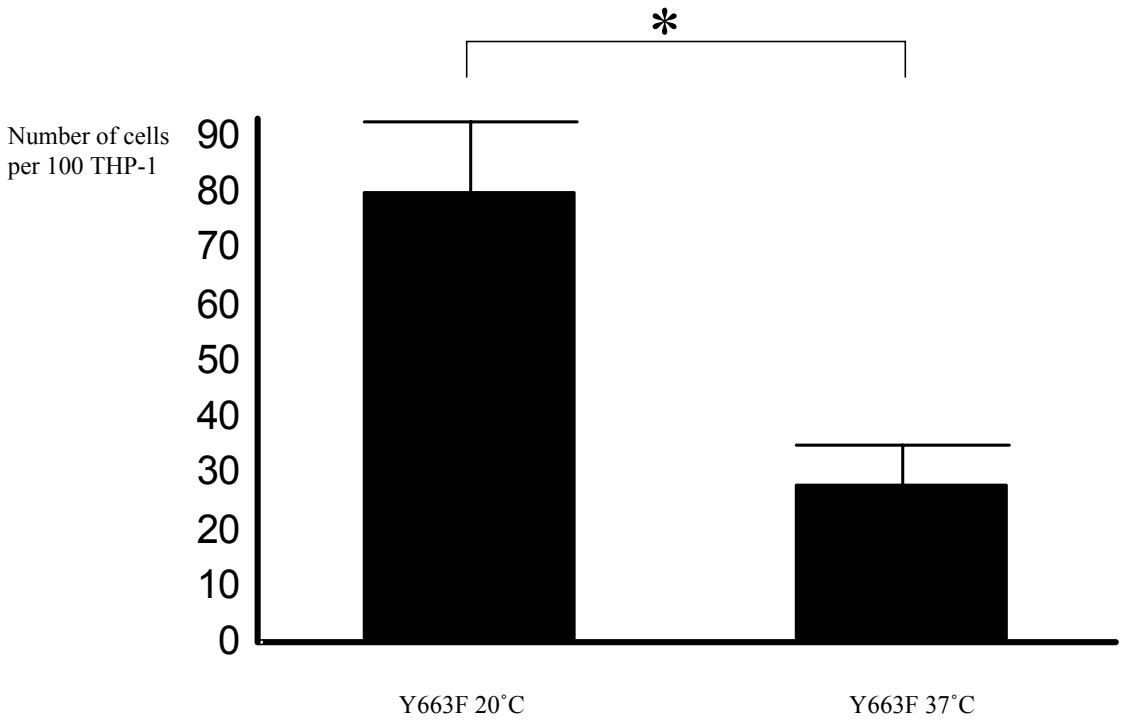

Figure 2.2:12. Y663F mutant Jurkats exhibit temperature dependent attachment to the THP-1 showing tyrosine 663 is dispensable for CD31 downstream signalling (p=0.021, n=3).

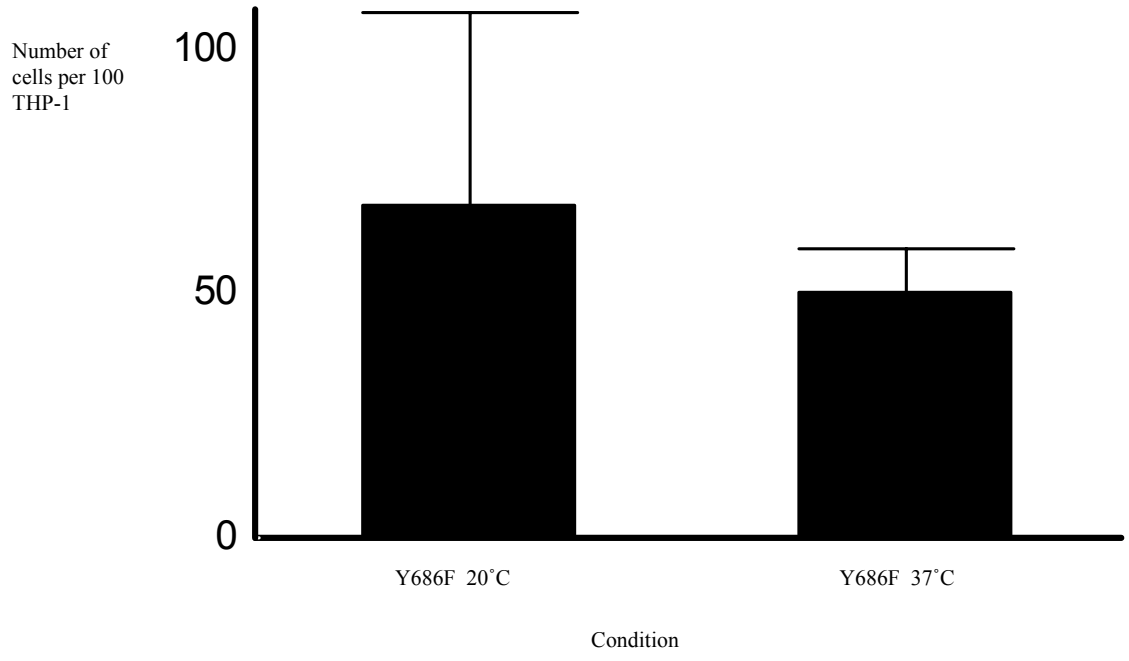

Figure 2.2:13. Y686F mutant Jurkats exhibit similar levels of attachment compared between room temperature and standard assay showing tyrosine 686 is required for SHP-2 binding and subsequent signalling (p=0.516, n=3).

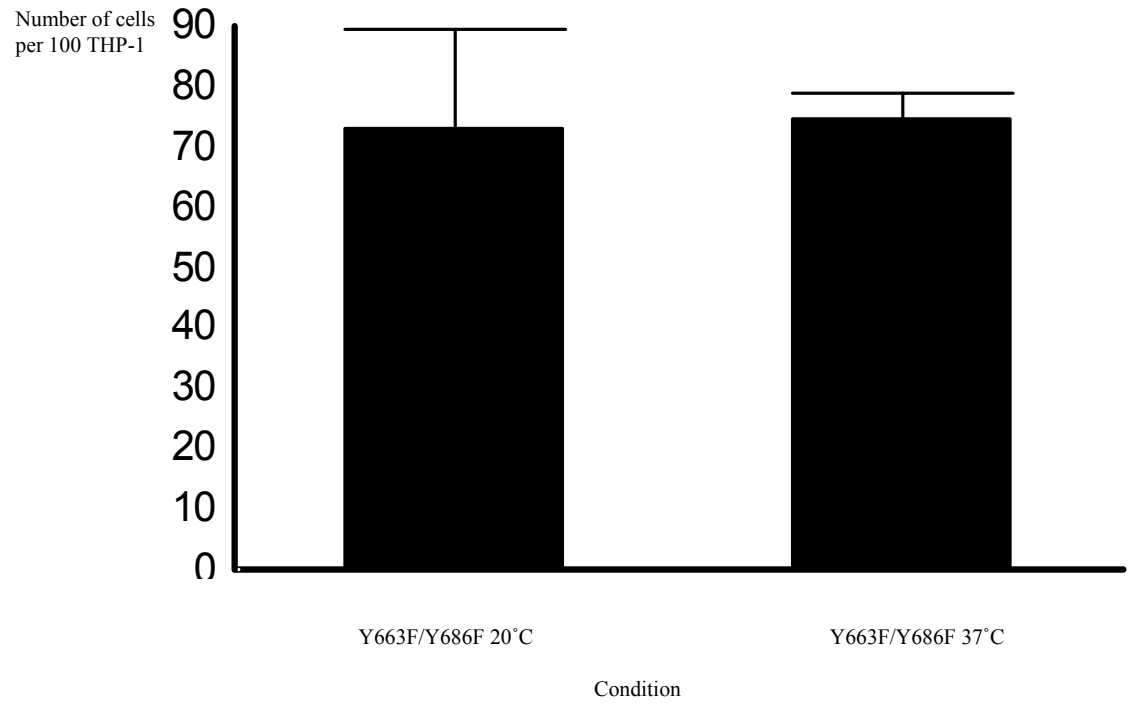

Figure 2.2:14. Y663F/Y686F Jurkats show similar levels of attachment to the THP-1 compared between room temperature and standard assay (p=0.8746, n=3), implying a role for the ITIM and downstream signalling effectors.

2.2.6 *Stibogluconate Treatment of CD31 Positive Jurkats*

SHP-1 and SHP-2 phosphatases have both been shown to bind to the cytoplasmic domain of CD31 [57,130]. To directly examine the role of SH2 phosphatases in detachment, and specifically the activation and role of the phosphatase domain, CD31 wild-type Jurkats were treated with sodium stibogluconate, a drug used in the treatment of leishmaniasis which inhibits only the catalytic activity of the phosphatases, but not their binding to CD31. Sodium stibogluconate inhibits SHP-1, SHP-2 and PTP1B. Previous studies indicate that at 10µg/ml, only SHP-1 will be targeted [131]. In this series of experiments, all assays were performed under standard conditions, with room temperature settling and inversion at 37˚C. Drug treatment did not affect the cell viability as assayed by annexin V/propidium iodide staining as described in Materials and Methods. Treatment with 10µg/ml sodium stibogluconate gave somewhat variable results. However there was little difference in attachment of stibogluconate treated cells compared with untreated Jurkats (Figure 2.2:15) (n=5, p=0.636). At higher concentrations of stibogluconate (100µg/ml), SHP-2 has been shown to be inhibited [131]. Treatment of Jurkats with this higher concentration did not affect the attachment, although again there was the same inconsistency in the results from different experiments (Figure 2.2:16) (p=0.371, n=3).

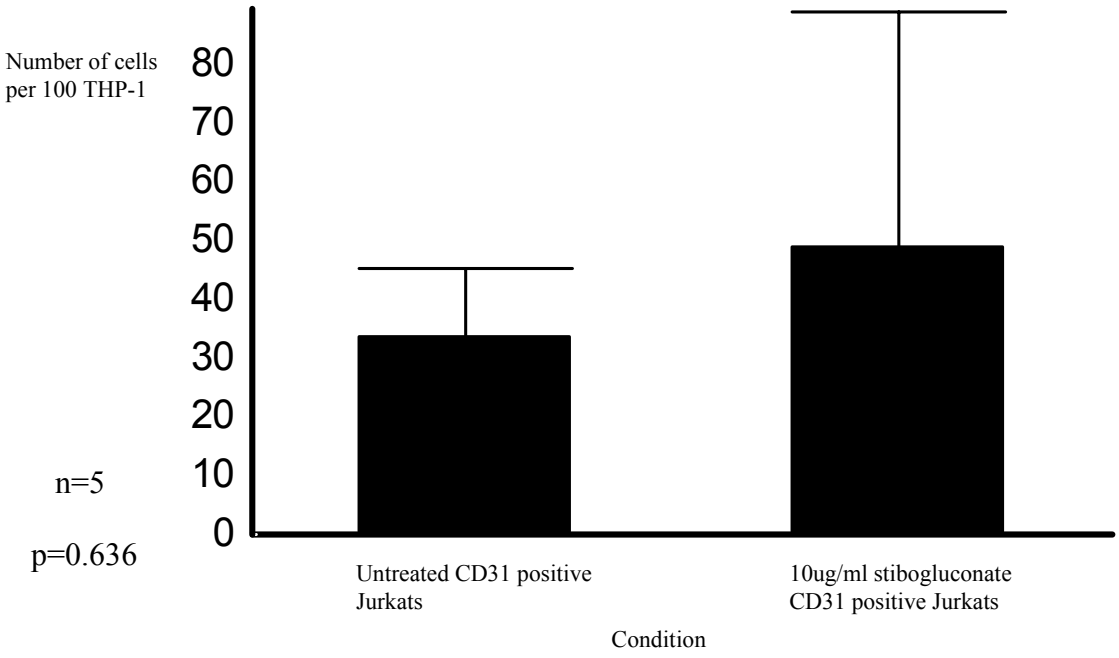

Figure 2.2:15. Stibogluconate treated CD31 positive Jurkats (10µg/ml) attachment under standard conditions remains unaffected compared with untreated Jurkats (p=0.636, n=5).

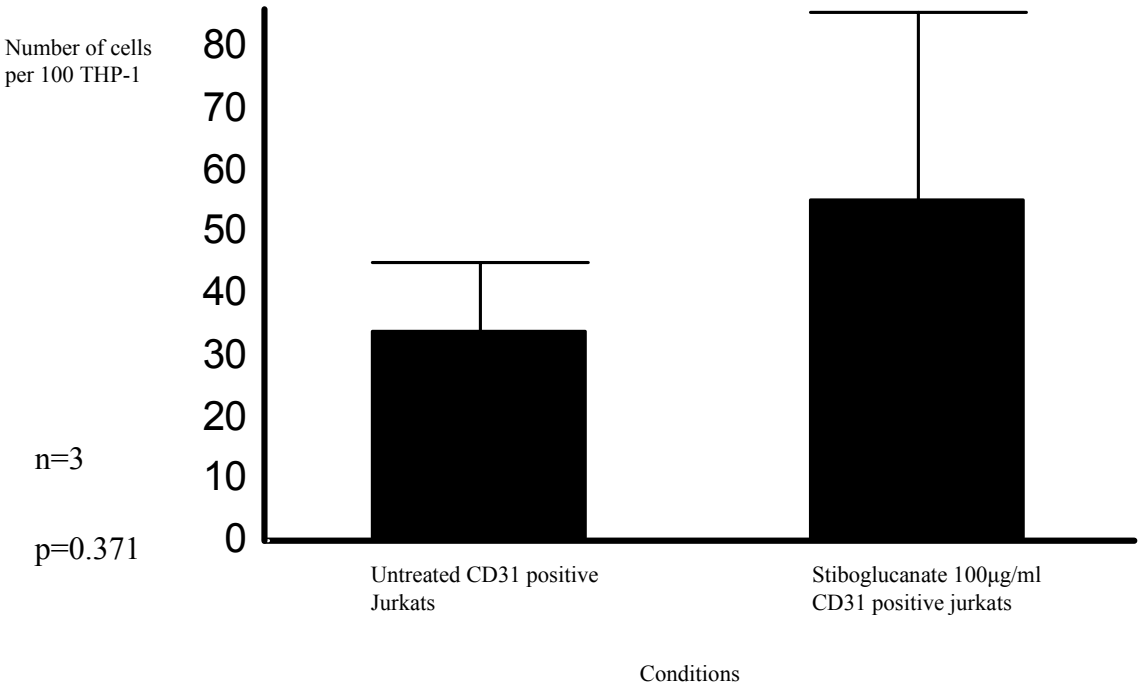

Figure 2.2:16. 100µg/ml stibogluconate treatment of CD31 positive Jurkats does not effect attachment under standard conditions (p=0.371, n=3).

2.2.7 *siRNA Knock-Down of SHP-2 in Jurkats*

RNA interference introduces double-stranded RNA into cells that is cleaved by Dicer into short 21 nucleotide sequences with an overhang of 2 bases at the 3' end. One strand of RNA is recognised by the RISC (RNA-induced silencing complex) and used to target the homologous sequence from the genome, thus targeting both for destruction by nuclease activity [132]. To target SHP-2, suspected as being involved in mediating detachment signals, for knock-down in Jurkats short-hairpin RNA (shRNA) constructs were generated for delivery into the cell by lentivirus.

As a pharmacological approach had been unsuccessful, a different approach to target SHP-2 was required. As SHP-2 is expressed in Jurkats, using siRNA to knock down SHP-2 expression could prevent the positive signalling through CD31, and therefore prevent detachment from macrophages. A SHP-2 sequence previously used to achieve knockdown in fibroblasts [133] was commercially produced (Dharmacon) and transfected into CD31 positive Jurkats by Amaxa electroporation. As a positive control a lamin A/C sequence produced by Dharmacon was used. The cells were harvested at 24, 48 and 72 hours post-transfection, lysed and assessed for protein expression of either SHP-2 or lamin A/C. There was a slight decrease in SHP-2 expression at 72 hours post-transfection observed with this method (Figure 2.2:17). Western blotting for lamin A/C also showed there to be some decrease in lamin A/C protein levels at 72 hours (Figure 2.2:18) (See Appendix for transfection troubleshooting). However, the decrease in protein expression observed was deemed insufficient to assess the effects of SHP-2 knockdown upon the ability of the Jurkat to detach from THP-1, so a different method of transfection of the siRNA was

sought. As electroporation induces cell death, lipid mediators were used. Both EPOCH and Dharmacon transfection reagents were used, but with no knock-down of either SHP-2 or lamin A/C detectable by Western blot (data not shown).

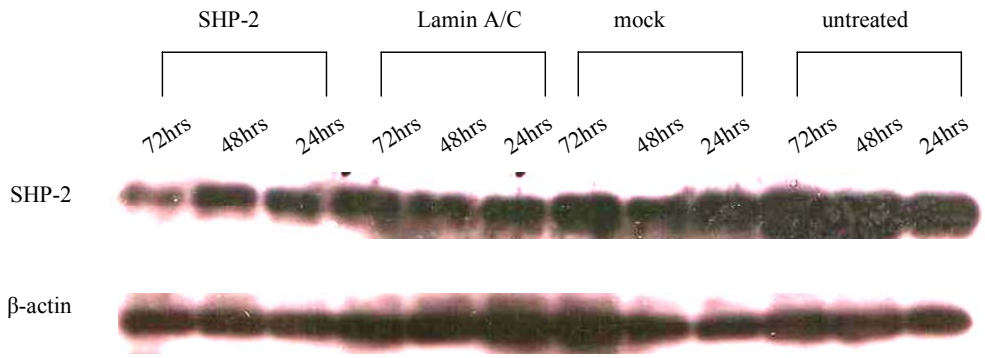

Figure 2.2:17. CD31 positive Jurkats transfected by Amaxa electroporation, untreated cells, electroporation only, SHP-2 RNA, or lamin A/C RNA were harvested at 24, 48 and 72hrs and probed for SHP-2, and loading control of β-actin.

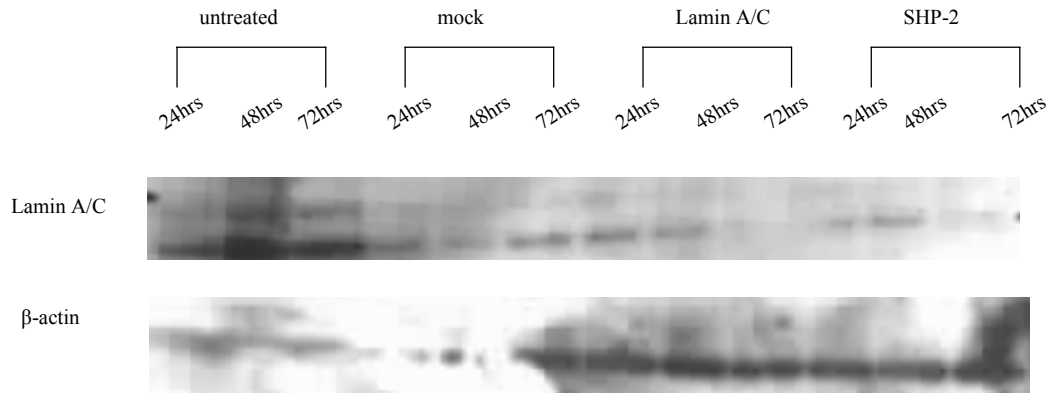

Figure 2.2:18. CD31 positive Jurkats transfected by Amaxa electroporation, untreated cells, electroporation only, SHP-2 RNA or lamin A/C RNA, harvested at 24, 48 and 72 hrs and probed for lamin A/C, and loading control of β-actin.

2.2.8 *Lentiviral Transduction*

Lentiviruses are a genus of the *Retroviridae* family, of which HIV-1 (human immunodeficiency virus-1) is a species utilised in the development of this technology. The viruses carry their genome as double-stranded sense RNA, and are capable of transcribing it to DNA once inside a cell. The virus particle contains reverse transcriptase, integrase and protease. The virus is surrounded by an envelope of host cell membrane, with the glycoprotein the only viral protein expressed on the surface. This glycoprotein interacts with the host cell surface proteins in order to infect the cell.

The genome contains *gag, pro, pol* and *env* genes required for virus replication. *gag* encodes the structural proteins, *pro* the protease required for cleaving *gag* and *gag-pol* and particle maturation, *pol* the reverse transcriptase and integrase required for transcription to DNA and integration into the host genome, and *env* encodes the glycoprotein expressed on the surface of the virion. Lentiviruses also encode accessory genes that regulate infectivity and replication.[134]

To infect a host cell, the virus binds to its receptor via the envelope glycoprotein, allowing fusion of the cell membranes and the introduction of the uncoated virus into the cytoplasm. The viral genome is then transported to the nucleus via the cell's nuclear transport system. The viral genome is reverse transcribed to DNA where it is stably integrated into the host cell genome (Figure 2.2:19).

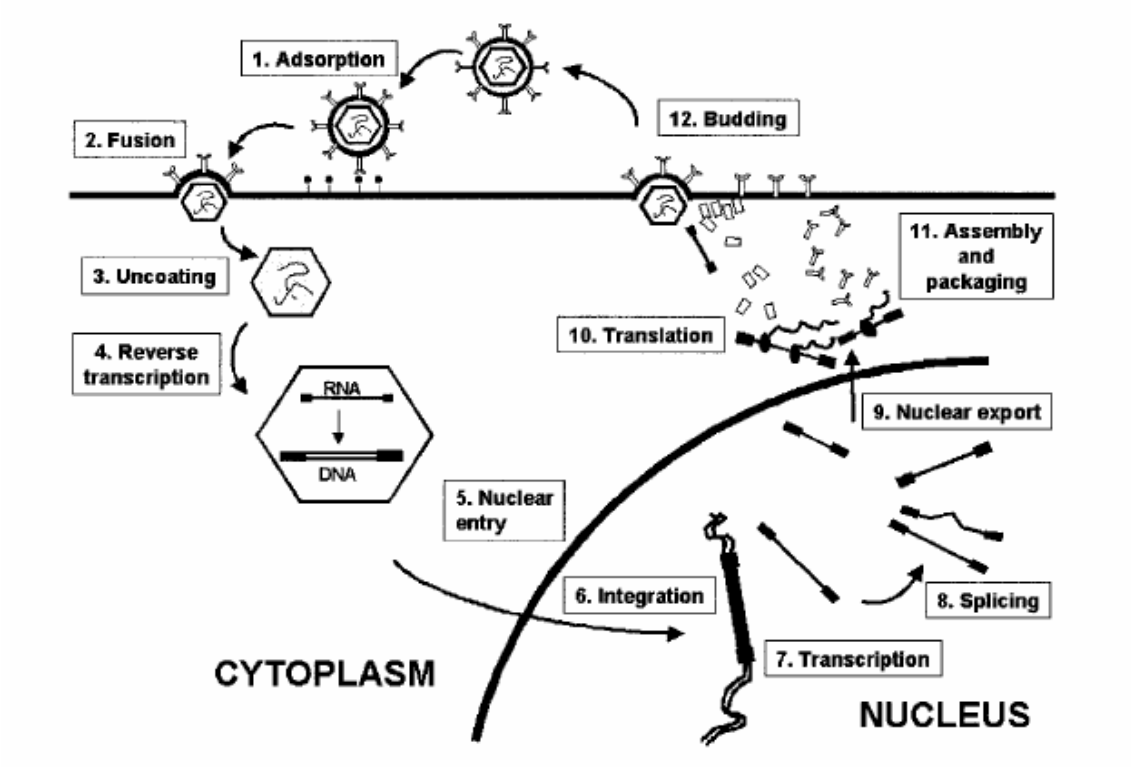

Figure 2.2:19 Retrovirus infection and replication cycle showing viral genome reverse transcription to DNA and integration into the cell's genome [134].

2.2.9 *Packaging and Transduction*

Once the insert of interest is cloned into the lentiviral vector, it is then ready to be packaged into virus particles. Third generation lentivirus vectors have been developed that have much reduced capacity of producing virions infective to workers, thus improving the biosafety. Two plasmids one containing the transgene and the other containing *gag, pol* and *env* (VSV-G *env* is used as it has a broad host range and can withstand concentration by ultracentrifugation) are transfected into the packaging cell line HEK 293T, developed from human embryonic kidney cells transfected with adenovirus E1 that activate the CMV promoter present in the transgene plasmid resulting in greater virus titre. HEK 293T cells are adherent and produce virus into the supernatant which can be harvested, and concentrated if desired [135]. The virus particles contain the transgene of interest and this can now be used to transduce the cells required.

2.2.10 *Proof of Concept Lentiviral Transductions*

CD31 positive Jurkats were transfected with a GFP EIAV (equine infectious anaemia virus) vector. The cells were then incubated under normal cell culture conditions for 48hrs before examination of GFP expression using a fluorescence microscope. The cells were transduced with nearly 100% efficiency (Figure 2.2:20). Jurkats were also transduced with pLenti Lac-Z, cells were incubated under normal cell culture conditions for 72 hours then stained with X-gal staining solution (as described in Materials and Methods) for a minimum of 3 hours before visualising under light microscopy show the cells can be transduced, albeit with a low efficiency (Figure 2.2:21). The titre of virus was not assessed and optimised for improved efficiency.

In view of these encouraging preliminary experiments that demonstrate the cells are able to be transduced, an siRNA construct for SHP-2 could be engineered into this system to target SHP-2 for future knock-down.

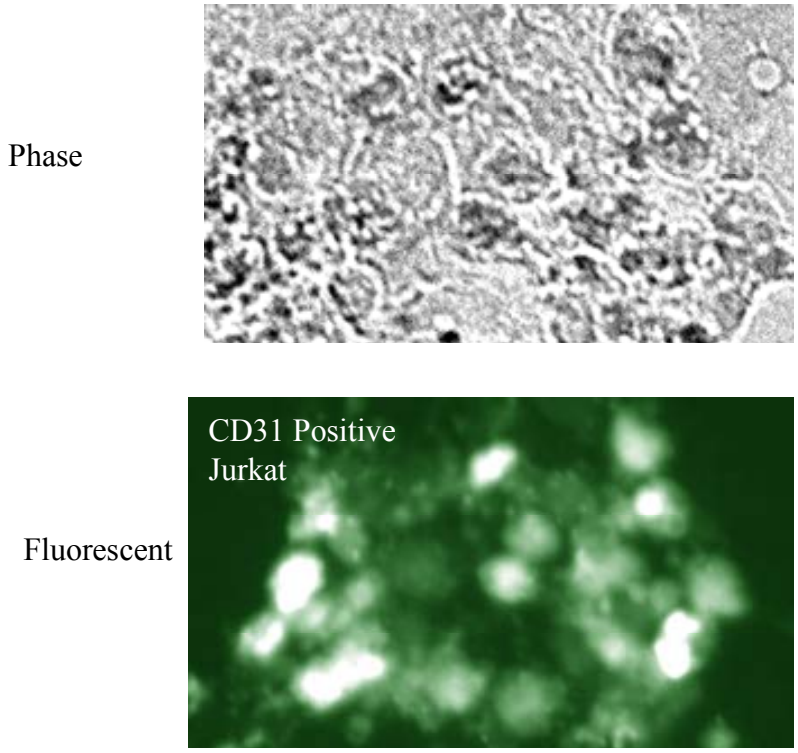

Figure 2.2:20. Transduction of CD31 positive Jurkats with EIAV-GFP lentivirus construct 48hrs post transduction shows high transduction efficiency.

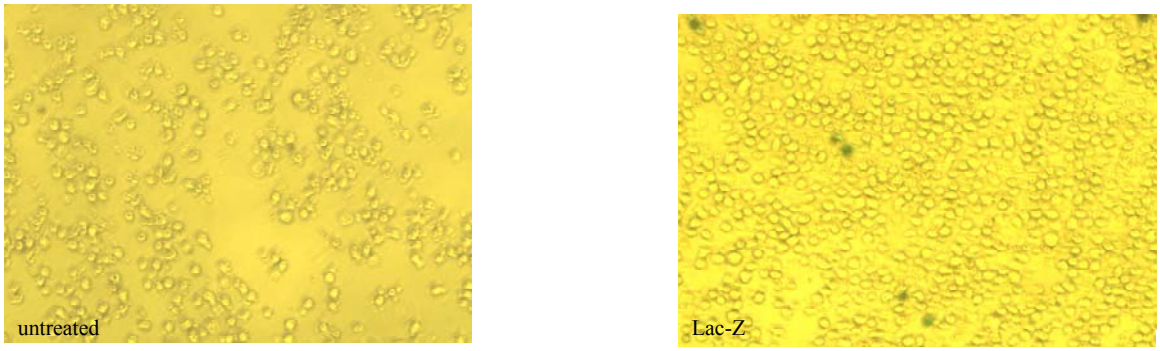

Figure 2.2:21. Transduction of CD31 positive Jurkats with Lac-Z-lentivirus at 48hours post transduction show the cells can be transduced but at low transduction efficiency.

2.3 Discussion

To study the role of CD31 in mediating viable leukocyte detachment from macrophages [84], a static assay was developed with the macrophage-like cell line THP-1, and leukemic cell lines U937, MM6, KG-1 and Jurkats stably transfected with CD31. This assay, in which cells were allowed to attach at 20°C and then detach at 37°C, revealed that there were low levels of binding of CD31 positive Jurkats and MM6 to the THP-1, whereas the U937 and KG-1 exhibited greater levels of binding. However, since this assay only quantified the cells that remained bound after inversion at 37˚C, it did not provide information relating to the initial binding signal when the chamber slide was incubated at 20°C, thus the assay was repeated with all steps at 20°C and compared with results when inversion was performed at 37°C. In previous studies, a difference in the number of cells bound would indicate a temperature dependent attachment effect.

MM6 cells did not exhibit temperature dependent attachment to THP-1. These cells have been shown to express CD38, which is a ligand for CD31. A study with MM6 showed that the CD31-CD38 interaction could be important for MM6 extravasation to sites of inflammation [136]. As THP-1 also express CD38, it could be that during the attachment assay, the MM6 are interacting with the THP-1 in a CD31-CD38 manner, which may not act to regulate adhesion in a temperature dependent way as suggested for homophilic CD31 interactions.

KG-1 cells also do not exhibit temperature dependent attachment when the inversion temperature was raised from 20˚C to 37˚C. These cells have been used as a model of

differentiated dendritic cells (DC) [137], so the interaction observed here may be more similar to that of an immature DC and a macrophage. In situ, interaction between immature DCs and macrophages in lymph nodes will be predisposed to be adhesive to allow communication of antigen and subsequent macrophage-induced maturation of the DC. So it is possibly more likely that the readily reversible adhesions required for observation of cellular detachment are more difficult to detect using KG-1 cells.

Monocytic–like U937 also do not exhibit temperature dependent attachment, in fact the cells became more adherent when the temperature was raised. It has previously been shown that U937 engage CD31 predominantly via $\alpha_v\beta_3$ in a heterotypic interaction together with a low level of homophilic CD31 binding. The study also showed a temperature-dependent adhesion (temperature range 37-4˚C) of the U937 to CD31 extracellular domain construct [9]. With the static attachment assay used here (temperature range 37-20˚C), we have shown a similar result, with more U937 adhering at 37˚C than at the lower temperature. This interaction may lead to a different signalling pathway in the U937 mediated by the integrin and not through CD31, which could lead to a more adhesive response through integrin activation.

In order to investigate the adhesive mechanisms described by the leukemic cell lines U937, KG-1 and MM6 further, antibody blocking studies could be used. Blocking the homophilic interaction of CD31 using monoclonal antibodies before performing the attachment assay may then shed light upon the involvement other molecules such as integrins.

CD31 negative Jurkats also were unable to exhibit temperature-dependent detachment, an observation which demonstrates that there was a CD31-independent

binding of Jurkats to THP-1 that is not temperature-sensitive. One unlikely possibility was that the population of cells that remain attached may not be viable, and could represent the apoptotic and necrotic cells in the culture. The differences observed between CD31 positive and CD31 negative Jurkats, and again with the Y663F/Y686F mutant Jurkats when compared with CD31 positive Jurkats could have been due to the different levels of death in these populations. However, as each cell population was growing well and had the levels of apoptosis and necrosis measured at each assay. The cells were found to be mostly viable, and the differences between each population was minimal, we were confident the differences in attachment were due to the properties of CD31, not due to differences in cell viability. Moreover, to overcome this, the population of cells could be depleted of PS expressing cells prior to the assay to remove apoptotic populations. This may have 'fine tuned' the assay and possibly improved the error between each assay. Alternatively, the temperature-insensitive binding could be due to firmer integrin-mediated adhesion, with CD31 on the THP-1 engaging β_1 integrins [138] on the Jurkat in the absence of CD31.

Jurkats stably transfected with full-length wild type CD31 exhibited less attachment to the THP-1 monolayer than CD31 negative Jurkats. This finding recapitulates previous work that CD31 mediates a detachment signal in the viable leukocyte [84], and prompted questions about which signalling and adapter molecules were binding to the cytoplasmic domain and how they were acting to drive the cell's motor machinery. SIRPα, an immunoglobulin superfamily member, binds SHP-2 via its ITIM and may be involved in a positive feedback loop to activate FAK and src

leading to MAPK activation and migration [139]. It is therefore conceivable that CD31, which is an immunoglobulin superfamily member containing an ITIM could engage similar signalling pathway following binding that would result in increased cell migration.

Utilising Jurkats provided a model leukocyte that could be genetically modified with mutations to the cytoplasmic domain of CD31 at key tyrosine residues 663 and 686 [59]. CD31 positive Jurkats with mutations in ITIM tyrosines 663, 686 and both 663 and 686 were used as viable leukocytes in the attachment assay. Only the Y663F/Y686F mutant Jurkat showed increased attachment when compared with CD31 wild-type and with the single Y663F and Y686F mutants. This observation suggests that the ITIM was essential for mediating the signals required for leukocyte detachment, and that mutating single tyrosines on their own did not have this effect. One implication of these data is that the signalling and adapter molecules are able to bind to either of the tyrosines present in the cytoplasmic domain. The SH2 domain containing phosphatase SHP-2 has been shown to bind to CD31 and transduce motility signals through binding to the ITIM tyrosines[59].

The assay was repeated at room temperature to assess initial binding of the Jurkats to the THP-1. Y663F mutant Jurkats were also found to exhibit temperature dependent attachment; since SHP-2 requires tyrosine residue 686 on CD31 for binding. SHP-2 is still able to bind to tyrosine 686 independently of tyrosine 663. Detachment may therefore be possible even in the absence of SHP-2 activation, as this has been shown

to require tyrosine 663 [60]. In contrast, the Y686F mutant did not show temperature dependent attachment. One interpretation of this data is that SHP-2 is unable to bind to the cytoplasmic domain of CD31 and provide a docking site for downstream signalling molecules. The Y663F/Y686F mutant Jurkat also does not show temperature dependent attachment, again recapitulating previous work in this laboratory [84], and strongly suggests that in the absence of the cytoplasmic ITIM motif, CD31-mediated motility is disabled.

As SHP-2 is able to bind to the ITIM of CD31, it is conceivable that the regulation of adhesion is initiated by SHP-2 acting as a docking protein. SHP-2 binding would be predicted to influence downstream signalling following this interaction. If SHP-2 was unable to bind to the cytoplasmic domain of CD31 because of mutation of the ITIM, the signalling pathway leading to disruption of adhesions may not occur, which could explain why the Y663F/Y686F Jurkat exhibited impaired detachment.

To explore the possibility of SH-2 domain containing phosphatases binding to the cytoplasmic domain of CD31 and exerting their catalytic activity by dephosphorylating substrates involved in downstream signalling, CD31 positive Jurkats were treated with the anti-leishmaniasis drug sodium stibogluconate. The drug specifically inhibits the catalytic activity of SHP-1 and SHP-2 and the inhibition does not require the SH-2 domain or C-terminal region. At a concentration of 10µg/ml SHP-1 catalytic activity is specifically inhibited, whereas at 100µg/ml SHP-2 activity is also inhibited. At both concentrations there was no difference in the levels of attachment observed for untreated and stibogluconate-treated cells, which

suggested the catalytic activity of SHP-1 and SHP-2 was not necessary for mediating downstream detachment signals.

One caveat to these experiments is that the efficiency of the drug treatment was not measured by assessing SHP-1 or SHP-2 phosphatase activity within the treated cells. There was some variability in the effects of stibogluconate treatment upon cell attachment. One possibility is that stibogluconate did not achieve consistent phosphatase inhibition. Further experiments would be necessary to test this possibility, for example using a range of stibogluconate concentrations and then measuring the activity of the phosphatases by phosphatase assay.

SH-2 domain containing phosphatases have been shown to have a critical role in signalling during cell migration. SHP-2 is involved in integrin-mediated adhesive signals. Fibroblasts negative for SHP-2 exhibited decreased ability to migrate and spread. This adhesion defect was rescued upon transfection of the fibroblasts with wild-type SHP-2. In focal adhesions, FAK and SHP-2 may work concurrently, with SHP-2 phosphatase activity deactivating FAK and thus allowing FAK regeneration and focal adhesion turnover throughout the process of cell migration [140]. A catalytic mutant of SHP-2 expressed in human carcinoma acted to reduce integrin-mediated activation of MAPK and consequently cell spreading. Consistent with this observation, neutralising SHP-2 activity decreases migration and is associated with an increase in formation of stable focal adhesion contacts [141].

Transfecting CHO cells with a catalytic mutant of SHP-2 were demonstrated to alter the cell morphology and reduced cell polarity. Transfected cells had increased numbers of actin stress fibres and focal adhesion contacts [142]. SHP-2 activity may

act to regulate focal adhesion turnover by dephosphorylating tyrosine phosphorylated substrates, and disruption of this activity by mutation may inhibit the disassembly of established focal contacts. Thus, recruitment of SHP-2 to focal adhesions may represent a mechanism for monitoring focal adhesion events and controlling the strength of adhesion to allow the cell to migrate [142].

SHP-2 has been shown to be involved in signalling pathways through receptor tyrosine kinases, such as Met, and has the ability to serve as a docking protein for Gab1. Met becomes phosphorylated and binds Gab1 on a specific tyrosine residue. Gab1 itself becomes tyrosine phosphorylated and provides binding sites for other downstream signalling molecules, including SHP-2 [143]. Gab1 is then able to bind the SH-2 domain of Crk II. This molecule binds to DOCK180 which together with ELMO acts as an guanidine exchange factor for Rac, leading to activation. Activated Rac has been shown to destabilise adherens junctions in MDCK cells [144].

In order to probe the role of SHP-2 in detachment we attempted to knock-down SHP-2 expression in CD31 positive Jurkats to examine the effect of this on the ability of the Jurkat to attach to the THP-1. Various methods of transfection of SHP-2 siRNA were attempted including electroporation and lipid mediators all without success. Electroporation resulted in a reduction in viable cell number and low transfection efficiency, whereas lipid mediators failed to increase transfection efficiency despite improving transfected cell viability.

As an alternative approach, retrovirus technology could be used to introduce the RNA into the cell. In particular, lentiviral plasmids have been developed to enable cloning of the sequence of interest into this system and transfected along with the vector containing the genes for virus replication, which by homologous recombination generates a vector with the sequence of interest plus the ability to make virus. This vector is then transfected into a packaging cell line, allowing production of virus containing short hairpin RNA (shRNA). When this virus is then transfected into the cell line of interest the shRNA is transcribed and is recognised by Dicer, an RNAse that cleaves the hairpin into small 21-23 nucleotide fragments; these are the small interfering RNAs (siRNA). The siRNAs are incorporated into the RISC complex, which unwinds and then guides the siRNA to its complementary mRNA. The endogenous mRNA is then destroyed and translation of the protein does not occur [145].

Due to the complexity of designing and engineering the siRNA constructs, time constraints precluded our ability to use these constructs experimentally. However, if the constructs were available, one would expect the knock-down of SHP-2 in CD31 positive Jurkats to impair the detachment of Jurkats from THP-1. As postulated the knock-down of SHP-2 expression would prevent SHP-2 acting as a docking protein for the recruitment of downstream signalling and adapter molecules to CD31.

As this work has been with cell lines, it would be interesting to confirm the findings *in vivo*. A model of macrophage-leukocyte interactions has previously been used in the laboratory, where mouse thymocytes are introduced into the greater omental lymphoid organ (GOLO), and recovered by lavage after a set time point. As was

previously shown with this model, more thymocytes from CD31 wild-type mice were recovered than from knock-out mice, when injected as a mixed population into wild type mice (Dr Simon Watson, personal communication, University of Edinburgh, UK), confirming previous results with the *in vitro* flow chamber model [84], and with work presented here, that CD31 is required for viable leukocytes to detach. This model could be adapted to introduce reconstituted knock-out leukocytes with either mutations in CD31 itself, or knock-down potential targets such as SHP-2 from CD31 positive leukocytes.

In summary, for viable leukocytes to actively detach from macrophages when bound via CD31, the leukocyte appears to require the ITIM of CD31 intact. This is most probably in order to recruit the signalling and adapter molecule SHP-2, which may initiate a downstream signalling pathway that culminates in the activation of cellular motor machinery.

3 GST Pulldowns

3.1 Introduction

3.1.1 *SHP-1 and SHP-2*

In addition to mediating homophilic interactions between cells, it has become apparent that CD31 also participates in intracellular signalling. In platelets, full-length CD31 participates in cell signalling by binding SHP-2, an SH2 domain containing phosphatase. Upon further investigation, CD31 phosphopeptides encompassing residues 658-668 and 681-691 were found to bind SHP-2 [130].

Several signalling proteins have previously been shown to bind to the cytoplasmic domain of CD31. A study using BIAcore analysis showed the SH2 domains of SHP-1, SHP-2, SHIP and PLC-γ bind CD31. SHP-2 binds CD31 preferentially via Y663, whereas SHIP binds via Y686. Binding of SHP-1 and PLC-γ to CD31 required both tyrosines [63].

The binding of SHP-1 and SHP-2 phosphatases is required for CD31-mediated B cell receptor regulation. When lysates from DT40 chicken B cells were incubated with phosphopeptides of the cytoplasmic domain of CD31, only tyrosine phosphorylated phosphopeptides bound SHP-1 and SHP-2; and binding was shown to be dependent on both ITIM tyrosines [62].

3.1.2 *Rho GTPases*

Rho family GTPases are involved in cell motility by modulating the actin cytoskeleton. Rac can also activate Rho, and it is likely that Rho GTPases regulate motility by acting as molecular switches. In fibroblasts Rho supports the production of stress fibres, and Rac the production of lamellipodia. Ras has also been shown to

be involved in regulating stress fibres and focal adhesions, and may regulate Rho through RasGAPp120 association with RhoGAPp190 [146]. A mechanism for the regulation of migration of endothelial cells was recently described [61] where CD31 influenced signalling through Rho, as CD31KO endothelial cells were found to have a defect in RhoGTP loading. Knocking down CD31 with siRNA in HUVEC also resulted in a decrease in levels of RhoGTP.

In endothelial cells, tyrosine phosphorylated β-catenin binds to CD31. In EOMA (haemangioendothelioma) cells, both CD31 and β-catenin was found to be tyrosine phosphorylated, allowing a complex with SHP-2 to be formed. This observation suggests that β-catenin dephosphorylation mediated by SHP-2 occurs on the CD31 scaffold. CD31 may modulate the phosphorylation and function of β-catenin as a reservoir of tyrosine phosphorylated β-catenin [65].

3.1.3 *Viable and Apoptotic Signalling*

In a flow-chamber system, both viable and apoptotic neutrophils adhered to macrophages at 20˚C, a temperature where cytoskeletal reorganisation was inhibited. When the temperature was raised to 37˚C, the viable cells actively detached from the macrophages, whereas the apoptotic cells remained attached. CD31 expressed on the surface of neutrophils was shown to mediate the interaction between the leukocyte and the macrophage. Viable Jurkat T cells stably transfected with a CD31 construct missing the ITIM tyrosines were also unable to detach, showing that fully-functional CD31 was required to transmit detachment signals, allowing the leukocyte to escape. CD31 on apoptotic leukocyte may be impeded from providing detachment signals

through the action of SHP-1 and SHP-2 phosphatases. SHP-1 did not constitutively associate with CD31, and SHP-2 was cleaved and did not bind the cytoplasmic domain upon pervanadate treatment [84]. The differential signalling in viable and apoptotic cells may account for the ability of the viable cell to escape engulfment.

During apoptosis of endothelial cells, CD31 was reported to be cleaved and then shed into the supernatant as a soluble extracellular fragment of 100kDa, leaving a truncated fragment of 28kDa comprising of a small portion of the extracellular domain, the transmembrane region and the cytoplasmic domain in the cell membrane. This truncated form was found to differentially associate with the cytoplasmic signalling molecule γ-catenin, but not with β-catenin, inhibit cell growth, and even promote apoptotic cell death when expressed in human colon carcinoma cells [92]. CD31 may therefore be recruiting different proteins in a viable cell compared with an apoptotic cell, and this provides an explanation as to why a viable cell is able to detach and an apoptotic cell is not able, and is therefore internalised.

3.1.4 *Experimental Approach*

To identify the proteins bound to the cytoplasmic domain of CD31, GST-CD31 fusion proteins were generated and used in GST pulldowns of viable CD31 negative Jurkat lysates. It was thought most appropriate to investigate the proteins that bind to CD31 in the viable cell initially, and then determine whether these interactions still hold true in an effete cell.

GST binds to glutathione with high affinity allowing the fusion proteins to be rapidly and specifically isolated together with potential binding candidates present in cell lysates; this is a common system that has been previously used in cell signalling studies of protein interactions [147]. Other high affinity interactions that could have been used included biotin-streptavidin and His-nickel. However, since the initial vectors containing the CD31 cytoplasmic domain used previously in the laboratory and by others (gift from Dr Michael Douglas, Birmingham University, UK) included an N-terminal GST tag, it was decided to make all constructs in this manner. Attempts were initially made to produce a cytoplasmic domain construct with an N-terminal biotin tag, but this was unsuccessful.

3.2 Results

Lysates from CD31 negative Jurkats were used in subsequent analysis unless stated otherwise to avoid substrate competition with endogenous CD31. All CD31 cytoplasmic domain constructs were produced (see Appendix for details of construction, induction and purification) with an N-terminal GST tag. The recombinant proteins were full length CD31 cytoplasmic domain, and point mutations at ITIM tyrosines Y663, Y686, Y663/686, and tyrosine 701 to phenylalanine and serine 620, 669, 673 and 702 to alanine mutant (QSA) (Figure 3.2:1).

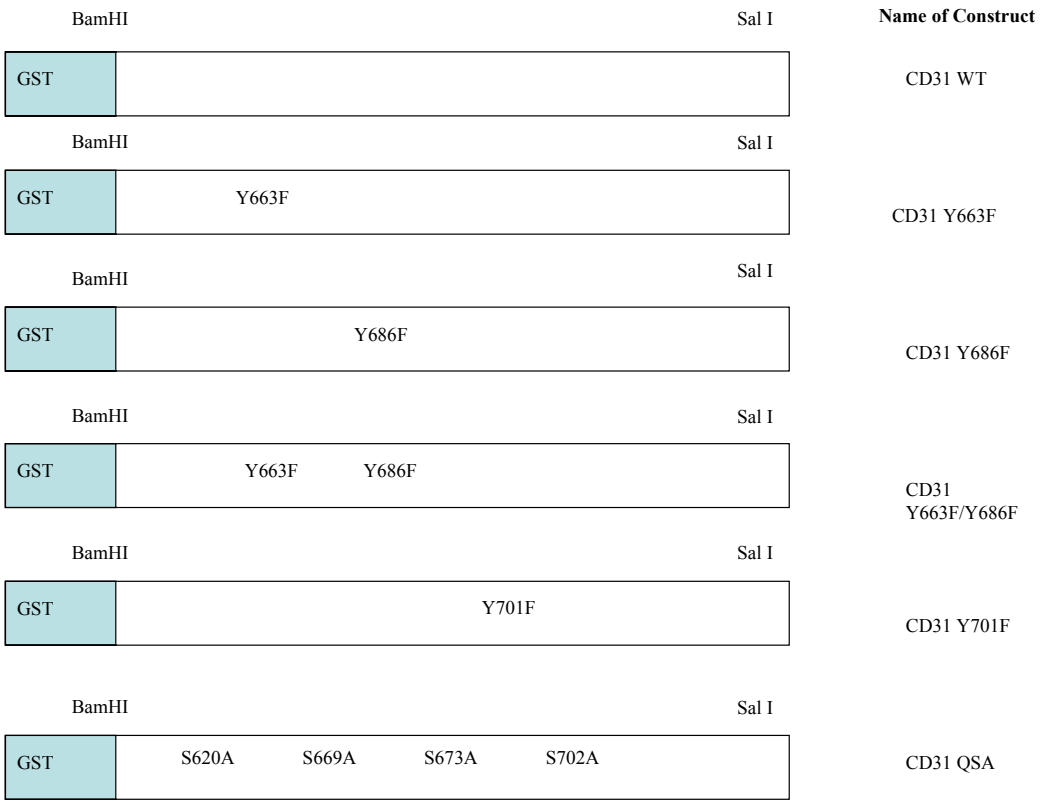

Figure 3.2:1. Diagrammatic representation of recombinant proteins generated, showing the N-terminal GST tag and the positions of the point mutations introduced.

GST-fusion protein pulldown analysis revealed that SHP-2 binds to the cytoplasmic domain of CD31, in an ITIM dependent manner, as the Y663F/Y686F construct did not bind SHP-2 (Figure 3.2:2). There was reduced binding of SHP-2 with Y663F and Y686F constructs, supporting previous work [62]. The blot was reprobed for GST to confirm equal protein loading.

SHP-1 binds to the cytoplasmic domain of CD31 at a lower level than SHP-2, and is dependent on intact ITIM tyrosines, which recapitulates previous work[57] (Figure 3.2:3). Equivalent protein loading was confirmed by reprobing for GST. The pulldowns were also probed for p120 RasGAP (Figure 3.2:4), and this was found not to bind to the cytoplasmic domain of CD31, equal loading was confirmed by reprobing with anti-GST antibodies.

Given the previous findings of β-catenin binding to CD31 in endothelial cells, and in complex with SHP-2 [65], GST pulldowns with either wild type and tyrosine mutant CD31 constructs show β-catenin did not bind to the cytoplasmic domain of CD31 (Figure 3.2:5), the blot was reprobed with GST to confirm equal protein loading.

Src family kinases have been shown to phosphorylate CD31, but src was not detectable in a GST-CD31 pulldown (Figure 3.2:6). Src may not be binding to CD31 directly, but may bind to other proteins the plasma membrane and phosphorylate CD31. The proteins pulled down by each GST-CD31 construct are summarised (Table 3.2:1).

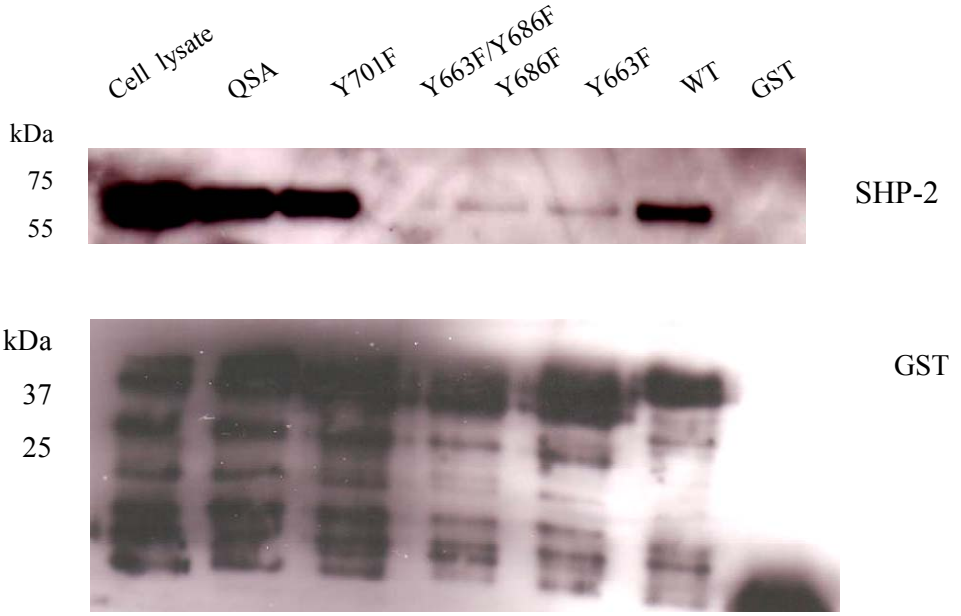

Figure 3.2:2. CD31 negative Jurkat lysates were incubated with GST-CD31 point mutant constructs in a GST pulldown assay, separated by 10% SDS-PAGE and Western blotted for SHP-2 (top) and GST to confirm equivalent protein loading (lower). SHP-2 binds to wild-type, QSA and Y701F CD31, with less binding to Y663F, Y686F and no binding with Y663F/Y686F. CD31 negative Jurkat cell lysate included as a positive control.

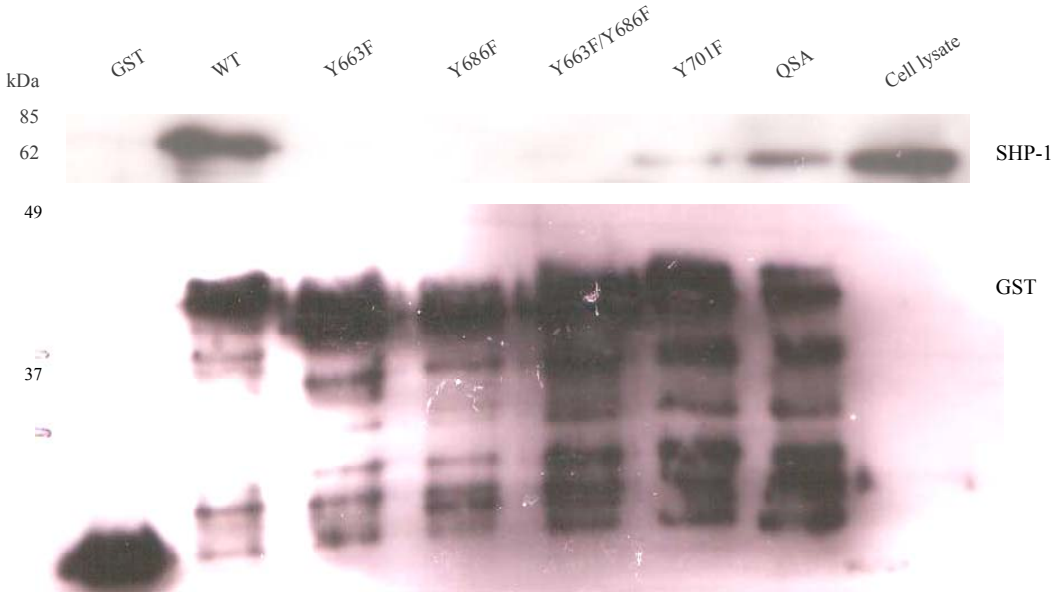

Figure 3.2:3. GST pulldown (as described previously [Figure 3.2:2]) of Jurkat lysates show SHP-1 binding to CD31 is dependent on intact ITIM tyrosines and is unaffected by QSA or Y701F mutations (top), reprobed for GST (lower) to confirm equivalent protein loading.

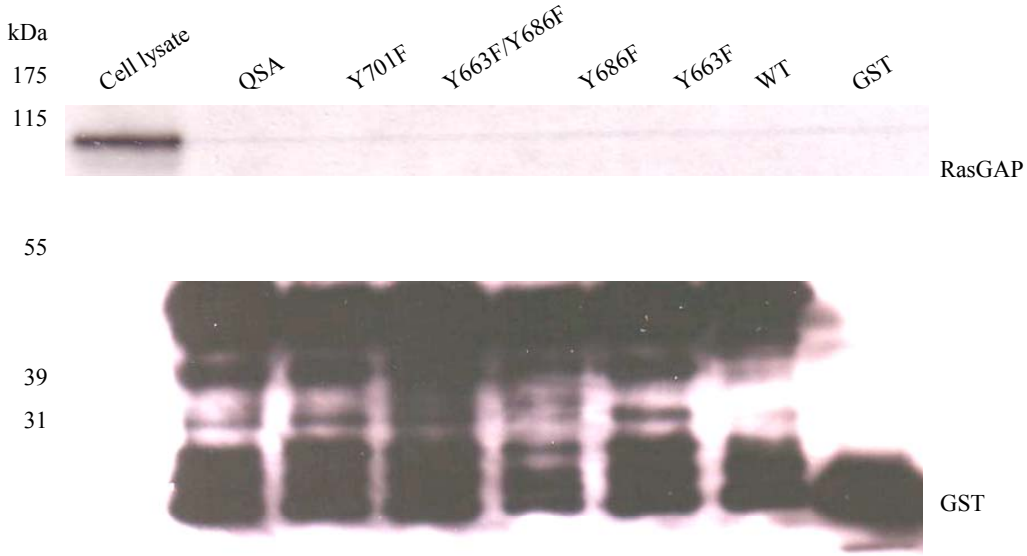

Figure 3.2:4. GST pulldown (as described previously [Figure 3.2:2]) of Jurkat lysates show p120 RasGAP does not bind to CD31 cytoplasmic domain (top) reprobed with for GST (lower) to confirm equal protein loading.

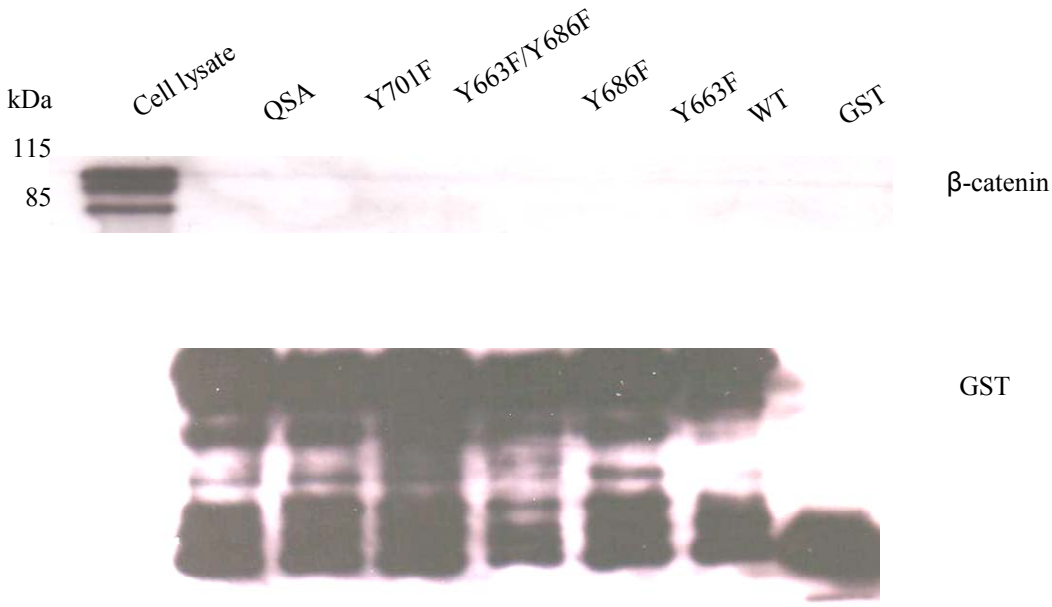

Figure 3.2:5. GST pulldown (as described previously [Figure 3.2:2]) show β-catenin does not bind to the cytoplasmic domain of CD31 (top), reprobed for GST (lower) to confirm equal protein loading.

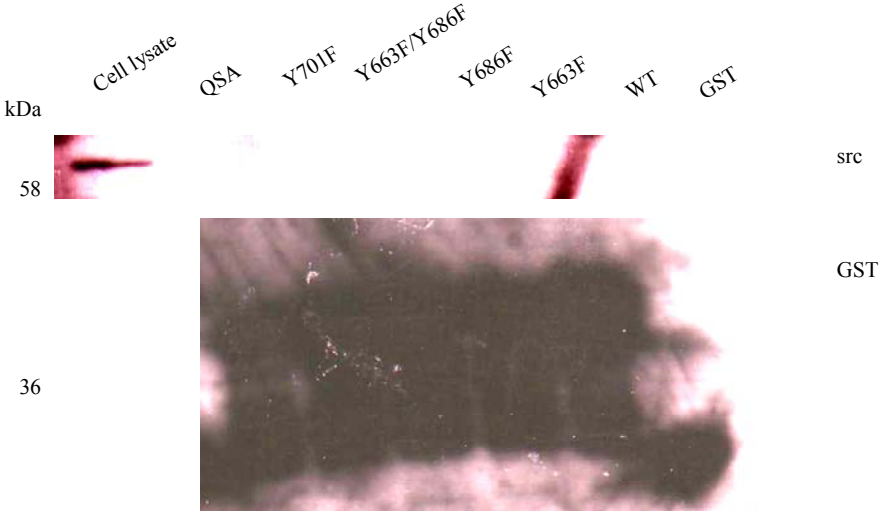

Figure 3.2:6. GST pulldown (as described previously [Figure 3.2:2]) show src does not bind to the cytoplasmic domain of CD31 (top), reprobed for GST (lower) to confirm equal protein loading.

It has been suggested that talin may be involved in CD31 mediated activation of integrins (Personal communication, Dr David Critchley, Leicester University, UK). To explore this we investigated whether there was a direct link between CD31 and talin, using a construct of the talin FERM domain with an N-terminal His tag in pulldown assays.

The His-talin construct was transformed into BL21 *E. coli* and purified with magnetic nickel-coated beads (see Appendix). Pulldowns using the original buffer condition as described [76] with either His-talin or GST-CD31, and probing for CD31 and talin respectively found no association between talin FERM domain and CD31 cytoplasmic domain. Changing the buffer conditions to those used in the optimised GST pulldowns, and probing for talin binding to CD31 did not detect any direct relationship between the two proteins (Figure 3.2:7).

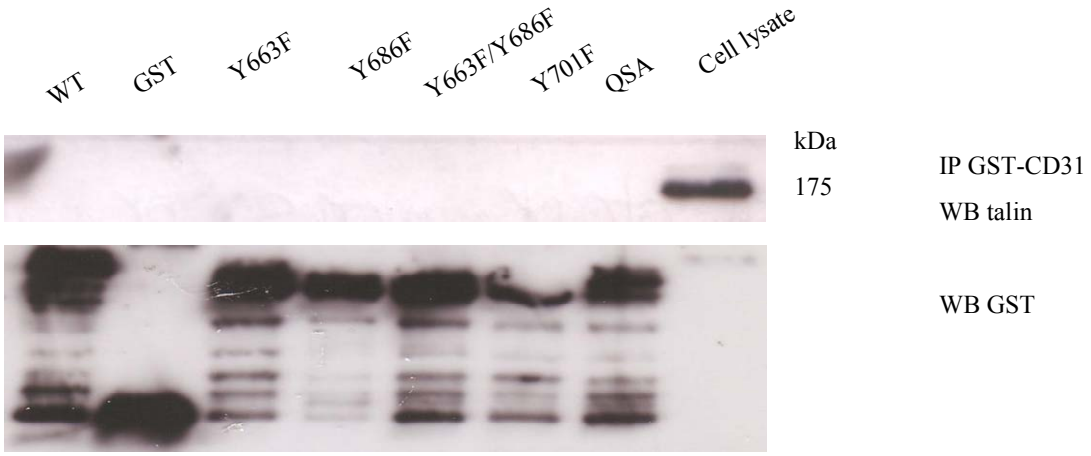

Figure 3.2:7. GST pulldown (as described previously [Figure 3.2:2]) with ITIM mutant, Y701F, QSA and wild type CD31 GST constructs show no association with talin.

Candidate Protein	GST	WT	Y663F	Y686F	Y663F/Y686F	Y701F	QSA
SHP-1	×	✓	✓	✓	×	✓	✓
SHP-2	×	✓	×	×	×	✓	✓
RasGAP p120	×	×	×	×	×	×	×
RhoGAP p190	×	×	×	×	×	×	×
β-catenin	×	×	×	×	×	×	×
c-src	×	×	×	×	×	×	×
Talin	×	×	×	×	×	×	×

Table 3.2:1. Summary table showing association between different GST-CD31 recombinant proteins (defined in Figure 3.2:1) and the candidate protein binding to each.

3.2.1 *Apoptotic vs Viable GST Pulldowns*

It has proven difficult to induce Jurkat cells to undergo apoptosis with minimal necrosis. Using a range of concentrations of Fas ligand (CH11) antibody together with various chemical treatments, the cells were found to be very resistant to apoptosis and progressed instead to necrotic cell death. Treatment of Jurkats with 10mM cycloheximide and 50μM etoposide induced massive necrosis (Figure 3.2:8). Inducing apoptosis with different concentrations of CH11 also produced high levels of necrosis (Figure 3.2:9). We therefore decided to use neutrophils as they undergo apoptosis readily following culture overnight *in vitro* with low levels of necrosis.

Apoptosis and necrosis was measured by annexin V/ propidium iodide (PI) staining and flow cytometric analysis (FACSCalibur, BD Biosciences). The outer membrane of the cell contains, amongst proteins, zwitterionic phospholipids, whereas the inner membrane has the aminophospholipids phosphatidylethanolamine (PE) and phosphatidylserine (PS). The aminophospholipid translocase catalyses the movement of aminophospholipids from the outer to the inner membrane. When the cell undergoes apoptosis, this translocase is inactivated, and PS becomes exposed on the cell surface [110].

Exposure of PS is detectable using annexin V, which can be conjugated to FITC, amongst other fluorochromes, and is detectable through the FL-1 channel. Cell membrane integrity is lost during the late stages of apoptosis and PI can enter the cell and bind DNA, this is detectable through the FL-2 channel. Viable cells have low annexin V/PI staining, whereas apoptotic populations have high annexin V and low PI, and necrotic cells have high PI and annexin V staining.

3.2.2 *Neutrophil Pulldowns*

Freshly isolated neutrophils were mostly viable (97.6% unstained, 0.28% annexin V positive, 0.73% propidium iodide positive and 1.43% both annexin V/propidium iodide). Aged neutrophils have 46.4% unstained, 44.4% annexin V positive, 5.03% propidium iodide positive and 7.19% annexin V/propidium iodide positive (Figure 3.2:10).

GST pulldowns were performed as described (Materials and Methods) with the following modifications; the lysates were not precleared with glutathione beads overnight as proteolysis occurred over this time frame. (Extra protease and phosphatase inhibitors were added in addition to those described in Material and Methods, 1 protease inhibitor cocktail tablet [Roche], 10mM β-glycerophosphate, 2mM levamisole, 10mM NaF, 10mM Na_3VO_4) with either freshly isolated or aged neutrophils (10 $X10^6$ cells/ml lysate).

As previously shown in viable Jurkats, SHP-1 binds to the cytoplasmic domain of CD31, in viable and aged neutrophils, SHP-1 binds to the cytoplasmic domain of CD31 (Figure 3.2:11). SHP-2 has also been shown to bind to CD31 in viable Jurkats, but is degraded in apoptotic Jurkats [84]. SHP-2 was present in both viable and aged neutrophils, and bound to CD31 in both conditions (Figure 3.2:12). Interestingly, we found that phosphotyrosine levels of CD31 were decreased following incubation with aged neutrophil lysates, which may suggest that aged neutrophils have increased levels of phosphatases (Figure 3.2:13).

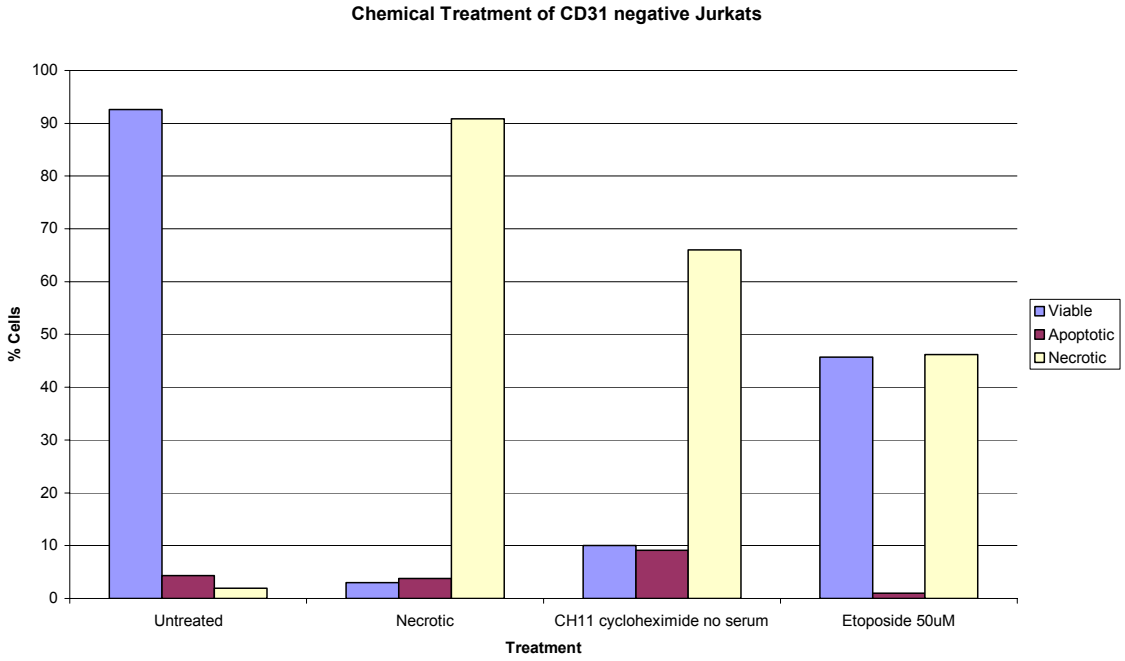

Figure 3.2:8. Treatment of CD31 negative Jurkats with CH11 and 10mM cycloheximide and 50µM etoposide shows a high percentage of cells are necrotic.

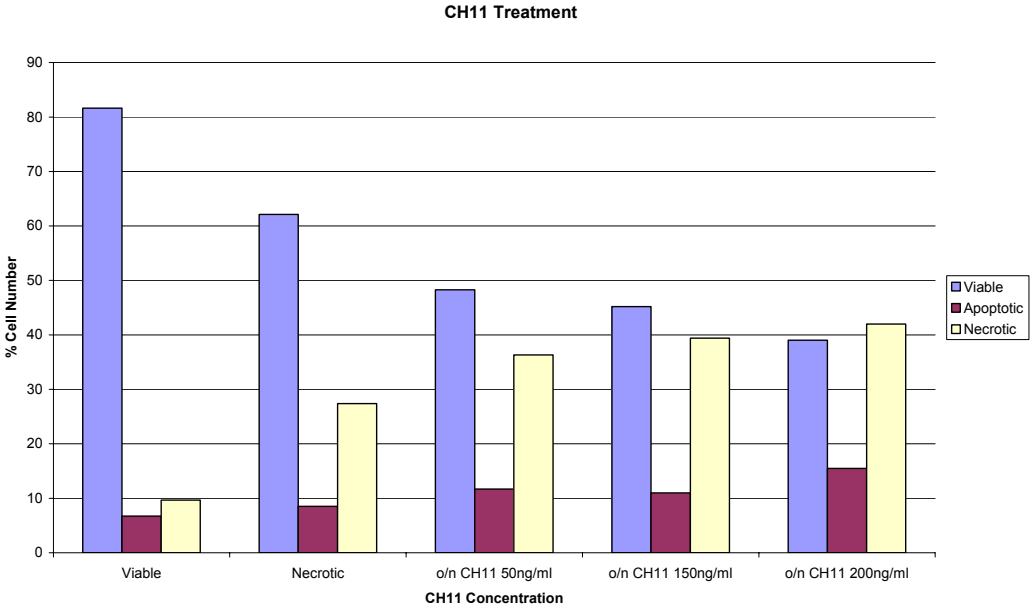

Figure 3.2:9. CH11 treatment of CD31 negative Jurkats at concentrations from 50 to 200ng/ml induces necrosis.

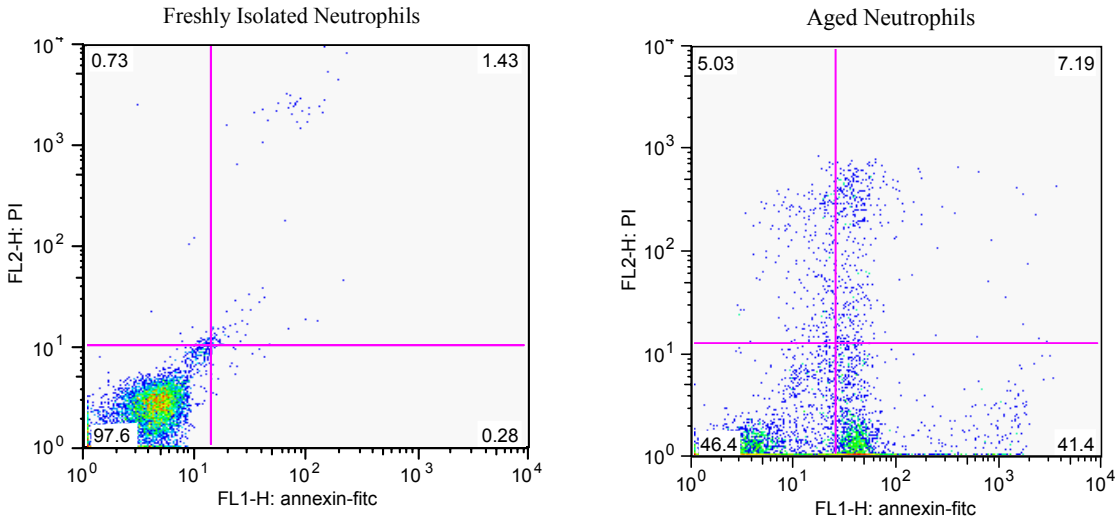

Figure 3.2:10. Freshly isolated and aged neutrophils stained with annexin V and propidium iodide show freshly isolated neutrophils have 97.6% unstained, 0.28% annexin V positive, 0.73% propidium iodide positive and 1.43% both annexin V/propidium iodide. Aged neutrophils have 46.6% unstained, 44.4% annexin V positive, 5.03% propidium iodide positive and 7.19% annexin V/propidium iodide positive. Representative of three independent blood preparations.

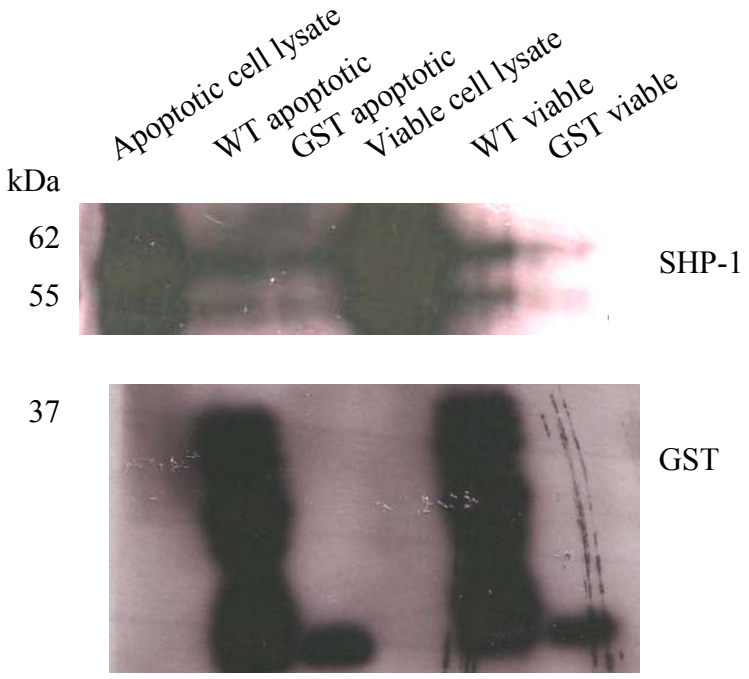

Figure 3.2:11. Freshly isolated and aged overnight neutrophil pulldown probed for SHP-1, shows binding of SHP-1 to CD31 in viable and aged neutrophils (top), reprobed for GST (lower) to confirm equal protein loading.

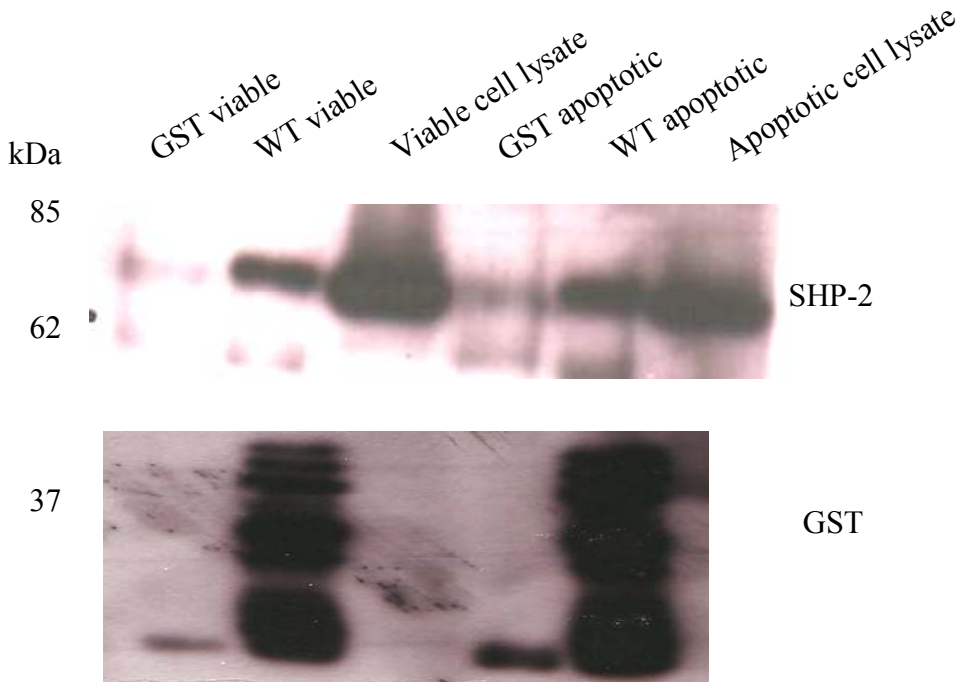

Figure 3.2:12. Freshly isolated and aged overnight neutrophil pulldown probed for SHP-2 shows CD31 binds SHP-2 in viable and aged neutrophils (top), reprobed for GST (lower) to confirm equal protein loading.

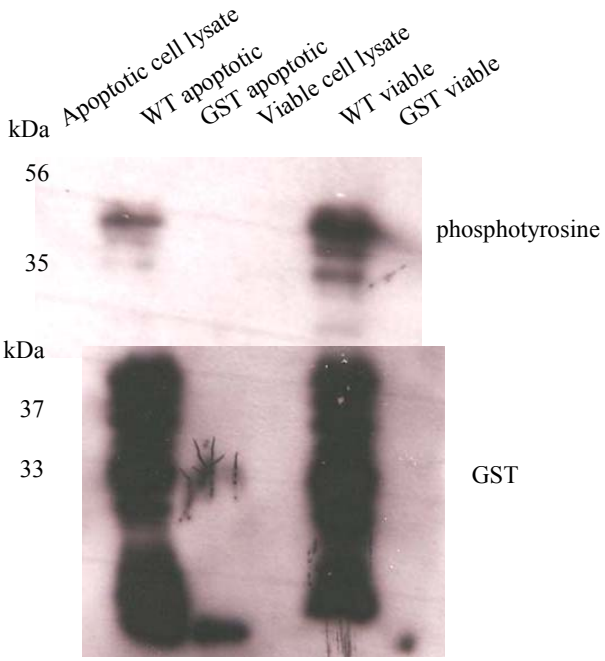

Figure 3.2:13. Freshly isolated and aged overnight neutrophil pulldown probed for phosphotyrosine (top) showing decreased tyrosine phosphorylation of CD31 in aged neutrophils, reprobed for GST (lower) to confirm equal protein loading.

3.2.3 *MALDI-TOF Protein Finger Printing*

As well as investigating GST pulldowns by Western blot for suspected binding partners, we also included an unbiased approach to identify novel candidates binding to the cytoplasmic domain of CD31. MALDI-TOF (matrix assisted laser desorption time of flight spectroscopy) protein fingerprinting provides an accurate method to identify unknown protein bands on a gel. Briefly, proteins are separated on SDS-PAGE and excised from the gel. The protein is then removed from the gel by washing with acetonitrile, and is then digested with trypsin. The protein fragments are then mixed with a matrix which is ionised by a laser. The fragments and matrix then fly down to a detector, and their time of flight is measured. Larger fragments take longer to reach the detector than smaller fragments. The detector then produces the results as peaks of protein mass, which can then be compared with a database of known proteins to allow identification of CD31 binding partners.

The GST pulldown was performed with GST alone to act as a negative control, wild-type, Y663F, Y686F, Y663F/Y686F, Y701F and QSA mutant constructs as described (Materials and Methods) and the proteins separated on an 8-16% Tris-glycine SDS PAGE. The bands were visualised by silver staining (Figure 3.2:14). Bands present in the GST alone pulldown were discounted as non-specific, and their presence in the other pulldowns was ignored. Between the different pulldowns it was noted that there were slight differences in the molecular weights of the proteins, particularly at the lower molecular weights. However, large differences were unlikely to be seen as the constructs used were point mutations.

The proteins binding to wild type cytoplasmic domain were of immediate interest, and this pulldown sample was sent for MALDI-TOF analysis (Fingerprints Proteomics Services, Dundee, UK). Utilising known binding partners from the literature or from work in this laboratory, the arrowed bands were selected as being potentially novel proteins (Figure 3.2:15). To compare between phosphorylated, (wild-type CD31) and unphosphorylated (Y663F/Y686F mutant) CD31, and determine whether there were different proteins associating due to phosphorylation of the cytoplasmic domain, pulldowns were performed and separated on SDS-PAGE (Figure 3.2:16). Bands unique to the CD31 lanes were excised for MALDI-TOF analysis. Table 3.2:17 shows the proteins identified from Swiss-prot database where the percentage confidence interval (% C.I.) was greater than 95%. 14-3-3ε is an adapter protein that acts as a 'molecular anvil' to bring two proteins together, and thereby facilitating an interaction. Proteins binding to 14-3-3ε must be phosphorylated [148], and since CD31 can be phosphorylated, and may be utilising 14-3-3ε to mediate interactions with other signalling molecules during migration.

During the formation of focal adhesions, structures termed spreading initiation centres (SIC) form at the point of contact in the cytoplasm. These structures contain focal adhesion markers, actin and RNA and RNA binding proteins [149]. CD31 may form these structures during the process of forming focal adhesion complexes, and this may be why the RNA helicase EIF3 was identified as binding to the cytoplasmic domain of CD31.

The other identified proteins, cyclophilin A, profilin, L-plastin, α-enolase and myosin have been shown to be glutathionated in T cells that are oxidatively stressed [150]. Using the GST-glutathione affinity system may have selectively pulled out these proteins, and they may not actually be binding to CD31, but to the GST tag.

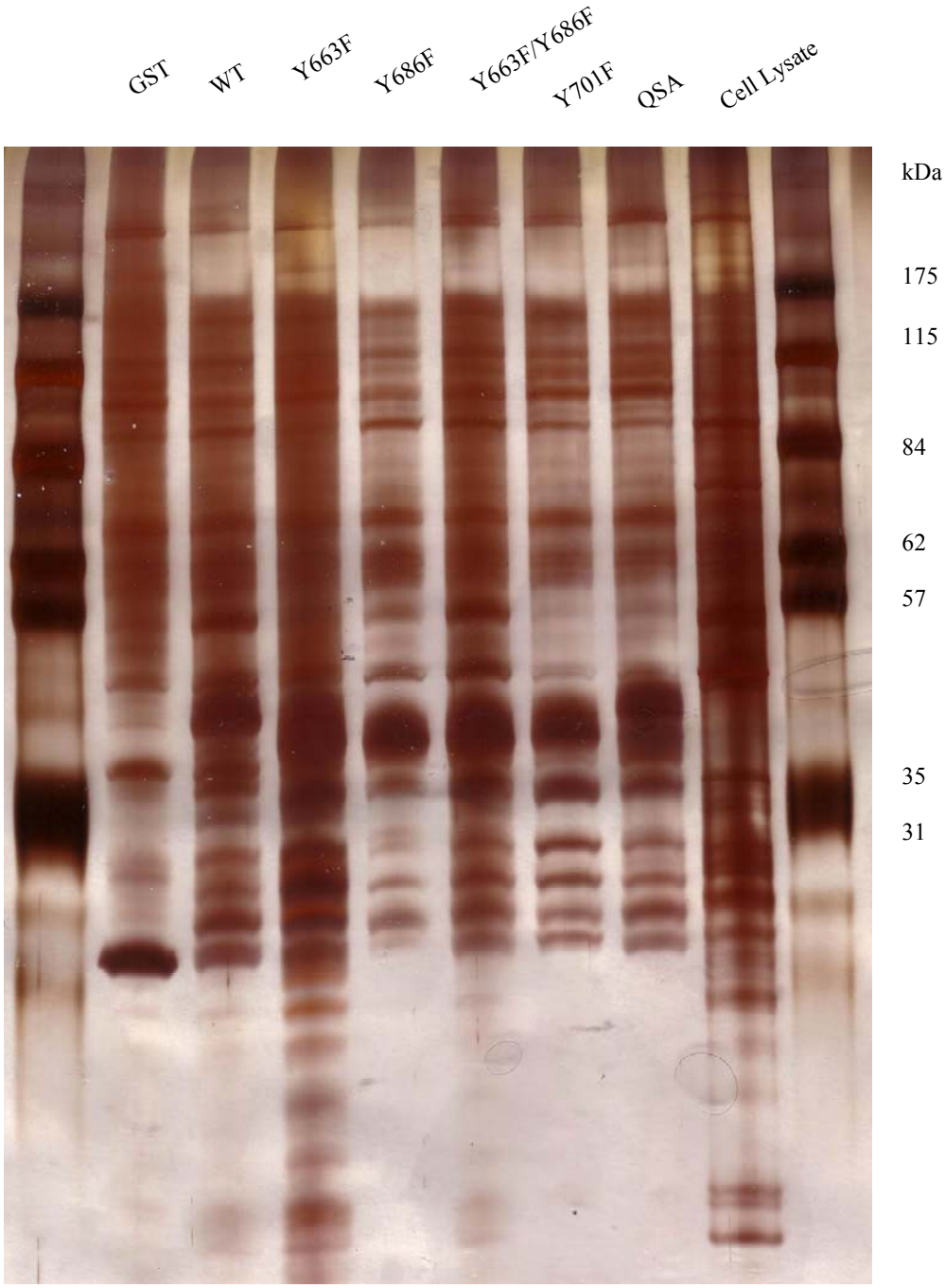

Figure 3.2:14. Silver stained 8-16% SDS-PAGE showing proteins of different molecular weights binding to the cytoplasmic domain constructs of CD31.

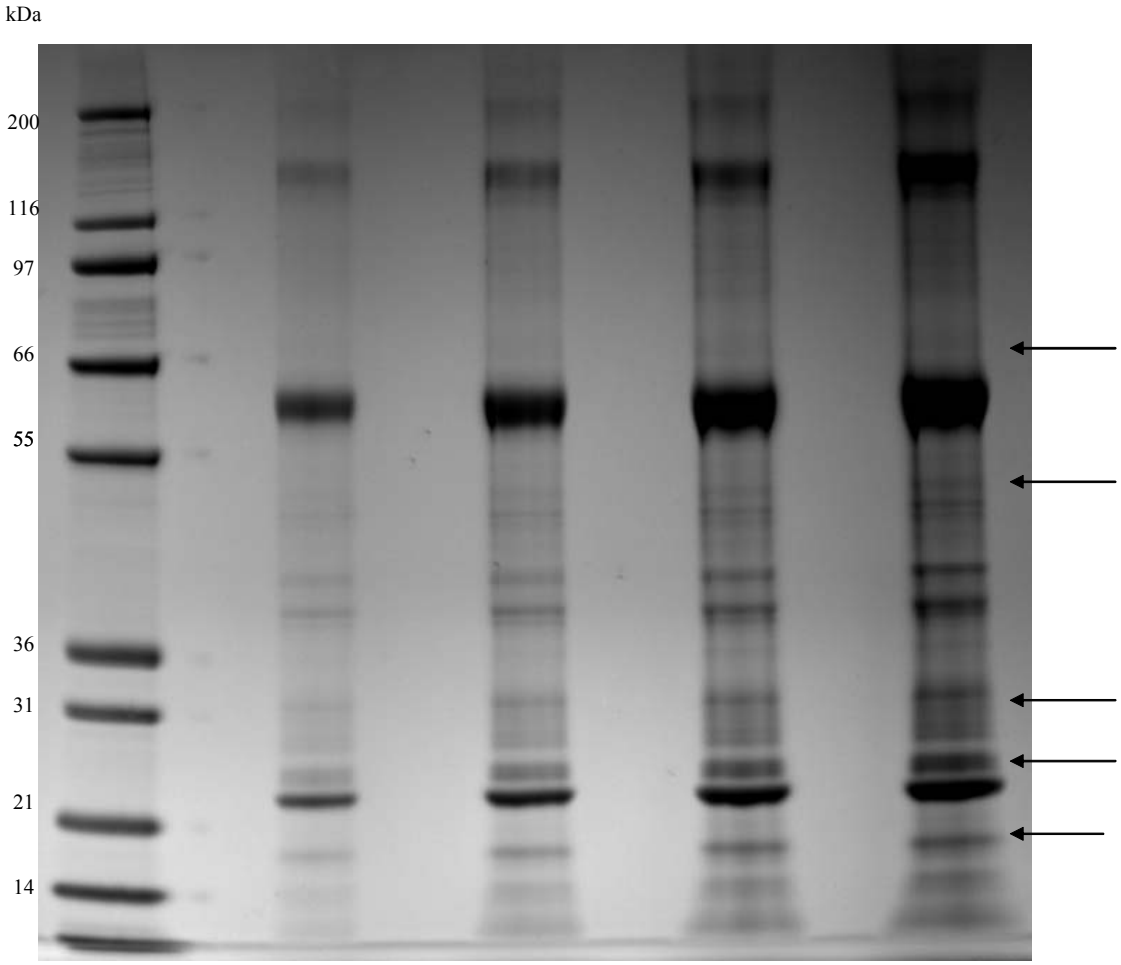

Figure 3.2:15. Coomassie stained 12-18% MOPS gel of GST pulldown from negative Jurkat lysates. The four lanes contain 5µl, 10 µl, 15 µl and 20 µl of the sample to gauge for overloading. The arrows show bands that were extracted for MALDI-TOF MS/MS analysis.

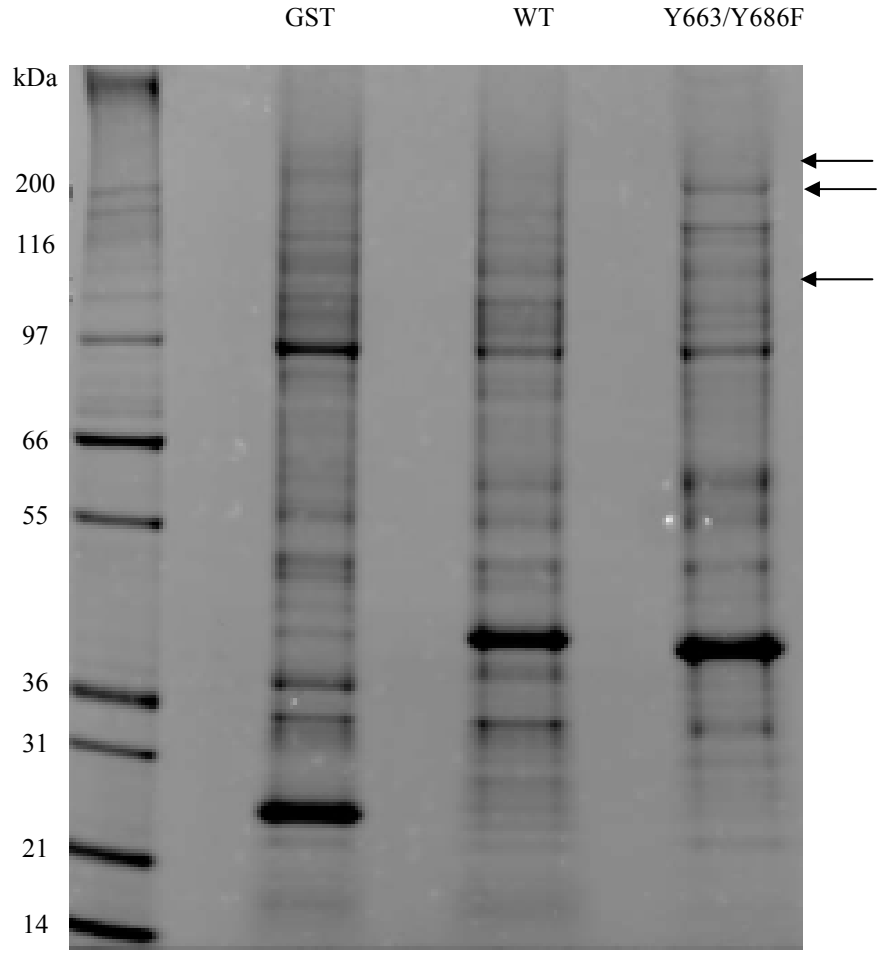

Figure 3.2:16. Coomassie stained 12-18% MOPS gel of GST-CD31 pulldowns from negative Jurkat lysates, with GST alone, wild type and Y663/Y686F CD31 as bait. The unknown bands unique to the CD31 lanes were taken for MALDI-TOF analysis (arrowed).

Protein	Function	Molecular Weight (kDa)	Construct Used
14-3-3ε	Adapter protein Binds SH-2 domain proteins	29	WT
Cyclophilin A	Immunophilin	18	WT
Profilin	Actin binding protein Binds Rho effectors	15	WT
L-plastin	Actin bundling protein Binds calmodullin	70	WT
Alpha enolase	Glycolytic enzyme Heat shock protein	47	WT
Myosin	Cytoskeleton component	228	Y663F/Y686F
eIF3	RNA helicase	53	Y663F/Y686F

Table 3.2:17. Table of results from MALDI-TOF analysis showing proteins identified, molecular weight and cytoplasmic domain constructs used to pull out.

3.3 Discussion

To investigate the proteins that were binding to the cytoplasmic domain of CD31, GST pulldown with N-terminal tagged CD31 constructs was used. However, this method required a lot of optimisation, as initial attempts with the affinity isolation yielded non-specific binding of SHP-2 and Hsp90 to the GST tag. Increasing concentrations of NaCl did not remove the non-specificity of molecular interactions, neither did the addition of a chaotrope (NaI) to destabilise hydrophobic interactions. Preclearing the lysates before pulldown with either beads or GST was also unsuccessful at removing the non-specific binding.

Performing a literature search found three published methods of pulldown that used different compositions of lysis buffer and washing conditions that were subsequently tested for minimal non-specific binding to the GST tag. The lysis buffer must contain both a detergent and NaCl, and the cell lysate must be precleared with glutathione-agarose beads overnight prior to performing the GST pulldown.

The GST-CD31 cytoplasmic domain constructs must also be phosphorylated *in vitro*, as they were not phosphorylated by being produced in the bacteria or by incubating with the cell lysate. Phosphorylation of the cytoplasmic domain was essential to bind the SH2 domain containing phosphatases and other signalling molecules dependent on tyrosine phosphorylation. There was no association of c-src with the cytoplasmic domain of CD31 from GST pulldown analysis, and this observation is consistent with previous work where although c-src is able to phosphorylate CD31, it does not co-precipitate with CD31 [54].

The tyrosine phosphorylated cytoplasmic domain of CD31 has been shown to associate with several signalling molecules in the cytoplasm. The SH2 domain containing phosphatases SHP-1 and SHP-2 bind to specific tyrosine residues identified as part of an ITIM (immunoreceptor tyrosine-based inhibitory motif). SHP-1 requires an intact ITIM for binding to CD31, whereas SHP-2 requires Y663. Phospholipase C-γ (PLC- γ) is also reported to bind to CD31 and requires an intact ITIM [63].

A complex of β-catenin and SHP-2 on the CD31 scaffold has been hypothesised to allow dephosphorylation of β-catenin and the recycling of β-catenin to the endothelial cell junction [65]. β-catenin binds the cytoplasmic domains of cell adhesion molecules such as VE cadherin and links VE cadherin to the actin cytoskeleton [151]. β-catenin did not bind to the cytoplasmic domain constructs in leukocytes which may suggest that it is not phosphorylated, or that it may function in a different manner in leukocytes compared with endothelial cells.

The association of signalling proteins with the cytoplasmic domain of CD31 in viable cells could explain why viable cells are able to actively detach from macrophages. However, in the apoptotic cell, this signalling pathway could be perturbed, with differential recruitment of signalling and adapter molecules resulting in the cell being unable to engage its motor machinery and escape engulfment.

Investigation with point mutant GST-CD31 cytoplasmic domain constructs showed that SHP-1 binding to CD31 is dependent on an intact ITIM, and SHP-2 binding

requires either tyrosine residue which confirms previous findings [63]. These phosphatases may be acting as docking proteins themselves for downstream signalling molecules in addition to their established function of dephosphorylating CD31. SHP-2 has been shown to bind to Gab1 and Grb2 via their SH-2 domains. Gab1 (Grb-associated binder-1) recruits a variety of signalling proteins including Crk and PLC-γ in the context of receptor-mediated signalling [152]. Crk binds to pleckstrin homology domains of various signalling proteins via its SH-3 domains including DOCK180; which is a guanidine exchange factor of Rac, and is involved in lamellipodia formation and cell motility [153].

Grb2 also recruits SOS (son of sevenless), which is an exchange factor of Ras, and this signalling pathway may lead to the activation of Ras [154], and the regulation of focal adhesion contacts [146].

In lysates of viable and aged neutrophils, SHP-1 and SHP-2 were found to be associated with the cytoplasmic domain of CD31, and there were decreased phosphotyrosine levels of CD31 in aged lysates. This result does not wholly confirm previous work with Jurkats [84] where SHP-2 was found to be degraded, and there was reduced SHP-1 association to CD31 in apoptotic leukocytes. However, there was reduced phosphotyrosine in both systems. In endothelial cells CD31 homophilic interactions suppresses cell death and dephosphorylating CD31 causes detachment and anoiksis [155]. Dephosphorylation of CD31 may be a consequence of apoptosis and altered signalling within the cell which may lead to firm attachment to macrophages and subsequent engulfment.

The modulation of the actin cytoskeleton by the regulation of Rho family members is required for cell motility [61]. The guanidine exchange factor RasGAP5 (p120) was not detected as binding to the cytoplasmic domain of CD31. However, the exchange factor may be acting indirectly with CD31 further downstream to regulate migration. Previous work has shown that CD31KO endothelial cells have a defect in RhoGTP loading, and RhoGTP is required for migration of CD31 positive endothelial cells [61], so it is likely that exchange factors for Rho family members are involved in CD31-mediated signalling.

The possible association of the integrin binding protein talin with CD31 was also explored, but these studies did not demonstrate binding of talin to the cytoplasmic domain constructs in Jurkats. As CD31 activates integrins, it could be binding talin to achieve this indirectly, but from the work presented here, this possibility is unlikely.

As well looking at suspected candidates binding to CD31 via Western blotting, an unbiased approach of pulldown then MALDI-TOF was taken to identify novel candidates. Although many proteins can be identified as binding to the cytoplasmic domain, the issue of specificity was raised. Washing the pulldowns with high stringency buffers can disrupt weaker interactions; conversely washing with a buffer of too low stringency can result in non-specific proteins binding. Running GST alone and a mutant of CD31 alongside the wild-type could be used to eliminate non-

specific interactions binding to the GST tag, or in the case of the mutant confirm the requirement of certain residues in the cytoplasmic domain for protein binding.

MALDI-TOF identified 14-3-3ε as binding to the wild-type cytoplasmic domain of CD31. This is an adapter protein that binds phosphorylated proteins, and SH-2-domain containing proteins [148]. 14-3-3ε could be mediating interactions between SHP-2 and other signalling molecules such as Grb2, facilitating the role of CD31 as a scaffolding molecule.

From the Y663F/Y686F mutant analysis, one interesting protein identified was eIF3 (elongation initiation factor 3). This is an RNA helicase, responsible for unwinding RNA prior to translation. Spreading initiation centres were recently discovered as initial points of adhesion during cell spreading and contain focal adhesion proteins, actin, RNA binding proteins and RNA [149]. CD31 may be participating in the formation of these structures prior to focal adhesions and firmer attachment.

Of the other proteins identified, cyclophilin A, profilin, L-plastin, α-enolase and myosin, all have been found to be glutathionated in T lymphocytes [150]. This suggests that these proteins represent non-specific contaminants that are binding to the GST and not to CD31. Using an alternative system for tagging the CD31 constructs such as His-nickel or biotin-streptavidin may eliminate this possibility. However, it is also possible that these protein interactions with CD31 may be real, and could further link CD31 to the actin cytoskeletal regulatory machinery which may therefore facilitate cell motility.

As SHP-2 was detected as binding to the cytoplasmic domain of CD31 and can also function as a docking protein, probing leukocyte lysates with a recombinant SHP-2 and SHP-2 with a point mutation in its catalytic site may elucidate the signalling pathway of CD31-mediated migration. A Western blotting and MALDI-TOF approach could also be used here. Once candidates have been identified, they could be subject to siRNA to knock-down expression in the functional attachment assay to determine whether the candidates have a role in leukocyte motility.

4 Hsp90

4.1 Introduction

4.1.1 *Project Background*

The potential interaction of Hsp90 with CD31 was discovered by others in this laboratory using a number of different, but complementary approaches, including genetic screens, CD31 cross linking and immunoprecipitation studies. To ascertain if Hsp90 binding to CD31 was a specific interaction, and to elucidate which residues in the cytoplasmic domain were important for mediating binding, investigation with GST pulldowns was performed.

4.1.2 *Chaperone Functions of Hsp90*

Hsp90 is an abundant (1% soluble cellular protein) cytoplasmic chaperone that is involved in ensuring correct folding and maturation of many proteins. An important regulatory function of Hsp90 is the binding of steroid hormone receptors that are free from hormone ligand. Binding of hormone causes dissociation of the Hsp90-receptor complex and dimerisation of the receptor, thereby allowing it to bind specific DNA glucocorticoid response elements and regulate transcription [156].

Hsp90 functions in co-operation with other co-chaperones Hsp70, Hop (hsp-organising protein), Hsp40 and p23 [157]. For efficient binding of hormone to the receptor, the chaperone complex must bind to the receptor prior to its engagement with steroid [158]. The steroid hormone receptor client protein binds Hsp70 and Hsp40 to form a complex capable of binding Hsp90. An ATP-dependent reaction then converts Hsp90 to its ATP-binding conformation, and this requires p23 to stabilise

and hold Hsp90 in this active state. The client protein and chaperone complex then associates with the immunophilins, peptidyl-prolyl isomerases, containing TPR (tetratricopeptide repeats) motifs, such as FKBP52[159]. The immunophilins bind to dynein, a motor protein that moves the client protein in the direction of the nucleus. Once inside the nucleus, the chaperone complex dissociates from the client protein, allowing the receptor-hormone complex to bind to chromatin and exert its effects upon the cell [160]. A schematic of the formation of the chaperone complex with steroid hormone receptor is shown (Figure 4.1:1)[161].

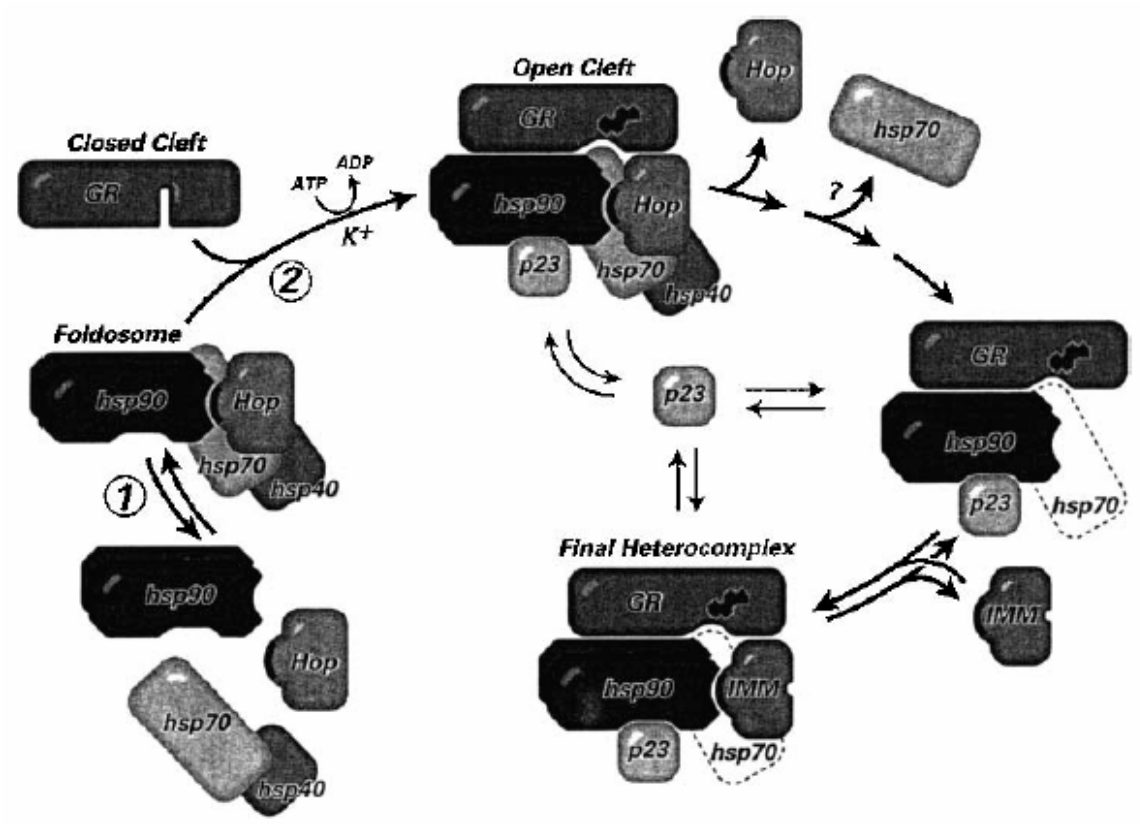

Figure 4.1:1. Schematic of Hsp90 function in steroid hormone receptor activation. Hsp90 forms a complex with Hsp70, Hsp40 and Hop. The chaperone complex binds to the inactive receptor, and in an ATP-dependent reaction cause the receptor to open and bind hormone. p23 binds to stabilise the reaction, then Hop and Hsp70 are released. The immunophilins (IMM) can then bind to Hsp90 via TPR motifs. The whole chaperone complex can then translocate to the nucleus where the receptor can bind to DNA and exert its effects upon transcription [161].

Calmodulin is involved in intracellular calcium signalling, and has been shown to bind to Hsp90 in complex with the glucocorticoid receptor [162]. Interestingly, calmodulin has been shown to associate with CD31 in platelets, an interaction that was dependent on the specific sequence ^{599}RKAKAK^{604} and the association is increased with the addition of Ca^{2+}. This interaction is thought to regulate the cleavage of the cytoplasmic domain of CD31 [163].

4.1.3 *Src Family Kinases*

Src family kinases are also substrates of Hsp90 with v-src from Rous sarcoma virus being the first to be identified. Immediately after v-src synthesis, Hsp90 was also co-precipitated. Binding of Hsp90 renders the kinase incapable of autophosphorylation, and reduces the capacity of v-src to phosphorylate its substrates. However, when the kinase is inserted into the membrane its kinase activity becomes maximal. Thus, Hsp90 prevents the inappropriate activation of v-src prior to reaching the membrane. Contrastingly, the cellular homolog c-src, interacts very weakly with Hsp90 upon its transit to the membrane [164]. Lck, another src family kinase member, requires Hsp90 during synthesis and transport to the membrane but the mature form does not require Hsp90 [165].

4.1.4 *Tetratrico Peptide Repeats*

Hsp90 interacts with co-chaperones that contain tetratrico peptide repeats (TPRs). The TPR fold is found in many organisms and mediates interactions between different proteins. TPR-containing proteins participate in a variety of cellular

processes including cell cycle control, transcription, protein transport, folding and turnover. The TPR is a 34 amino acid motif containing amino acids with basic charges and the following consensus residues –W-LG-Y-A-F-A-P. TPR motifs form amphipathic helices, containing both hydrophilic and hydrophobic residues, comprising of approximately 50% α-helices, where the helices form domains A and B [166]. Domain A spans residues W, LG and Y, and domain B residues A, F, A and P. The TPR motifs are arranged in an antiparallel fashion at angles of 24˚ to form a right-handed 'staircase', creating an amphipathic channel with which proteins interact [167-170].

The TPR is important in mediating the interactions between Hop, Hsp70 and Hsp90. Hop contains three three-TPR motifs, the N-terminal TPR binds Hsp70, the middle repeat binds Hsp90, the binding partner for the third TPR motif has yet to be discovered [171].

4.2 Results

4.2.1 *ITIM Point Mutations of CD31*

GST pulldowns with wild-type, tyrosine 663 (Y663F), 686 (Y686F) and both 663 and 686 (Y663F/Y686F), 701 (Y701F) and serine (QSA) point mutant CD31 demonstrated that Hsp90 was capable of interacting with the cytoplasmic domain of CD31, and that this interaction was independent of the ITIM, Y701 or serine mutation, and hence independent of phosphorylation of the cytoplasmic domain of CD31 (Figure 4.2:1).

4.2.2 *Truncation of CD31*

To determine the residues of CD31 critical for Hsp90 binding, a series of truncated constructs were generated (Figure 4.2:2). The constructs are numbered from the first residue after the transmembrane region and the truncated regions are denoted with the prefix Δ. To begin with, the constructs CD31TM30Δ88 (i.e. is the first 30 amino acids with a truncation of the last 88), CD31TMΔ25,93, CD31TMΔ50,68 and CD31TM104,Δ14 were generated. When these constructs were used in GST pulldowns the only construct for which binding to Hsp90 could not be demonstrated was CD31TMΔ50,68 (Figure 4.2:3).

The CD31TMΔ50,68 construct became a focus for further C-terminal truncation, as the results thus far suggested there were critical amino acids present in the distal region of the cytoplasmic domain required for Hsp90 binding. Further truncations of this region were generated CD31TM31,Δ87, CD31TM37,Δ81 and CD31TM41Δ77. In the course of the production of these proteins, the GST pulldown method was optimised for other proteins to remove non-specific binding to the GST alone. With optimisation achieved, the pulldowns with all truncated constructs including the new ones were performed (Figure 4.2:4). Both CD31TM30,Δ88 and CD31TM19,Δ109 were found to bind Hsp90, perhaps because both of these constructs contain the calmodulin binding region (KCYFLRKAK) [163].

CD31TMΔ25,93 , CD31TMΔ50,68, and CD31TM104,Δ14 also bind Hsp90. Hsp90 association with CD31TM30,Δ88 and CD31TM104,Δ14 was similar to that observed with the original pulldown method, but surprisingly Hsp90 was now binding to

CD31TMΔ50,68 construct. The further truncations CD31TM37,Δ81 and CD31TM41Δ77 did not bind Hsp90, suggesting there are residues required for binding to the cytoplasmic domain present in the missing regions (residues MEANSHYGHNDDVG). The blot was reprobed for SHP-2 binding, as SHP-2 associates with phosphorylated CD31, this provides a positive control for correct folding, as expected only constructs with an intact ITIM were able to bind SHP-2 (wild-type CD31, CD31TMΔ25,93, CD31TM31,Δ87, CD31TMΔ50,68, and CD31TM104,Δ14). A summary of the ability of each construct to bind both Hsp90 and SHP-2 is shown (Figure 4.2:5). The blot was also reprobed for GST to confirm loading levels.

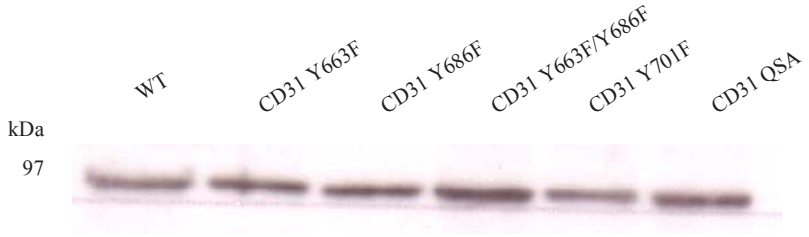

Figure 4.2:1. GST pulldown performed with tyrosine and serine mutants showing Hsp90 binding to CD31 is independent of the ITIM tyrosines, Y701 or serine mutation.

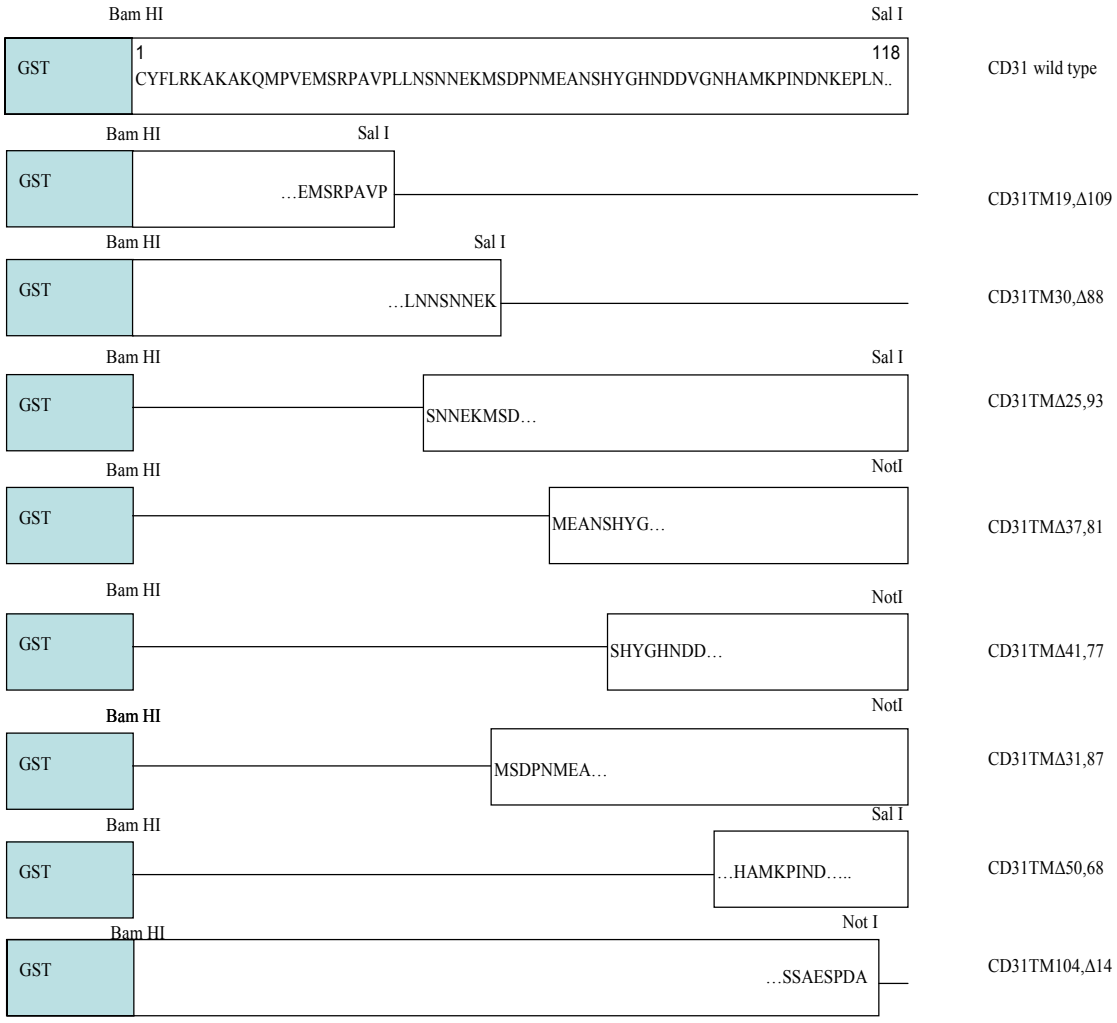

Figure 4.2:2. Schematic showing truncated CD31 constructs. The residues highlighted show the beginning or ending of the amino acid sequence at the position of the truncation, the truncation itself is denoted by a solid line.

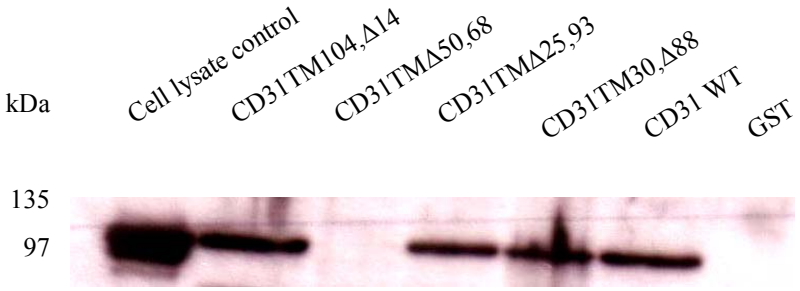

Figure 4.2:3. GST pulldowns with CD31 wild-type, CD31TM30,Δ88, CD31TMΔ25,93, CD31TMΔ50,68, and CD31TM104,Δ14, shows CD31TMΔ50,68 to be the only construct not binding Hsp90.

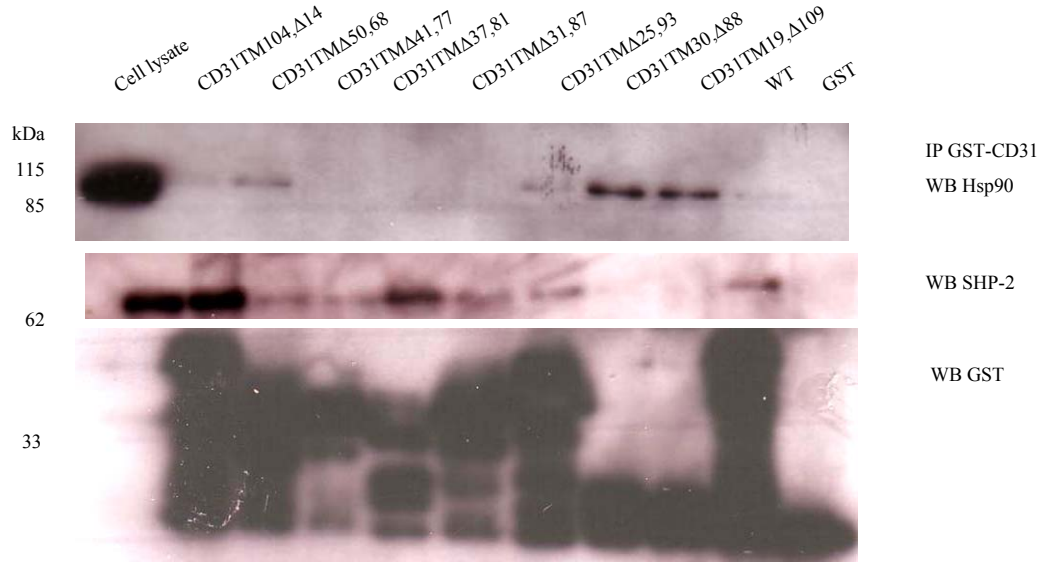

Figure 4.2:4. Optimisation of the GST pulldown method and truncation of the cytoplasmic domain of CD31 reveals multiple binding sites for Hsp90. Reprobing the membrane for SHP-2 shows the constructs to be correctly folded, with those possessing an intact ITIM able to bind SHP-2. Blot reprobed to confirm equal protein loading levels.

Name of Construct	Hsp90 Binding	SHP-2 Binding
GST	✗	✗
CD31 wild-type	✓	✓
CD31TM19,Δ109	✓	✗
CD31TM30,Δ88	✓	✗
CD31TMΔ25,93	✓	✓
CD31TMΔ37,81	✗	✓
CD31TMΔ50,68	✓	✓
CD31TM37,Δ81	✗	✓
CD31TM41,Δ77	✗	✓
CD31TM104,Δ14	✓	✓

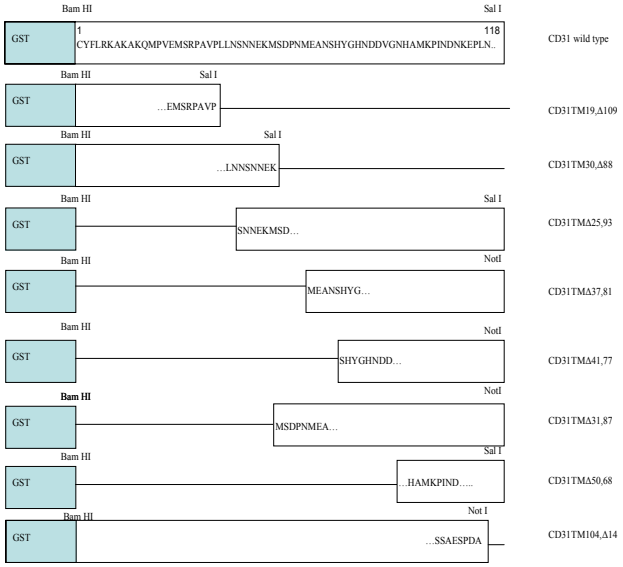

Figure 4.2:5. Summary of truncated GST-CD31 constructs with amino acid sequence and ability to bind Hsp90 and SHP-2 from CD31 negative Jurkat lysates.

4.2.3 *Sequencing Alignment*

A ribbon diagram of a TPR-containing protein demonstrates the A and B helix regions and shows the residues important for Hsp90 binding (Figure 4.2:6). A 3-dimensional model shows the amphipathic helix and carboxylic clamp that TPR-containing proteins use to bind Hsp90 (Figure 4.2:7). Sequence alignment with other TPR-containing proteins that bind Hsp90, such as FKB51 and Hop, which is part of the chaperone complex with Hsp90 and Hsp70, shows CD31 may have some sequence homology. The most conserved regions are highlighted, and the position of the putative helix regions is shown. Aligning the truncated constructs shows that a conserved region containing the sequence SNNEK is missing from the construct (CD31TMΔ50, 68) that was originally found not to bind Hsp90 (Figure 4.2:8).

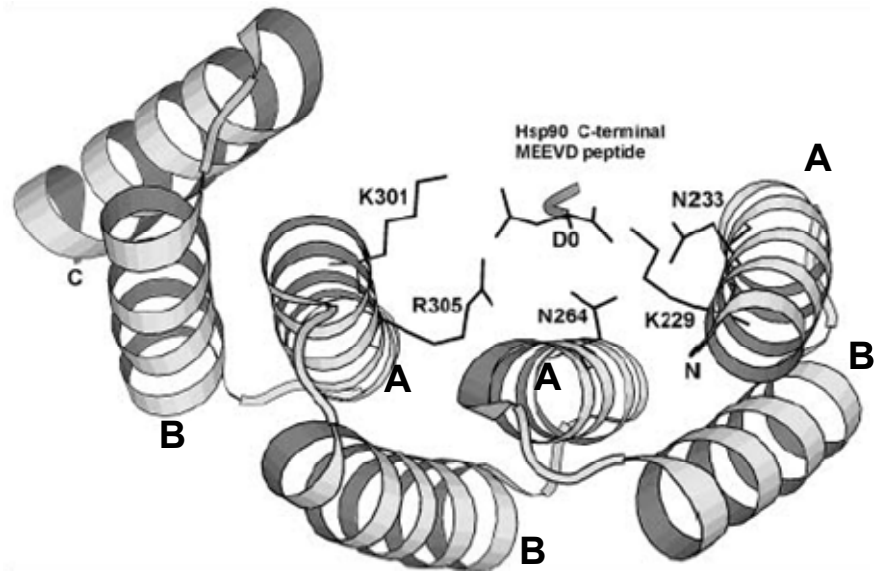

Figure 4.2:6. Ribbon drawing of an Hsp90 binding protein showing the helix regions A and B and the Hsp90 binding cleft amino acids denoted by single letter code (Personal communication Dr Simon Brown, University of Edinburgh).

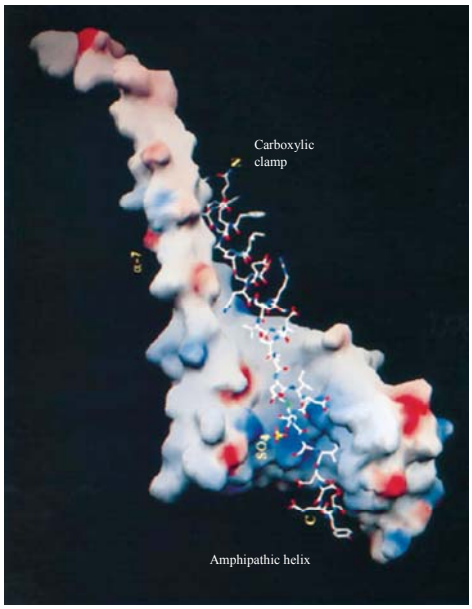

Figure 4.2:7. 3-dimensional model of an Hsp90 binding protein showing the amphipathic helix formed around Hsp90 (ball and stick model) (Personal communication, Dr Simon Brown, University of Edinburgh).

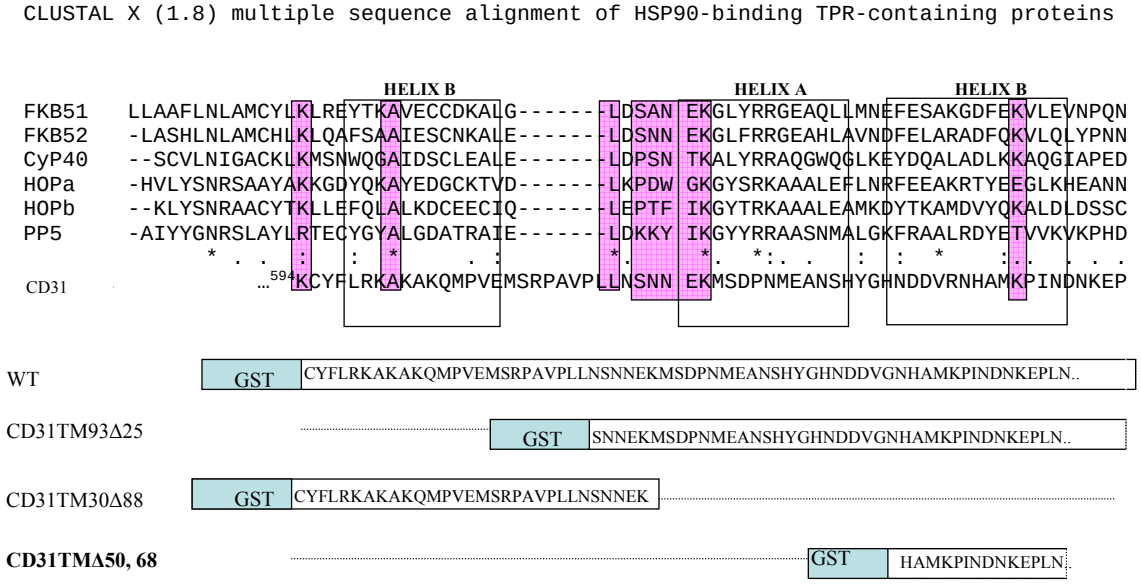

Figure 4.2:8. Clustal X CD31 cytoplasmic domain amino acid sequence aligned with known Hsp90 binding proteins containing TPR motifs. The boxes marked helix A and B denote putative helix regions. The pink boxes show the most conserved regions between the Hsp90 binding proteins and CD31. Amino acid sequence examination of the truncated constructs shows CD31TMΔ50,68 to be missing a conserved region, SNNEK.

4.2.4 *Site-Directed Mutagenesis of CD31*

Comparing the sequence of CD31 with TPR-containing proteins show conserved regions SNNEK and downstream lysines. Site-directed mutagenesis was employed to specifically target these particular residues. Site directed mutagenesis requires the target sequence to be in a plasmid from *E. coli* which is methylated. Primers containing the mutation required are annealed to the plasmid and PCR amplification of the whole plasmid occurs, generating a nicked plasmid with the mutation in the target sequence. The original plasmid template that does not have any mutations is methylated, is therefore sensitive to Dpn I digestion, whereas the synthetic mutant plasmid is not. The pure synthetic mutant plasmid can then be transformed into competent cells that repair the nicks.

Mutations of the conserved residues were generated, N27 to A, N27 to D, (E28 to A/K29 to A/M30 to A), K54 to A, (K85 to A/K86 to A) (Figure 4.2:9). (For details of construction, and purification see Appendix).

Pulldowns with these constructs revealed the mutation CD31N27A from asparagine to alanine did not bind Hsp90, but changing this residue to aspartic acid did not prevent the binding of Hsp90. Mutating three amino acids including the basic lysine residue K29 (CD31E28A/K29A/M30A in the putative TPR motif) did not have any effect on Hsp90 binding, suggesting that single mutation of the cytoplasmic domain of CD31 may not impact upon the binding surface required by Hsp90.

The single lysine mutation CD31 K54A did not prevent Hsp90 binding, suggesting that this basic amino acid is not required for Hsp90 associate with CD31. Mutation

of the lysines 85 and 86 reduced Hsp90 binding to the cytoplasmic domain of CD31. These lysines are postulated to be part of the carboxylic clamp region that may grasp Hsp90 in another region downstream of the TPR motif. All mutagenesis constructs were capable of binding SHP-2, which demonstrates the proteins are correctly folded. Blots were also reprobed for GST to confirm equivalent protein loading levels (Figure 4.2:10).

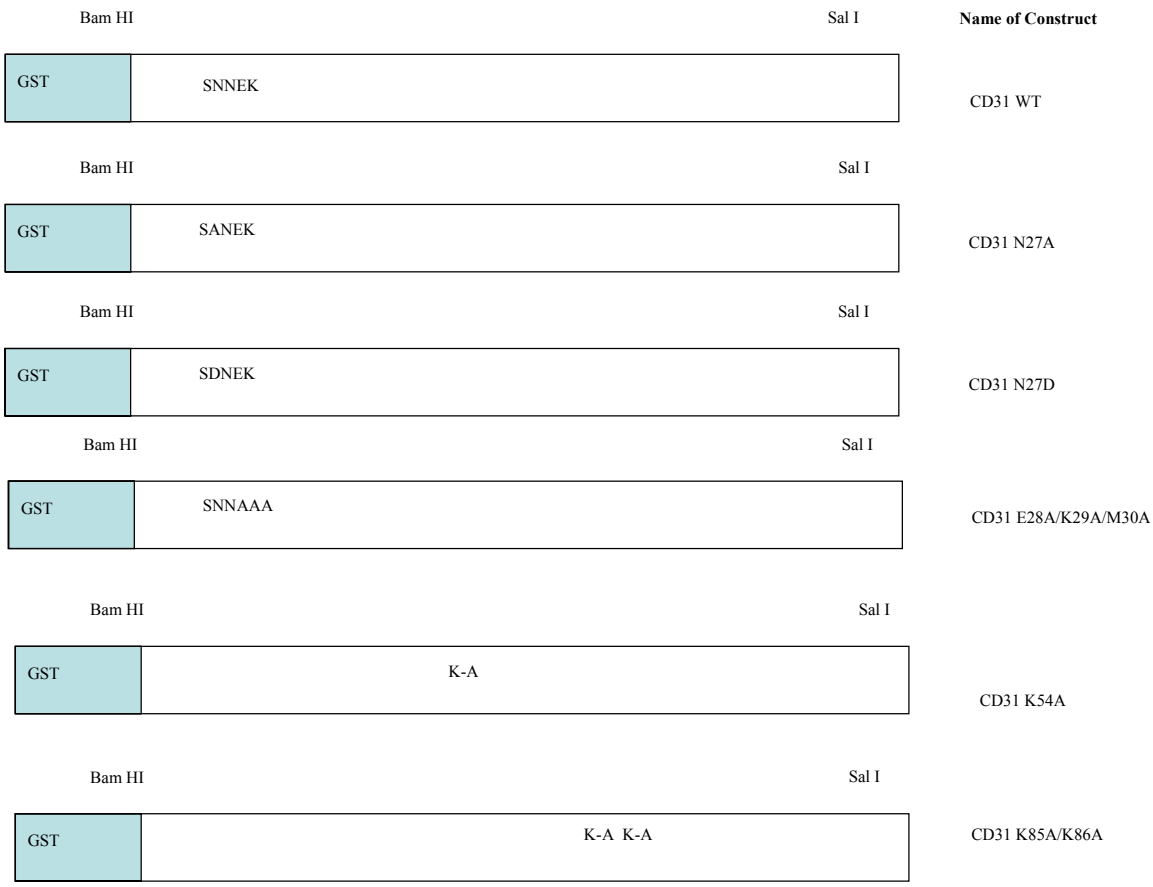

Figure 4.2:9. Schematic of site directed mutagenesis constructs showing the SNNEK region and lysine mutants.

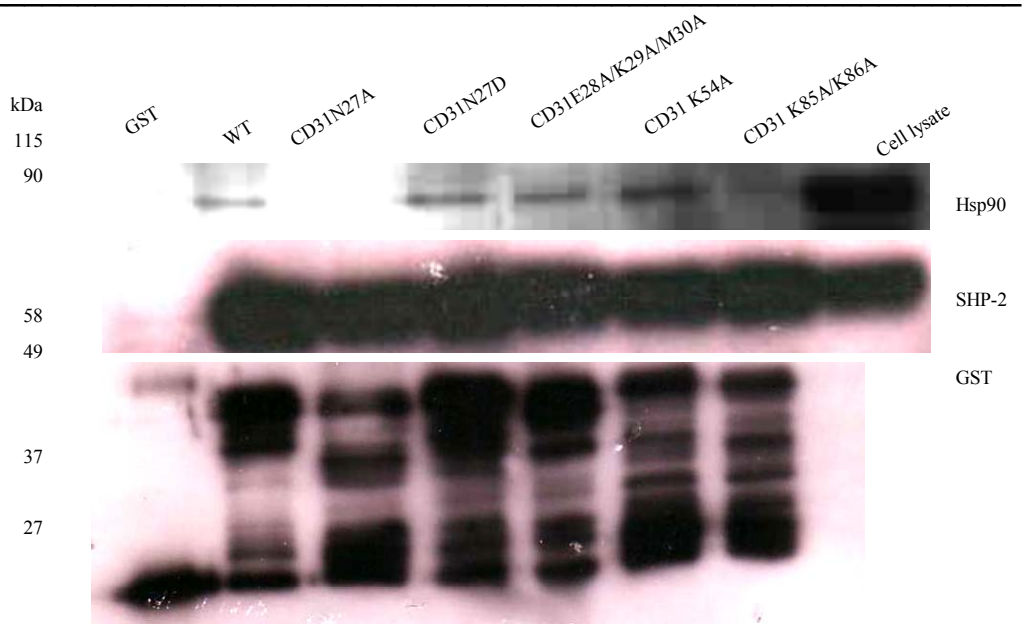

Figure 4.2:10. Site-directed mutagenesis of CD31 cytoplasmic domain shows conserved downstream lysines K85 and K86 are required for Hsp90 binding. The blot was reprobed for SHP-2 to confirm correct folding of the constructs, and again for GST to confirm loading levels.

4.3 Discussion

Utilising the CD31 cytoplasmic domain constructs already available (Y633F, Y686F, Y663F/Y686F, Y701F and QSA), Hsp90 was shown to bind independently of the ITIM tyrosines and the serine residues, and hence tyrosine phosphorylation of the cytoplasmic domain of CD31. Examination of the sequence alignment of the CD31 cytoplasmic domain with other Hsp90 binding proteins, revealed conserved regions; in particular the possibility of the cytoplasmic domain containing a TPR motif. Truncation of the cytoplasmic domain to perturb the potential TPR and other conserved residues revealed multiple binding sites for Hsp90.

CD31 has been shown to bind calmodulin in platelets [163], and Hsp90 binds to calmodulin in complex with the glucocorticoid receptor[162]. Truncations containing the calmodulin binding site (KAFYLRKAKAK) were able to bind Hsp90 and possibly mediate an indirect interaction, but truncations missing this region were not. From GST pulldowns (Chapter 2) and subsequent MALDI-TOF analysis of low molecular weight proteins, calmodulin was not found binding to CD31 in the system, neither has calmodulin been found by CD31 crosslinking studies and subsequent Western blotting (personal communication, Dr Simon Brown, University of Edinburgh, UK).

From pulldown experiments using a further set of truncations a region of the CD31 cytoplasmic domain downstream from the calmodulin binding region containing the sequence (SNNEKMSDMEANSHY) was identified as being required for Hsp90 binding. Of note was the observation that the level of Hsp90 binding decreased

when the constructs were able to bind SHP-2, which suggested phosphorylation and subsequent SHP-2 recruitment may compete with Hsp90 for binding of the cytoplasmic domain of CD31.

These findings raised the possibility of there being a TPR motif in the cytoplasmic domain of CD31, therefore site-directed mutagenesis was used to change the basic charge of key amino acids within the TPR motif to determine whether Hsp90 binding to the cytoplasmic domain of CD31 conformed to consensus TPR binding interactions.

The most conserved region of CD31 (when compared to the other Hsp90 binding proteins that also contain a TPR) S**N**NE**K**, was subjected to site-directed mutagenesis, at the first N (asparagine 27), and K (lysine 30). Mutating this residue from asparagine to alanine abrogated Hsp90 binding, but changing this residue to aspartic acid allowed Hsp90 association. This apparent discrepancy may be due to the mutation involving aspartic acid altering the structure of the cytoplasmic domain of CD31 allowing Hsp90 to utilise the first asparagine of the S**N**NEK motif (N 26) and thus still bind. Changing the basic amino acid that was most conserved (lysine 30) to an alanine did not prevent Hsp90 binding to the cytoplasmic domain of CD31. A further downstream conserved lysine at amino acid position 64 allowed Hsp90 binding, however two further lysines at 85 and 86 (85 is part of the putative carboxylic clamp) were also targeted by site directed mutagenesis, and prevented Hsp90 binding to CD31.

These data suggest that this region of the cytoplasmic domain of CD31 could conform to a TPR motif. However, there were some caveats to the results. The conserved residues targeted were postulated to contain a TPR motif, and mutations of these were thought to prevent Hsp90 binding. As not all conserved residue mutation prevented Hsp90 binding, perhaps single amino acid changes are insufficient to perturb the structure of CD31 so that Hsp90 is unable to bind. Double mutations of both the postulated TPR and carboxylic clamp of CD31 are required to examine this possibility.

To explore the functional consequences of this interaction, particularly in the context of CD31-mediated migration, constructs of the cytoplasmic domain that do not bind Hsp90 (CD31TMΔ37,81, CD31TMΔ31,87 and CD31TMΔ41,77) could be introduced into CD31 negative Jurkats and their ability to transduce motility signals measured in the detachment assay.

There is a possibility that the association of Hsp90 with the cytoplasmic domain of CD31 may be due to its function as a chaperone, and could be recognising the GST constructs as being improperly folded. However, as particular regions of amino acids of the cytoplasmic domain of CD31 seem to be required for Hsp90 binding, perhaps CD31 is a client of Hsp90 and Hsp90 is required for the maturation of the receptor. Hsp90 may also be using CD31 as a scaffold to bring src kinases to the membrane thereby facilitating CD31 phosphorylation.

5 General Discussion

5.1 General Discussion

CD31 is an immunoglobulin superfamily member involved in the process of mediating leukocyte transmigration to sites of inflammation. The work in this thesis set out to test the hypothesis that there is differential recruitment of signalling and adapter molecules to the cytoplasmic domain of CD31 in viable and apoptotic leukocytes. In addition, we have attempted to ascertain the role of cytoplasmic binding partners for CD31 in viable leukocyte attachment to macrophages, and their subsequent detachment.

To explore the role of CD31 in leukocyte detachment from macrophages, we screened a panel of leukemic cell lines expressing CD31 for their ability to attach to the myelomonocytic cell line THP-1 that had been differentiated into a 'macrophage-like' phenotype.

Neither MM6, U937 nor KG-1 cells attached to the THP-1 in a temperature dependent manner. Jurkats stably transfected with wild-type CD31, exhibited less ability to attach to the THP-1 than Jurkats negative for CD31 [84]. Thus, although the binding at room temperature observed with both CD31 positive and CD31 negative Jurkats was similar, only CD31 positive cells showed temperature-dependent attachment at 37˚C. This observation implies that CD31 is mediating signalling in the Jurkat to permit active disengagement from the THP-1.

Experiments using CD31 positive Jurkats with double tyrosine mutations in the ITIM showed that the ITIM was essential for the temperature-dependent attachment of

viable Jurkats. This finding implied that signalling molecules involved in mediating the detachment signal require the ITIM intact. Molecules that bind to the cytoplasmic domain of CD31 via the ITIM include the protein tyrosine phosphatases SHP-1 and SHP-2. Experiments examining the attachment at room temperature with cells having single tyrosine mutations demonstrated that Y663F Jurkats exhibit temperature-dependent attachment. SHP-2 has been shown to preferentially bind to Y686 [63], and therefore act as a docking protein for downstream signalling molecules involved in motility. Consistent with this argument, the lack of temperature-dependent binding observed with Y686F Jurkats could be explained by the loss of SHP-2 binding to Y686, and consequently a failure to activate downstream signalling pathways.

There has been some controversy surrounding the role of the ITIM of CD31 and what role it plays in mediating migration of endothelial cells. Wound healing migration was impaired when endothelioma cells were transfected with a CD31 ITIM mutant, suggesting CD31 requires the ITIM to recruit SHP-2 and consequently may regulate focal adhesion turnover by dephosphorylating FAK during migration [59]. A similar study with a lung endothelial line showed cells transfected with an ITIM-deficient CD31 had increased migration, implying that recruitment of SHP-2 to the ITIM acted like a 'brake' to regulate migration. Increased β-catenin phosphorylation was also observed which could have loosened adherens junctions and enhanced migration [60]. However, another study by the same group[61] showed transfection of a mesothelioma cell line with an ITIM mutant CD31 made no difference to the ability of the cells to migrate, suggesting migration was independent of SHP-2 recruitment.

Instead, they showed that migration was dependent on a balance between Rac and Rho activity, with Rho activity required for the production and extension of lamellipodia. The work presented in this thesis suggests the ITIM of CD31 has a positive role in mediating leukocyte migration, which may allude to CD31 having different functions in leukocytes compared with endothelial cells.

Both SHP-1 and SHP-2 were targeted pharmacologically by the selective phosphatase inhibitor sodium stibogluconate. At 10µg/ml stibogluconate SHP-1 activity is blocked, and at 100µg/ml SHP-2 activity is inhibited [172]. Overall, attachment was unaffected at either concentration of the drug, but there was some inconsistency between results from each individual assay. The efficacy of the drug treatment was not tested, and this could be the reason for the variability.

Specifically targeting SHP-2 in Jurkats with siRNA to knock-down protein expression would confirm the role of the phosphatase in mediating leukocyte attachment to macrophages. SHP-2 could be acting as a docking protein for downstream signalling molecules, or could be involved in dephosphorylating CD31 to allow binding of alternative proteins that are normally inhibited from interacting with tyrosine phosphorylated CD31.

Having demonstrated that CD31 has a role in leukocyte motility *in vitro*, an *in vivo* model could have been developed. A model of leukocytes disappearing in the murine GOLO (greater omental lymphoid organ) has been used in this laboratory. The model demonstrated that when thymocytes were injected from either CD31

wild-type or CD31KO mice, more CD31 wild-type thymocytes were recovered in lavages than CD31KO thymocytes showing CD31 is mediating thymocyte detachment from peritoneal macrophages. The model could be adapted to target specific candidate molecules, such as SHP-2, by siRNA prior to injection into the mouse.

We postulated CD31 may be recruiting SHP-2 to the ITIM, where SHP-2 in itself acts as a docking protein for other SH2 domain containing proteins downstream that leads to the activation of Rac. Rac has been shown to destabilise adherens junctions and thus facilitate cell migration [144].

Investigation with GST pulldowns and subsequent MALDI-TOF analysis revealed eIF3 (Elongation initiation factor-3) which is an RNA helicase and myosin, a cytoskeletal component bound uniquely to the Y663F/Y686F mutant CD31 construct, and were not present in the wild type pulldown. These findings suggest CD31 may participate in a different signalling pathway in the absence of tyrosine phosphorylation. As CD31 is intimately involved in the turnover of focal adhesions, it is possible that CD31 could also contribute to the formation of spreading initiation centres (SIC). SIC have been shown as the precursors to focal adhesions and contain RNA and RNA binding proteins and actin [149].

Investigation with GST-CD31 constructs in a GST pulldown assay of Jurkat lysates revealed that SHP-1 was able to bind to the cytoplasmic domain of CD31 and that both ITIM tyrosines were required, which recapitulates previous work [57]. SHP-2 was

also found to bind CD31 via the ITIM tyrosines, with weak association demonstrated when either Y663F or Y686F single mutant tyrosine were used as bait, also confirming previous findings [62]. The pulldown method required much optimisation, to reproducibly demonstrate CD31 interaction with cytoplasmic proteins. When the original published method was used[60], high levels of non-specific binding to the GST tag were found. Removing non-specific binding required the cell lysate to be precleared with glutathione-agarose beads, and the presence of a detergent in the lysis buffer, in addition to extensive washing.

A number of proteins were screened by GST pulldowns and Western blot that were thought to bind to the cytoplasmic domain of CD31 and be involved in downstream signalling from SH-2 domain containing proteins. Interestingly, p120 RasGAP was found not to bind to the recombinant CD31 protein. However, RasGTP was recently found to bind to a Δexon15 isoform of CD31 in endothelial cells, and transduce intracellular signalling by activating ERK (extracellular signal-regulated kinase) and MAPK (mitogen-activated protein kinase)[70]. During leukocyte extravasation through the endothelium, ERK and MAPK activation is necessary for the leukocyte to migrate, as inhibiting the activation of these signalling molecules does not allow migration to take place[173].It could be that although the effector molecule RasGTP is capable of binding CD31, the guanidine exchange factors themselves may not associate directly with CD31.

β-catenin has been shown to bind to tyrosine phosphorylated CD31 in endothelial cells, where CD31 plays a role in the cycling of β-catenin from endothelial cell junctions through interactions with SHP-2. SHP-2 causes the dephosphorylation of

β-catenin, which then dissociates from CD31 allowing it to rejoin the adherens junction [65]. It was postulated that the interaction of β-catenin with CD31 may also occur in leukocytes and hence be involved in a signalling pathway during leukocyte migration. However, GST pulldowns analysis failed to demonstrate β-catenin binding to the cytoplasmic domain of CD31, which implies that β-catenin may have a different function in leukocytes compared with endothelial cells.

CD31 has been shown to be phosphorylated by src family kinases [54], and prior to use in pulldown analyses the GST-CD31 constructs required phosphorylation *in vitro* by recombinant c-src. Since the GST-CD31 constructs were not phosphorylated either when produced in the bacteria or in the cell lysate, and consistent with previous observations with endothelial CD31 showing CD31 is phosphorylated by src, but a GST-CD31 cytoplasmic domain fusion protein did not co-precipitate with src [54]. Results obtained by GST pulldown from Jurkat lysates demonstrated there was no binding of c-src to the cytoplasmic domain of CD31.

CD31 activates β_1 integrins during transendothelial migration of T cells [4]. Talin binds to both the β_1 integrin cytoplasmic domain and actin, thereby linking integrins to the actin cytoskeleton, thus talin binding can modulate integrin function. It had been suggested that CD31 binds talin via the cytoplasmic domain (personal communication, Dr David Critchley, Leicester University, UK), and CD31 might activate integrins via its association with talin. A study with NK cells showed talin associated with actin after CD31 induced rearrangement of the cytoskeleton [174].

However, investigation with GST pulldowns from Jurkat lysates did not confirm talin binding to the cytoplasmic domain of CD31. These data suggest although talin may be involved in CD31 induced integrin activation, it does not bind directly to CD31 cytoplasmic domain.

As previously shown, SHP-2 in apoptotic Jurkats was degraded in a caspase-dependent manner, whereas SHP-1 levels remained unchanged when compared with viable Jurkat lysates [84]. In order to test the hypothesis of differential recruitment of signalling and adapter molecules to the cytoplasmic domain of CD31, attempts were made to induce apoptosis in CD31 negative Jurkats. However, this proved problematic, with the treatments of Fas ligand, etoposide and cycloheximide inducing a high proportion of necrotic cells (20-60%) with low levels (<20%) of apoptosis. It was decided to use neutrophils as an alternative as they undergo constitutive apoptosis with little necrosis during overnight culture. Surprisingly, comparison of binding partners of CD31 in lysates of viable and aged neutrophils showed no change in SHP-1 or SHP-2 levels in binding to CD31 cytoplasmic domain in freshly isolated or aged neutrophils. However, the tyrosine phosphorylation levels of the cytoplasmic domain construct were decreased in aged neutrophils, which suggested there may be increased phosphatase activity in apoptotic neutrophils. CD31 dephosphorylation in neutrophils may be due to altered utilisation of signalling pathways during apoptosis, as shown in endothelial cells undergoing programmed cell death CD31 is dephosphorylated, resulting in the cellular detachment [155].

In preliminary studies by others in the laboratory, the 90kDa heat shock protein (Hsp90) has been shown to bind to CD31. The work undertaken in this thesis set out to elucidate which residues of the cytoplasmic domain of CD31 were important for the interaction with Hsp90. GST pulldowns from CD31 negative Jurkat lysates with the CD31 constructs Y663F, Y686F and Y663F/Y686F showed that the ITIM, and hence by inference tyrosine phosphorylation of the ITIM, was not required for Hsp90 binding. Pulldowns using a series of truncations of the cytoplasmic domain revealed two distinct regions that were required for Hsp90 binding, (CYFLRKAKAK) and (SNNEKMSDMEANSHY). (CYFLRKAKAK) has previously been shown to be a calmodulin binding region in platelets [163], and Hsp90 binds to calmodulin in complex with the glucocorticoid receptor [162]. This finding raises the possibility that Hsp90 may be binding to CD31 indirectly through calmodulin bound to CD31. However, analysis of low molecular weight bands (~17kDa) present in GST pulldowns of Jurkat lysates with MALDI-TOF failed to identify calmodulin. Repeating the GST pulldowns with non-phosphorylated truncated CD31 constructs showed no binding of Hsp90 to CD31, which suggested that Hsp90 requires the cytoplasmic domain tyrosine phosphorylated independently of the ITIM. There are two tyrosines upstream of the ITIM of CD31, Y596 and Y636, which could be phosphorylated and either bind an intermediary protein, or bind Hsp90 directly. However, Y595 did not need to be phosphorylated to bind calmodulin [163], which would further suggest that the intermediary protein may not be calmodulin. The same study also showed a CD31 peptide containing Y636 or phosphorylated Y636 did not bind calmodulin [163],

which adds weight to the suggestion that the intermediary protein is not calmodulin. Generating further mutations of CD31 at Y595 and Y636 to probe Jurkat lysates for Hsp90 binding would determine whether these residues are crucial for Hsp90 association and help us to identify if an intermediary protein is also required.

The region (SNNEKMSDMEANSHY) was also required for Hsp90 binding to CD31, containing the conserved region SNNEK which potentially could represent a helix region of a putative TPR motif. Further exploration of the TPR motif via site-directed mutagenesis of the basic amino acids revealed that whilst mutation N27A abrogated Hsp90 binding, mutating N27 to D did not prevent Hsp90 binding. This may be due to an alteration to the structure of the cytoplasmic domain of CD31 allowing Hsp90 to utilise the first asparagine of the S**N**NEK motif (N 26) and thus still bind. Downstream mutation of basic lysine residues 85 and 86 also prevented Hsp90 binding. These residues are postulated to be part of the carboxylic clamp which acts in concert with the TPR to mediate protein binding. The data presented here leaves open the possibility of the cytoplasmic domain of CD31 conforming to a TPR motif, however double mutations of both the TPR and carboxylic clamp would be necessary to confirm this.

The functional consequences of Hsp90 binding to CD31 were not explored in this work, for example the possibility of a role for CD31-Hsp90 interaction during leukocyte motility. Jurkats could be transduced to express CD31 with mutations in the regions required for Hsp90 binding identified here, and then assayed for the ability of the Jurkats to detach from a THP-1 monolayer.

As well as probing GST pulldowns for suspected CD31 binding partners, we also chose a non-biased approach of MALDI-TOF protein fingerprinting. By separating the GST pulldowns by SDS-PAGE and targeting unknown proteins we hoped to discover novel binding proteins of CD31. Of the proteins identified by this method, 14-3-3ε was of particular interest. 14-3-3ε is a member of the large family of 14-3-3 proteins which have diverse roles in cellular processes including ligand binding and protein localisation. This protein has been described as a 'molecular anvil' that binds proteins and changes their conformation enabling them to participate in intracellular signalling [148]. 14-3-3 proteins also bind SH-2 domain containing proteins [148], and could be participating in signalling through binding CD31 directly or by binding SHP-2 associated with CD31.

CD31 has been shown recently to activate a non selective cation channel, in response to hydrogen peroxide in endothelial cells. The regulation of ion channel function requires an intact cytoplasmic domain, as well as an intact ITIM, as mutation of the CD31 ITIM resulted in no activation [175]. Recent work in this laboratory has shown CD31 may be capable of inhibiting the repolarisation of macrophages through the potassium channel HERG (human ether-a-go-go related gene) following a depolarising stimulus (Brown *et al.* 2006 submitted). The adapter protein 14-3-3ε also binds to PKA phosphorylated HERG, and is involved in stabilising the HERG phosphorylation state. 14-3-3ε binds as a dimer by protecting HERG from the action of phosphatases which function to decrease HERG activity and enhance the activity of HERG, [176]. The data from GST pulldowns and MALDI-TOF studies raises the possibility of CD31 binding 14-3-3ε to regulate the function of HERG. β_1 integrins

are activated by CD31 during leukocyte transmigration [6]. Since HERG has been shown to be physically linked to β_1 integrins, and modulate their activation [177], CD31 could be regulating HERG to allow integrin activation during leukocyte migration. Also of interest given the finding of association between Hsp90 and CD31 is the requirement of HERG for the chaperone Hsp90 probably in complex with Hsp70 and other co-chaperones for HERG folding and maturation [178].

Although the function of the signalling and adapter molecules alluded to in this work have not been elucidated, they nevertheless suggest a number of novel and potentially exciting pathways to pursue. Particularly the possibility of CD31 in viable leukocytes, upon ligation of CD31 forming a macromolecular complex that will encompass different signalling and adapter molecules dependent on the tyrosine phosphorylation state of CD31, which could have implications for leukocyte migration (Figure 5.1:1). Phosphorylation of the ITIM tyrosines of CD31 recruits SHP-2, which could act as a docking protein for the recruitment of the SH2-domain containing protein Grb2. Grb2 may bind Gab1 and then associate with DOCK180 bound to ELMO. This complex could promote the activation of Rac and drive the formation of membrane ruffles and lamellipodia, and thus motility of the cell. The adapter protein 14-3-3ε may have multiple roles in cellular function, and as it is capable of binding to HERG and β_1 integrins, and may provide a mechanism for CD31-mediated activation of integrins and adhesion during the early stages of transmigration. Hsp90 may be acting as a transporter for src kinase movement to the membrane where it could phosphorylate CD31 both on the ITIM tyrosines and at

tyrosines 596 and 636. Hsp90 is required for HERG maturation [148], and has also been shown to bind to CD31, so may also be involved in the maturation of CD31.

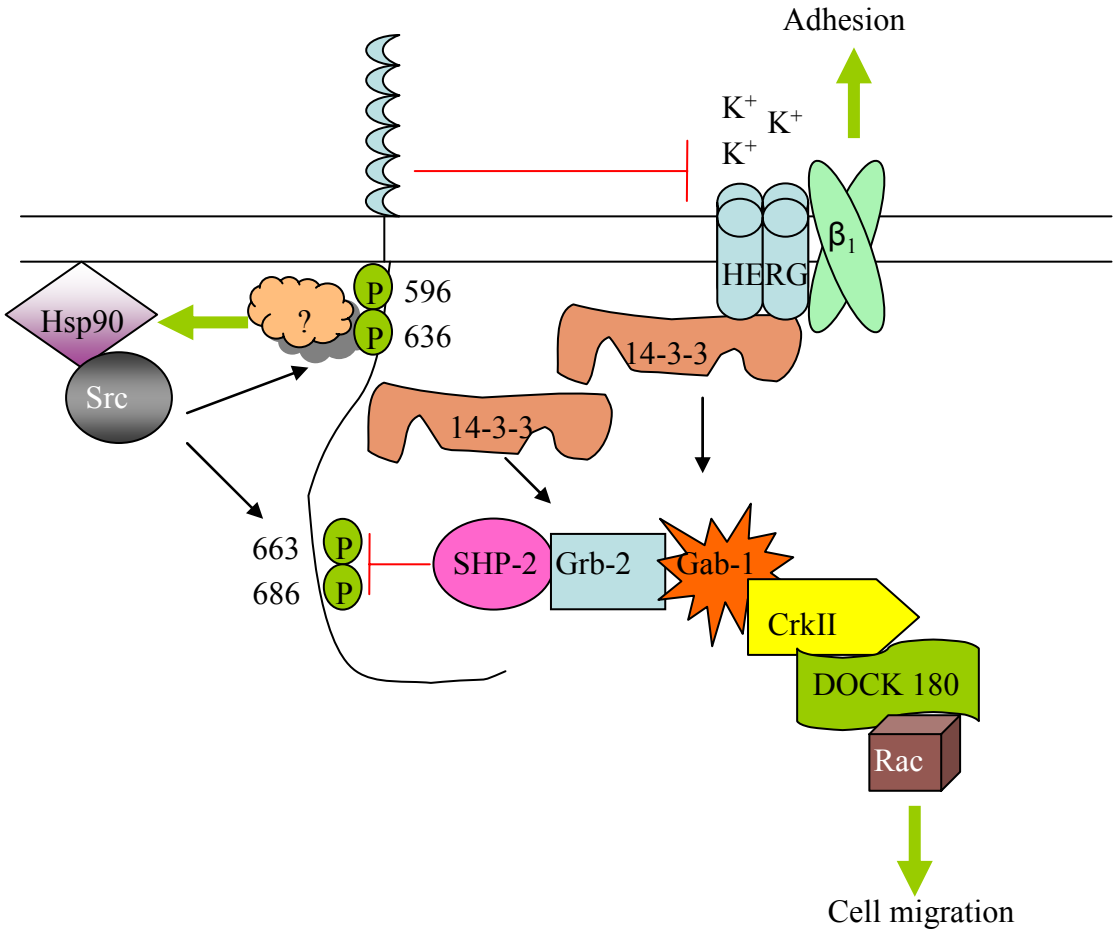

Figure 5.1:1. CD31 may be forming a macromolecular complex in viable leukocytes. A signalling pathway through SHP-2 binding to phosphorylated ITIM tyrosines and acting as a docking protein for the binding of SH2 domain containing proteins Grb2 and Gab1 which bind DOCK180, an exchange factor of Rac, which could regulate the activation of Rac. Hsp90 binding of CD31 through the potential association of an unknown intermediary protein may serve as a chaperone or transporter of src kinase, or of HERG, which could regulate β_1 integrin function.

5.2 Future Work

In view of the results presented in this thesis, future work with the attachment assay, in particular the use of siRNA delivered by lentivirus to target SHP-2, would be of major importance. Knocking-down the expression of SHP-2, and thus preventing the postulated signalling pathway from taking place, we would have expected to see a defect in temperature dependent attachment of viable CD31-expressing Jurkats to the THP-1 monolayer. To extend the attachment assay, the development of a suitable *in vivo* model of leukocyte attachment would be an important goal. A model of murine leukocyte-macrophage interactions in the GOLO has been used by others in this laboratory. Preliminary experiments introducing either wild-type or CD31 knock-out thymocytes into the GOLO have shown better recovery of wild-type thymocytes than knock-out (Dr Simon Watson, personal communication). This model could be adapted to knock-down SHP-2 expression in murine thymocytes, and assay the recovery of the thymocytes, where we would expect a defect in migration and more recovery. We would predict that SHP-2 phosphatase-dead mutant thymocytes in this assay exhibit reduced migration and thus confirm the *in vitro* findings presented here.

Data from GST pulldowns showing Hsp90 binding to CD31 provided biochemical evidence of an interaction between the two proteins, and further mutations of CD31 of both the postulated TPR motif and the carboxylic clamp region could be generated and assayed for Hsp90 binding. However, attributing function to the association of

Hsp90 with the cytoplasmic domain of CD31 may shed light on the question of Hsp90 involvement in mediating migration signals. Transducing Jurkats negative for expression of CD31 with constructs missing key residues identified by this work and then assaying their ability to attach to THP-1 cells, we expect to see an attachment defect if Hsp90 is either directly involved in a signalling pathway or is required for the correct folding of CD31. As has been postulated in this thesis, SHP-2 signalling through its association with CD31 may represent a critical event in providing viable leukocyte detachment signals. Generating a SHP-2 construct to use in GST pulldowns, both wild-type and a catalytic mutant, would then allow detailed dissection of the signalling pathway and identify which additional proteins are involved.

6 Materials and Methods

6.1 MOLECULAR BIOLOGY

6.1.1 *E. coli Competent Cell Preparation*

A single colony from an LB plate was picked and grown up in 2.5ml LB medium at 37°C with shaking overnight. The culture was diluted 1:100 in fresh LB supplemented with 1M $MgSO_4$ and grown at 37°C with shaking until the OD600nm read between 0.4 and 0.6. Cells were centrifuged at 4500g at 4°C for 5 minutes. The cell pellet was resuspended in 0.4 volume ice-cold filter-sterilised TFB1 buffer pH 5.8. The cells were centrifuged again and resuspended in 0.25-volume ice-cold filter-sterilised TFB2 pH 6.5 for 30 to 60 minutes. Cells were aliquoted and quick-frozen in liquid nitrogen before storage at -70°C.

6.1.2 *Polymerase Chain Reaction (PCR)*

CD31 Products were amplified from constructs in pcDNA3, for details of primer sequences, restriction sites added and PCR programme see Appendix.

6.1.3 *Cloning*

The amplified fragments were ligated into pGEMTeasy (Promega), by virtue of the overhanging A bases added by Taq polymerase during amplification. The ligations were transformed into DH5α competent *E. coli* cells and colonies selected on LB agar supplemented with ampicillin 100mg/ml overnight. Positive colonies were selected based on blue/white screening, where the addition of an insert into pGEMTeasy vector disrupts the β-lactimase gene, resulting in no metabolism of the X-gal substrate. Single white colonies were grown up in 5ml LB supplemented with

ampicillin 100µg/ml with shaking overnight at 37°C. Plasmid DNA was extracted using a kit (Qiagen) and digested with Bam HI and Sal I restriction enzymes. The resulting digest was separated on 1% agarose gel and the fragment extracted from the agarose (Qiagen).

The digested DNA fragments were cloned into pGEX vector containing a glutathione-S-transferase (GST) sequence, transformed into XL-1 blue competent cells and selected on LB agar supplemented with ampicillin 100mg/ml. Single colonies were picked and the plasmids extracted as described. Purified plasmids were sequenced with the primers described in Table 7.1:10.

6.1.4 *Site-directed Mutagenesis of CD31*

Primers were designed to introduce the mutation required into CD31. PCR was carried out on wild-type CD31 in pcDNA3 as described to generate a super primer, which is 100-200bp double-stranded DNA (Table 7.1:10). The super primer was then ran on 1% agarose gel and purified using Qiagen gel purification kit. The super primer is then used in PCR with proof-reading DNA polymerase Pfu Turbo to replicate the whole plasmid. The reaction was digested with 2µl Dpn I, 8µl 10X buffer and 20µl distilled water for 6 hours to remove methylated original DNA template. The reaction was heat-inactivated at 65˚C for 10 minutes and cooled at room temperature for 10 minutes. 8µl of the reaction was used to transform 100µl chemically competent *E. coli*. Single colonies were picked into LB medium supplemented with 100µg/ml ampicillin overnight with shaking at 37˚C. Minipreps

were carried out to purify the mutated plasmid DNA and the mutation was confirmed by sequencing.

6.1.5 *Reconstitution of Plasmid DNA from Filter Paper*

The plasmid on filter paper was added to 300µl distilled water and incubated at room temperature for 10-15 minutes. The tube was centrifuged at 13000rpm for 3 minutes. 5µl of the reconstituted DNA was transformed into JM109 chemically competent bacteria and plated onto LB-agarose supplemented with 100µg/ml ampicillin overnight at 37˚C.

6.1.6 *Chemically Competent Bacteria Transformation*

An aliquot of competent *E. coli* was allowed to thaw on ice. In a separate Eppendorf, 2-5µl of ligation mix was transferred, and mixed with the thawed bacteria, on ice for 30 minutes. The cells were heat shocked for 1 minute and then returned to ice for 2 minutes. 400µl SOC media was added and the cells incubated at 37˚C with shaking for 30 minutes. The cells were centrifuged at 200g for 4 minutes and the media discarded. The cells were plated onto LB-agarose supplemented with ampicillin 100µg/ml overnight at 37˚C.

6.1.7 *Bacterial Glycerol Stock Preparation*

A single colony from a selection plate was picked into 2ml LB medium supplemented with 100µg/ml ampicillin and incubated with shaking at 37˚C

overnight. 1ml of the culture was added to 80% glycerol and mixed. The stock was stored at -80˚C.

6.1.8 *Electroporation of Competent Bacterial Cells*

An aliquot of electrocompetent BL21 *E. coli* cells were defrosted on ice and 2µl of ligation mix were added to the cells and mixed. The cells and DNA were transferred to an electroporation cuvette and the pulse was triggered with the following parameters employed: Voltage 2500V, capacitor 25µF and shunt resistor 201R. 1ml of SOC medium was added, and the cells were transferred into an Eppendorf and incubated at 37°C with shaking for 30 minutes. The cells were plated onto LB-agarose supplemented with 100µg/ml ampicillin and incubated at 37˚C overnight.

6.2 RNA Methods

6.2.1 *RNA Isolation*

1ml of Trizol was added per 5 million cells and the cells were homogenised, then incubated at room temperature for 5 minutes and 200µl of chloroform was added. The tube was shaken vigorously for 15 seconds, and incubated at room temperature for 5 minutes. The tube was centrifuged at 12000***g*** and 4˚C for 15 minutes to separate the phases. The aqueous phase was transferred to a fresh tube and 500µl Trizol and 200µl chloroform was added. The tube was shaken vigorously for 15 seconds and incubated at room temperature for 5 minutes. The tube was centrifuged at 12000***g*** and 4˚C for 15 minutes to separate phases. The aqueous phase was transferred to a fresh tube and 500µl isopropanol was added. The tube was incubated

at room temperature for 15 minutes and centrifuged at 12000***g*** at 4˚C for 10 minutes. The supernatant was removed and 1ml 75% ethanol was added and the tube shaken vigorously. The tube was centrifuged at 7500***g*** for 5 minutes. The supernatant was removed completely and the pellet was allowed to dry. The pellet was resuspended in DEPC treated distilled water.

6.2.2 *Conversion of RNA to cDNA*

To each reaction tube 5µl of 10X reverse transcription buffer, 11µl 25mM $MgCl_2$, 10µl dNTPs, 2.5µl random hexamers, 1µl RNAse inhibitor, 1.25µl reverse transcriptase and 200ng RNA was added. The volume was made up to 50µl with RNAse-free distilled water. The reaction was incubated in a PCR machine with the following programme: 25˚C for 10 minutes and 95˚C for 5 minutes.

6.2.3 *siRNA Delivery by Electroporation of Jurkats*

SHP-2 and lamin A/C RNA was prepared according to the manufacturer's instructions and 2µg was transfected into 1 million CD31 positive Jurkat cells using Amaxa protocol A17. The cells were incubated at 37˚C and 5% CO_2 for 24, 48 and 72 hours. Knock-down was analysed by western blot.

6.2.4 *siRNA Construction for Lentiviral Delivery in Jurkats*

siRNA short hairpin constructs were generated with Sal I and Hind III restriction sites at both 5' and 3' end, and containing a loop TCAAGAG for insertion into pLenti6MCS-H1.CMV-GFP vector.

Name	siRNA Sequence
SHP-2 sense strand	CGACCGAATATGGCGTCATGCGTGT**TCAAGAG**ACAC GCATGAGCGCATATTGTTTTTG
SHP-2 antisense strand	GGGCTTATAGCGCAGTACGCACA**AGTTCTC**TGTGCG TACTCGCGTATAACAAAAACAGCT
Lamin A/C sense strand	TCGACCCGGGTGGTGACGATCTGGGCT**TCAAGAG**AG AGCCCAGATCGTCACCACCGTTTTTG
Lamin A/C antisense strand	GGGCCCACCACTGCTAGACCCGA**AGTTCT**CTCGGGT CTAGCAGTGGTGGCAAAAACAGCT
Scrambled sense strand	TCGACCCGAACAGATGAATATAACAATC**TCAAGAG**G ATTGTTATATTCATCTGTTCGTTTTTG
Scrambled antisense strand	GGGCCTTGTCTACTTATATTGTTAG**AGTTCT**CCTAAC AATATAAGTAGACAAGCAAAAACAGCT

Table 6.2:1. Sequence of siRNA sense and antisense strands for SHP-2, lamin A/C and scrambled including the Sal I restriction site at both 5' and 3' ends, and in bold the loop for generation of short hairpin RNA.

6.3 Protein Chemistry

6.3.1 *Preparation of Agarose Beads*

100µl (GST pulldowns) or 500µl (protein purification) of glutathione-agarose beads (Amersham, Bucks, UK) were washed twice with 500µl/2.5ml of PBS, the supernatant was cleared by centrifugation at 500***g*** for 5 minutes and discarded. Cell lysate or recombinant protein was added directly to the prepared beads.

6.3.2 *GST Fusion Protein Purification*

A single colony from a transformation plate was picked into 20ml LB supplemented with 100µg/ml ampicillin and grown overnight at 37°C with shaking. The culture was diluted 1:10 in LB and 100µg/ml ampicillin and grown for 60 minutes at 37°C with shaking. 0.1mM IPTG was added and the culture grown for 3 to 5 hours. The cells were pelleted at 4000rpm for 20 minutes at 4°C. The pellet was resuspended in 10ml 1% Triton-X100/PBS buffer on ice. The cells were sonicated at 50% power for four pulses of 30 seconds in duration. Trypan blue staining checked lysis, with lysed cells turning blue. The cell lysates were centrifuged at 20000g for 30 minutes at 4°C and the supernatant transferred to a fresh tube. A 50% solution of 25mM Tris, 140mM sodium chloride and glutathione-agarose beads (Sigma) was added to the supernatant and rotated for 30 minutes at 4°C. The sample was centrifuged at 500g for 5 minutes and the supernatant discarded. The beads were washed with PBS three times and the GST fusion protein was eluted with 1ml elution buffer rotating for 10 minutes at room temperature. The elution was repeated twice. Eluted fractions were read at 280nm to determine protein concentration in mg/ml.

6.3.3 *Purification of His-talin*

The His-talin protein was purified using a Magnehis kit (Promega). A 1ml 3 hour culture of transformed BL21 bacteria was read at OD_{600} and centrifuged at 10000***g*** for 2 minutes and the supernatant discarded. For every 1 OD_{600} unit, the supplied lysis buffer was diluted ten times with ultrapure water, and added to the bacteria pellet. 1µl DNAse was added and the mixture incubated at room temperature with shaking to lyse the bacteria. 0.3g/ml NaCl was added to improve the magnetic bead binding to the his-tagged protein. 30µl of his-nickel beads were added per 1.1ml lysate, and mixed for 2 minutes. The tubes were placed against a magnetic stand to capture the magnetic beads. The supernatant was carefully removed with a pipette. The beads were washed three times with supplied wash buffer. The purified protein was eluted from the beads incubating for 2 minutes at room temperature in supplied elution buffer containing 500mM imadazole.

6.3.4 *His-talin Pulldown in Capture Buffer*

50µg of purified his-talin was added to CD31 positive Jurkat lysates and incubated with rolling at 4˚C for 30 minutes. 100µl his-nickel magnetic beads were added and incubated at 4˚C with rolling for 2 minutes. The beads were washed three times in 500µl capture buffer for 2minutes. The beads were resuspended in 100µl elution buffer, a total of three times. The eluate was precipitated overnight in 95% ethanol at -20˚C. The precipitate was centrifuged at 5000***g*** for 10 minutes and the pellet air dried. 50µl of sample buffer was added to resuspend the pellet and then boiled for 5 minutes. 10µl of the sample was loaded onto a 10% acrylamide gel.

6.3.5 *Pre-optimised GST Pulldown Assay*

All steps were performed at 4°C with rotating. 100µg of GST-CD31 protein were added to cell lysates for 30 minutes. 500µl of 50% glutathione-agarose beads/PBS were added for 30 minutes. The beads were pelleted at 500***g*** for 2 minutes at 4°C and then washed in 500µl GST pull-down buffer for 30 minutes. The beads were pelleted at 500***g*** for 2 minutes then the protein eluted using 500µl elution buffer, rotating at room temperature for 10 minutes. The eluted protein was precipitated in 95% ethanol overnight at -20˚C. The precipitated protein was centrifuged at 15000***g*** for 10 minutes at 4˚C, the ethanol removed and the pellet dissolved in 50µl Laemmli sample buffer, with vortexing. The sample was boiled for 5 minutes before loading onto 10% reducing SDS Tris-glycine gel.

6.3.6 *Recombinant Protein Coupling to Beads*

10µg of recombinant GST or GST-CD31 protein was added to prepared glutathione-agarose beads and rolled at room temperature for 30 minutes. The beads were washed with 500µl of PBS and centrifuged at 500***g*** for 5 minutes to remove unbound protein. Cell lysate was added directly to the prepared beads in accordance with the protocol.

6.3.7 *Method 1 GST Pulldown*

The beads were combined with recombinant protein and the lysate added with rolling at 4˚C for 90 minutes. The beads were centrifuged at 500***g*** for 5 minutes and the

supernatant discarded. The beads were washed three times in lysis buffer and resuspended in sample buffer before being loaded onto a 10% reducing SDS-PAGE gel.

6.3.8 *Method 2 GST Pulldown*

The cell lysate was precleared with 100µl glutathione-agarose beads overnight at 4˚C. The beads were centrifuged at 500***g*** and the supernatant removed, then added to recombinant protein coupled to fresh glutathione beads and rolled at 4˚C for 2 hours. The beads were washed three times in lysis buffer and once in PBS, then the beads were resuspended in 50µl PBS before being combined with an equal volume of sample buffer and boiled and applied to a 10% reducing SDS-PAGE gel.

6.3.9 *Method 3 GST Pulldown*

Glutathione-agarose beads were combined with recombinant protein and added to the cell lysate at 4˚C with rolling for 2 hours. IP buffer was added and the mixture rolled for another 2 hours. The beads were centrifuged at 500***g*** and the supernatant discarded. The beads were washed once with IP buffer and resuspended in sample buffer before being applied to a 10% reducing SDS-PAGE gel.

6.3.10 *In vitro Phosphorylation*

10µg recombinant protein was combined with 0.01U recombinant src kinase, 1µM ATP to a total volume of 50µl with phosphorylation buffer, and incubated at room temperature for 15 minutes.

6.3.11 *Preparation of Protein Samples for MALDI-TOF*

GST pulldowns were prepared as described, and lyophilised. The sample was reduced with 60µl of reducing sample buffer, vortexed and incubated at 70˚C for 10 minutes. In a laminar flow hood, the sample was separated by electrophoresis on a 4-12% MOPS-SDS gradient gel at 200mV for 1 hour. The gel was washed three times with deionised water and stained with colloidal blue stain with rocking for 1 hour at room temperature. The gel was destained three times with deionised water. The bands of interest were excised from the gel and chopped into small pieces. 250µl of 100mM ammonium bicarbonate was added to each gel piece, and the gel pieces were shaken for 15 minutes. The liquid was removed from the gel pieces and 250µl 50% acetonitrile was added for 10 minutes with shaking. The liquid was the removed and the gel pieces dried by speed vacuum. 50µl DTT dissolved in 100mM ammonium bicarbonate was added and the gel pieces incubated at 56˚C for 1 hour. 50µl of 9.25g/ml iodoacetamide solution was added and the gel pieces were incubated in the dark at room temperature for 30 minutes. The liquid was removed and 200µl ammonium bicarbonate were added for 15 minutes at room temperature with shaking. The liquid was removed and 200µl 50% acetonitrile were added at room temperature with shaking. 30µl of trypsin buffer were added to the gel pieces plus 10µl of trypsin solution (12.5µg/ml trypsin and 1mM HCl in ammonium bicarbonate). Incubate the reaction at 30˚C overnight with shaking. Centrifuge sample to collect gel pieces and add an equal volume of acetonitrile. Spot 0.5µl onto a sample well of a MALDI-TOF plate and allow to dry before spotting another. Add 0.5µl of matrix solution and allow to dry completely before analysis.

6.3.12 *Silver Staining of SDS-PAGE gel*

Incubate the gel in solution A for 30 minutes at room temperature. Wash the gel in solution B for 15 minutes then three times in bidistilled H_2O. Sensitise the gel in solution C for 2 minutes and wash three times in bidistilled H_2O for 30 seconds each wash. Stain for 25 minutes in solution D and wash three times for 1 minute each in bidistilled H_2O. Develop in solution E for 5 to 10 minutes and stop in solution F for 10 minutes. Rinse the gel in bidistilled H_2O.

6.3.13 *Western Blotting*

Protein was transferred from polyacrylamide gel onto PVDF membrane at 100V for 1 hour with ice pack and stirring. The membrane was blocked in 5% milk/PBS overnight at 4˚C, then washed three times in 0.1%Tween 20/PBS for 10 minutes each. The primary antibody was added (SHP-1, SHP-2 1:500, Hsp90 1:500, GST 1:5000, src 1:1000, β-catenin 1:1000, p120 1:1000, talin 1:1000) diluted in 0.1% Tween 20/PBS for 2 hours at 4˚C. The membrane was washed as described and the secondary antibody conjugated to HRP was added at 1:1000, diluted in 0.1% Tween 20/PBS for 1 hour at 4˚C. The membrane was washed a further three times in 0.1% Tween 20/PBS for 10 minutes each. ECL plus reagents were added to the membrane, and the membrane was exposed to X-ray film and developed in an Xograph film developer

6.4 Cell Biology

6.4.1 *Cell Culture*

Jurkats and THP-1 were routinely maintained in suspension in RPMI medium supplemented with 10% heat inactivated foetal calf serum, 10mM glutamine, 10mM penicillin-streptomycin at 37˚C and 5% CO_2.

HEK-293T cells were maintained in DMEM medium supplemented with 10% heat inactivated foetal calf serum, 10mM glutamine, 10mM penicillin-streptomycin at 37˚C and 5% CO_2 at 30-50% confluence. To split the cells 5ml trypsin/EDTA was added for 5 minutes at room temperature. The flask was banged to release the cells and 10ml of medium was added and pipetted up and down the side of the flask to wash cells off. The cells were then centrifuged at 220rpm for 5 minutes and resuspended in fresh media.

THP-1 were differentiated in an 8-well chamber slide in RPMI with 10ng/ml PMA for 5 days. The cells became adherent and their morphology became spindle-like.

6.4.2 *Isolation of Human Neutrophils*

40ml of freshly isolated venous blood was added to 4ml 3.8% sodium citrate in a 50ml tube and mixed carefully. The tube was centrifuged at 12000rpm for 20 minutes with the brake off. The supernatant containing protein-rich plasma (PRP) was removed and 25ml was reserved. To make serum the remaining PRP was aliquoted into glass tubes and incubated with 400µl 1M $CaCl_2$ at 37˚C until the solution cleared. PRP was centrifuged at 300rpm for 15 minutes to provide platelet pellet and protein-poor plasma (PPP); the PPP was decanted into a fresh tube. To the

remaining cells 5ml 6% dextran was added and made up to 50ml with 0.9% NaCl, and mixed carefully. The cell mixture was incubated at room temperature for 15-30 minutes until it separated into two layers. The top leukocyte-containing layer was removed and centrifuged at 1000rpm for 6 minutes. The supernatant was discarded and the leukocytes were resuspended in 2ml PPP. Gradients of 42% and 51% percoll/PPP were made in separate tubes and vortexed to mix. The leukocytes were underlaid with the 42% gradient then with 51% gradient avoiding bubbles at fluid interface. The gradients were centrifuged at 1000rpm for 10 minutes with the brake off, monocytes separated at the top layer, neutrophils at the bottom layer. The neutrophil layer was removed and made up to 50ml with serum-free medium. The neutrophils were centrifuged at 12000rpm for 5 minutes, and the supernatant was removed and the neutrophils resuspended in media at a concentration of 4 million cells per ml.

6.4.3 *Inducing Apoptosis in Jurkats*

Cells were counted and centrifuged at 220g for 5 minutes, the media was discarded and the cells resuspended in RPMI without serum and supplemented with 10mM glutamine, 10mM penicillin-streptomycin. 1:1000 dilution of CH11 (anti-FasL) antibody was added and mixed gently. The cells were incubated at 37˚C and 5% CO_2 overnight. Apoptosis was assessed by annexin V and propidium iodide staining.

6.4.4 *Inducing Apoptosis in Neutrophils*

Freshly isolated human neutrophils were resuspended in IMDM media with 10mM glutamine, 10mM penicillin-streptomycin in the absence of serum, and incubated at 37˚C and 5% CO_2 overnight. Apoptosis was measured by annexin V and propidium iodide staining.

6.4.5 *Attachment Assay*

2 $X10^6$ THP-1 were differentiated into 8 well chamber slides as previously described over 5 days at 37˚C and 5% CO_2 [179]. The media was replaced with fresh containing no serum. The cells were stained with 0.1µl of 1mg/ml Celltracker orange for 15 minutes at room temperature. 1 X 10^6 Jurkats were counted and resuspended in 4ml media without serum and stained with 0.1µl of 1mg/ml Celltracker green for 15 minutes. 0.5ml Jurkat suspension was added to each of the wells and left to settle for 15 minutes at room temperature. The plate was immersed in a bath of prewarmed media (37˚C) and inverted under the liquid taking care not to introduce any bubbles. The plate was then incubated at 37˚C for 30 minutes. The plate was turned upright and removed from the media bath. The media was removed and 0.5ml trypsin/EDTA added to each well. The plate was incubated at 37˚C for 15 minutes. An equal volume of media was added to each well to neutralise the trypsin. Cells were harvested by pipetting up and down, centrifuged at 500***g*** for 5 minutes and resuspended in 0.5ml FACS buffer and analysed by flow Cytometry (Beckman Coulter).

6.4.6 *Annexin V and Propidium Iodide Staining*

Cells were centrifuged at 220***g*** for 5 minutes and resuspended in annexin binding buffer. Four tubes were set up as follows, unstained cells, Annexin V-FITC only for 20 minutes on ice, propidium iodide only and both annexin-V and propidium iodide. Propidium iodide was added to the cells immediately before analysis by flow cytometry.

6.4.7 *CD31-FITC Antibody Staining*

Cells were centrifuged at 220***g*** for 5 minutes and resuspended in 0.5ml FACS buffer. CD31-FITC or isotype control IgG-FITC was added at 1:100 dilution of stock, incubating on ice for 1 hour. The cells were centrifuged again and washed with 1ml FACS buffer. Cells were resuspended in 0.5ml FACS buffer and analysed by flow cytometry.

6.4.8 *Neutrophil Lysis*

50 million neutrophils were lysed in 5ml cell lysis buffer 2 with 2mM levamisole, 10mM β-glycerophosphate, 10mM NaF, 10mM Na_3VO_4, and 1 tablet of protease inhibitor cocktail (Roche) on ice for 20 minutes. Lysis was confirmed by trypan blue staining. The lysate was cleared by centrifugation at 13000rpm for 15 minutes.

6.5 Lentiviral Methods

6.5.1 *Packaging Virus*

HEK-293T cells at 30-50% confluency (cultured in DMEM with 10% heat inactivated foetal calf serum, 10mM glutamine, 10mM penicillin-streptomycin at 37˚C and 5% CO_2), were transfected with plasmid packaging mix. For each transfection 1462.7µl of Optimem and 45.3µl FuGene (Roche) were mixed together and incubated at room temperature for 5 minutes. 10.2µg of the SHP-2 or SHP-2 C-S pLenti plasmid was mixed with 5.1µg of GagPol plasmid (pESYNGP), 2.5µg Rev plasmid (pPLP-2) and 0.2µg Env plasmid (pVSV-G). The plasmid mix was added to the transfection reagent mix and 1560µl of the resultant mixture was added drop-wise to each plate of cells. The cells were incubated at 37°C with 5% CO_2. For vectors containing the CMV enhancer/promoter, 300µl of sodium butyrate was added to each plate after 24 hours to induce expression. The medium was changed to fresh complete medium (DMEM with 10% FCS, 100mM penicillin-streptomycin, 10mM glutamine) after 6 hours of incubation at 37ºC. Approximately 16-18 hours later, the virus-containing medium was aspirated from the plates and was filtered to remove cellular debris using a 150ml filter (0.44µm; Nalgene). The unconcentrated virus is then aliquoted into 1ml cryovials and stored at -80˚C.

6.5.2 *Lentivirus Transduction of Cells*

1 $X10^6$ cells (CD31 negative Jurkats) were centrifuged at 220***g*** for 5 minutes, and resuspended in 100µl fresh medium in a 48 well plate. 250µl lentivirus (CD31-pLenti, SHP-2-pLenti, SHP-2 C-S-pLenti) vector solution was added to the cells and mixed. The cells were incubated overnight at 37˚C and 5% CO_2. 300µl of fresh media is then added to each well and incubated overnight again. Approximately 48-72hrs post-transduction the cells were ready to test for expression of protein by either

surface antibody staining (CD31) or by western blotting (SHP-2). Stable integration was confirmed by RT-PCR.

6.5.3 *X-Gal Staining Solution*

Transduced cells were washed twice with PBS and 500µl of X-gal staining solution was added. The cells were incubated at 37˚C and 5% CO_2 for 3 hours before visualisation under a light microscope.

6.6 Buffer Composition

All reagents were purchased from Sigma unless otherwise stated.

TFB1
30mM potassium acetate
50mM manganese chloride
10mM calcium chloride
100mM rubidium chloride
15% glycerol
Adjust pH to 5.8

TFB2
10mM MOPS
75mM calcium chloride
10mM rubidium chloride
15% glycerol
Adjust pH to 6.5

GST Pulldown Buffer
50mM Tris
100mM sodium chloride
100mM β-mercaptoethanol
0.5% Tween 20

Laemmli Sample Buffer
0.6ml 1M Tris-HCl pH 6.0
5ml 50% glycerol
2ml 10% SDS
0.5ml β-mercaptoethanol
1ml 1% bromophenol blue
0.9ml distilled water

GST Elution Buffer

25mM Tris

140mM sodium chloride

5mM reduced glutathione

Jurkat Lysis buffer +Tx100

20mM Tris pH8

137mM sodium chloride

2mM EDTA

1mM sodium fluoride

1mM sodium pervanadate

10% glycerol

1% triton-X

1mM protease inhibitor cocktail

SOC Medium

2g Bactotryptone

0.5g Bactoyeast extract

1ml 1M NaCl

0.25ml KCl

1ml 2M Mg^{2+} stock

1ml 2M glucose

Add tryptone and yeast to 97ml deionised water, dissolve and add NaCl and KCl. Autoclave and allow to cool before adding glucose and Mg^{2+} stock. Filter through 0.2µm filter and store at 4˚C.

Mg^{2+} Stock

20.33g $MgCl_2.6.H_2O$

24.65g $MgSO_4.7H_2O$

Dissolve in 100ml distilled water and filter sterilise.

LB medium

10g Bactotryptone

5g Bactoyeast extract

5g NaCl

Add deionised water to 1 litre. Adjust pH to 7.5 with NaOH and autoclave.

Trypsin Buffer

70µl of 1% nog (n-octyl-nβpyranoside)

630µl of 20mM ammonium bicarbonate solution

TBE Electrophoresis Buffer (10X)

108g Tris

55g Boric acid

40ml 0.5M EDTA

Make up to 2 litres with distilled water and autoclave.

PAGE Running Gel (10%)

4ml distilled water

3.3ml 30% acrylamide

2.5ml Tris pH 8.8

100µl 10% SDS

100µl 10% ammonium persulphate

4µl TEMED

PAGE Stacking Gel

2.1ml distilled water

0.5ml 30% acrylamide

30µl 10% SDS

30µl 10% ammonium persulphate

3µl TEMED

Sealing Gel for PAGE

0.5ml acrylamide

2ml distilled water

10µl TEMED

25µl 10% ammonium persulphate

Coomassie Blue Stain

0.25g Coomassie blue

90ml 1:1 v/v methanol/water

10ml acetic acid

Anode Buffer

30g Tris

5g SDS

Make up to 5 litres with distilled water and adjust pH to 8.6

Cathode Buffer

144g Glycine

30 g Tris

5g SDS

Make up to 5 litres with distilled water.

Transfer Buffer

3.35g Tris

14.42g glycine

200ml methanol

Make up to 1 litre with distilled water.

TE Buffer

10mM Tris-HCl ph 7.5

1mM EDTA

FACS Buffer

0.5% BSA

0.05% sodium azide

Dissolve in PBS without calcium/magnesium

Capture Buffer

10mM imadazole

1mM NaF

1mM β-mercaptoethanol

Dissolve in PBS

Annexin Binding Buffer

10mM HEPES

140mM NaCl

5mM KCl

1mM $MgCl_2$

2.5mM $CaCl_2$

Adjust pH to 7.4

High/Low Salt Cell Lysis Buffer

10mM Tris

1mM EDTA

1mM 1,10-phenanthroline

1mM NaF

1mM sodium pervanadate

1mM protease inhibitor cocktail

(For high salt add 200mM NaCl)

Bead Wash Buffer 1

10mM Tris

100mM β-mercaptoethanol

Bead Wash Buffer 2

10mM Tris

GST Pulldown Buffer 1

20mM Tris

200mM NaCl

Adjust to pH8

GST Pulldown Buffer 2

20mM Tris

200mM NaI

Adjust pH to 8

Amido Black Stain

0.1% amido black

25% IPA

10% acetic acid

Amido Black Destain

25% IPA

10% acetic acid

Silver Stain Solution A

100ml 50% methanol

10% acetic acid

Prepare in bidistilled H_2O

Silver Stain Solution B

100ml 50% methanol

Silver Stain Solution C

0.2g sodium thiosulphate

1 litre of bidistilled H_2O

Silver Stain Solution D

200mg silver nitrate

100ml bidistilled H_2O

Silver Stain Solution E

3g sodium carbonate

50µl formaldehyde (37% stock)

2ml solution C

Make up to 100ml bidistilled H_2O

Silver Stain Solution F

1.4g sodium-EDTA

100ml bidistilled H_2O

Method 1 Cell Lysis Buffer

20mM Tris pH7.4

1% Triton-X_{100}

2mM $MgCl_2$

150mM NaCl

1mM NaF

1mM Na_3VO_4

1mM protease inhibitor cocktail

Method 2 Cell Lysis Buffer

50mM Tris-HCl pH7.4

1% IPEGAL 40

250mM NaCl

1mM NaF

1mM Na3VO4

1mM protease inhibitor cocktail

Method 3 Cell Lysis Buffer

50mM Tris pH7.4

1% IPEGAL 40

10% glycerol
150mM NaCl
1mM Na3VO4
1mM NaF
1mM protease inhibitors

Method 3 IP Buffer
50mM Tris pH7.4
1% Triton-X100
150mM NaCl
5mM EDTA

X-Gal Staining Solution
0.025g potassium ferricyanide
0.032g potassium ferrocyanide
30µl 1M MgCl
150µl 50mg/ml X-gal
15ml PBS

7 Appendix

7.1 CD31 Mutant Cytoplasmic Domain Construction

7.1.1 *The Discovery of CD31*

A 135kDa protein was identified from monoclonal antibody Hec7 screening of endothelial cell proteins, and found to localise at intracellular junctions on the surface of endothelial cells *in vitro* and *in vivo* [49].

CD31 was first identified from an endothelial expression library, where positive clones were revealed by epitope selection. The positive clones reacted against a 130kDa protein found at intracellular junctions, and was designated platelet-endothelial cell adhesion molecule-1 (PECAM-1) [180]. In HUVEC (human umbilical cord endothelial cells) a monoclonal antibody panel was used to screen for protein localised to cell-cell contacts. A cDNA library was produced from proliferating HUVEC, and positive clones, identifying CD31 were produced by transient transfection of Cos cells [181].

7.1.2 *CD31 Cloning*

CD31 (wild-type and tyrosine mutants) was cloned into pcDNA3 (Figure 7.1:1) from a cDNA library, and then PCR amplified into pGEX 4T (Figure 7.1:2) for protein production [63]. I have amplified wild-type, tyrosine mutant (Y663F, Y686F, Y663F/Y686F, Y701F) and serine mutant (S620A, S669A, S673A, S702A-designated QSA) CD31 cytoplasmic domains from pcDNA3 constructs (Dr Michael Douglas, Birmingham University, UK). Site-directed mutagenesis was utilised to create

SNNEK and lysine mutants from wild-type CD31 in pcDNA3. For SNNEK and lysine mutants, and truncated constructs amplification was from full-length wild type CD31 in pcDNA3. The PCR products were amplified to include 5' Bam HI site and either a Sal I or Not I 3' site. The fragments were subcloned into pGEMTeasy (Figure 7.1:3). Taq polymerase adds overhanging A bases which enable the PCR fragments to be cloned in either way into pGEMTeasy due to its overhanging T bases. The PCR fragments were then cloned into pGEX 4T for protein production.

DNA and amino acid sequence of CD31 cytoplasmic domain shows the position of the tyrosines (mutated to phenylalanine) and serines (mutated to alanine) (Figure 7.1:4). A diagrammatic representation of each of the constructs generated shows the N-terminal GST tag and position of mutations and truncations (Figure 7.1:5 and Figure 7.1:6).

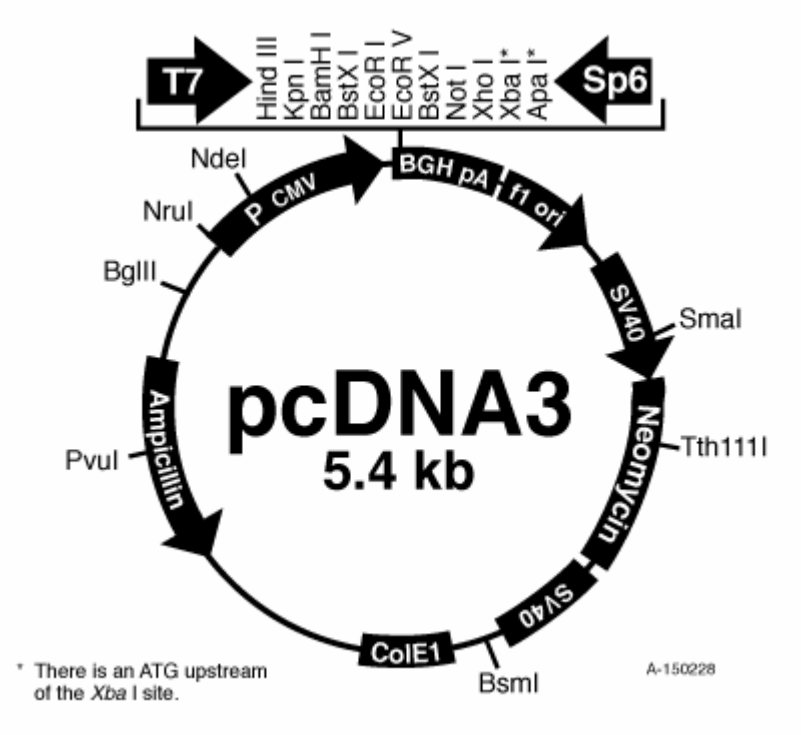

Figure 7.1:1. pcDNA3 (Invitrogen) vector map showing the restriction sites available and the ampicillin resistance gene. CD31 was cloned into this vector using BamH I and Not I restriction sites.

-

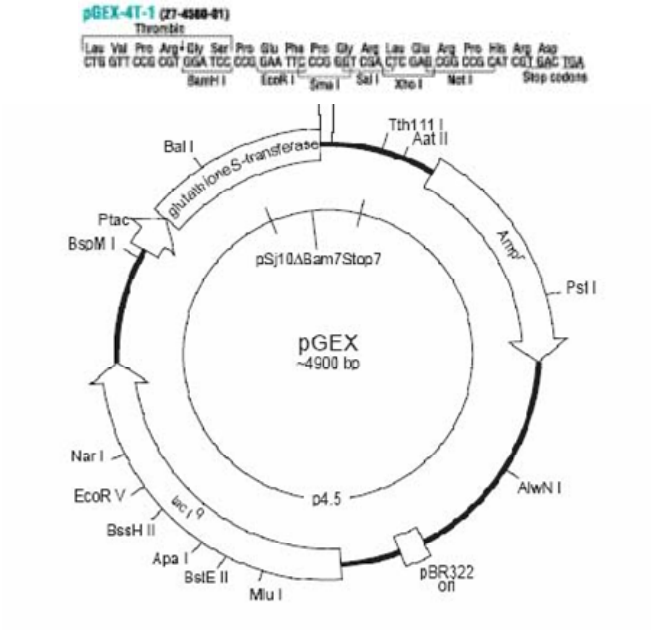

Figure 7.1:2. pGEX 4T (Amersham) vector map showing the ampicillin resistance gene, the N-terminal GST tag and the restriction sites available. CD31 was cloned into this vector with Bam HI and either Sal I or Not I restriction sites.

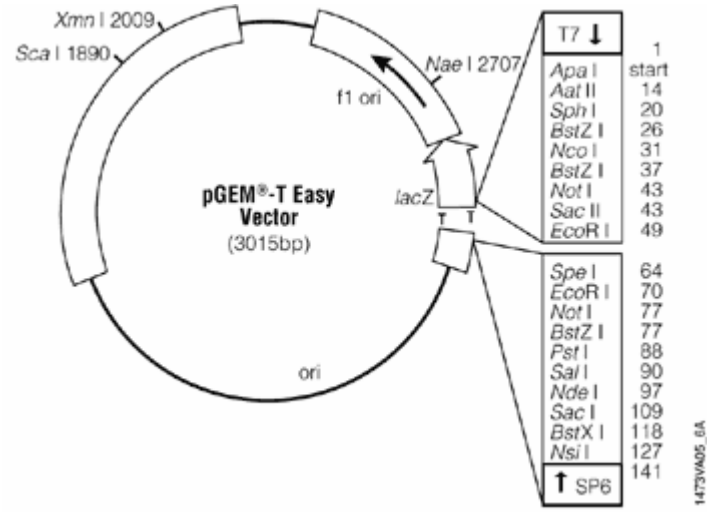

Figure 7.1:3. pGEMTeasy (Promega) vector map showing the restriction sites available. CD31 PCR products were subcloned directly into this vector by virtue of the overhanging A bases added by Taq polymerase.

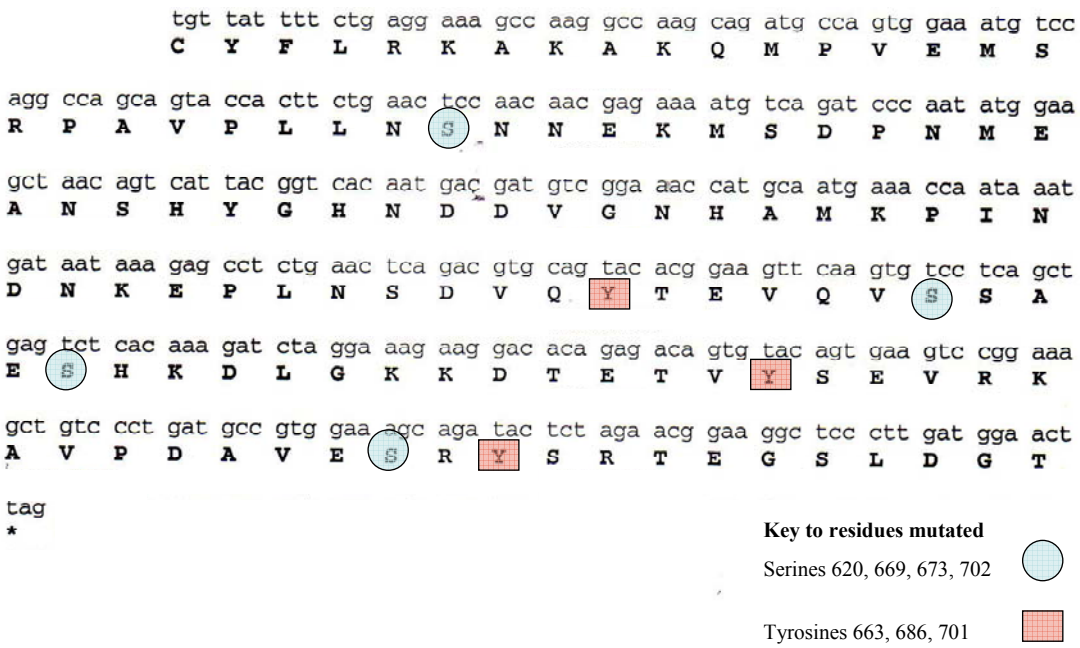

Figure 7.1:4. DNA sequence of the cytoplasmic domain of CD31 showing the tyrosine and serine residues mutated.

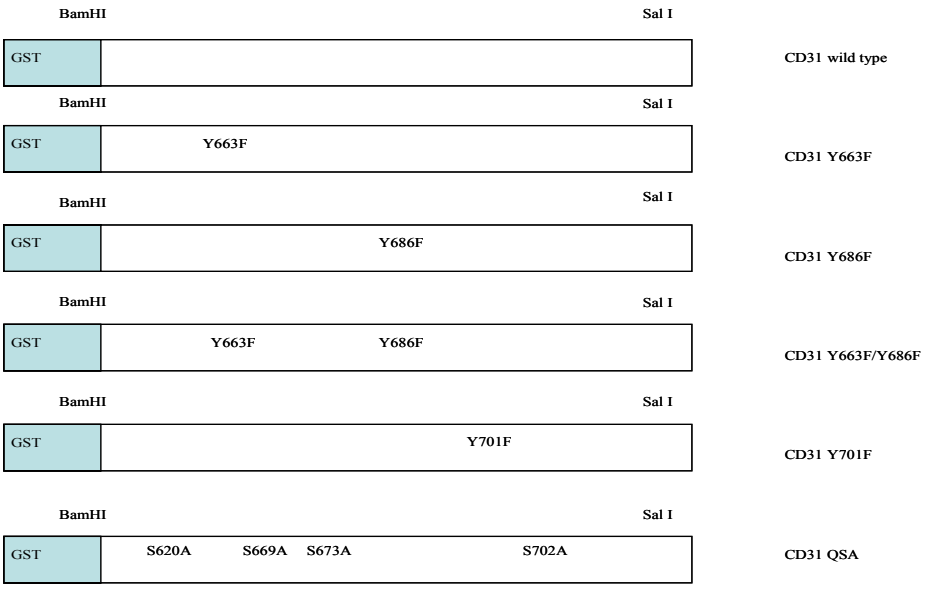

Figure 7.1:5. GST-CD31 constructs showing position of tyrosine and serine mutations.

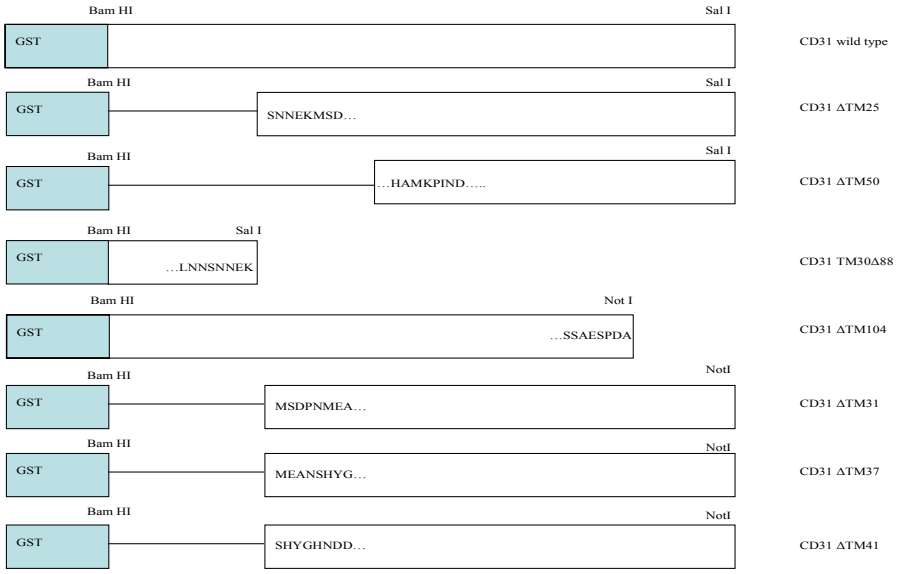

Figure 7.1:6 . Truncated CD31 constructs.

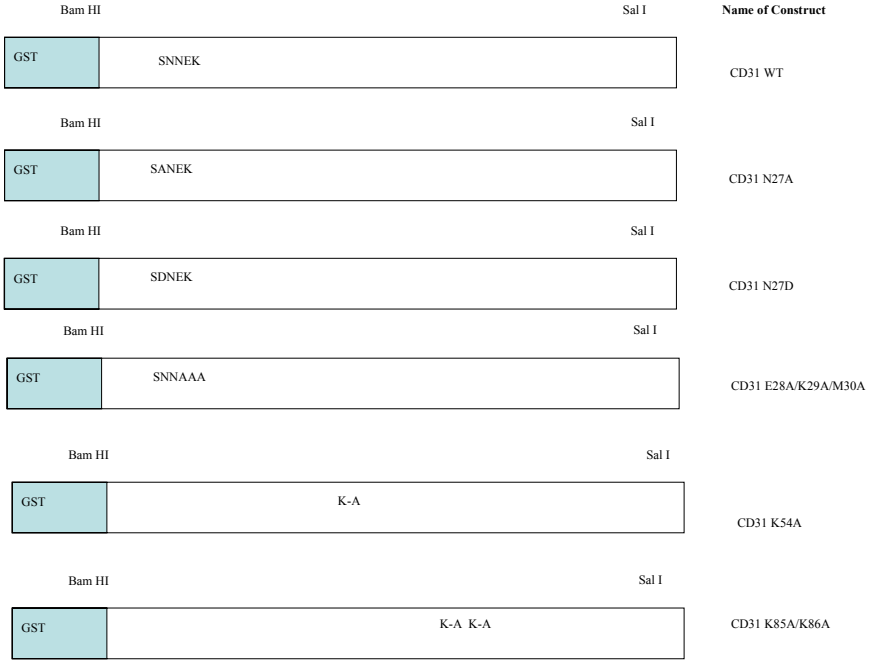

Figure 7.1:7. Site-directed mutagenesis constructs.

7.1.3 *PCR and Subcloning*

The programme for PCR amplification, the primers used and the restriction sites added to all constructs are shown (Table 7.1:10).

The CD31 cytoplasmic domain fragments (wild-type, tyrosine and serine mutants) of 400bp (Figure 7.1:12 and Figure 7.1:13) were amplified from pcDNA3 vectors incorporating a 5' Bam HI and 3' Sal I restriction site. Truncated and SNNEK and lysine mutants were also amplified from pcDNA3 (Figure 7.1:14 and Figure 7.1:15).

The PCR fragments were gel extracted using Qiagen spin gel extraction kit and subcloned into pGEMTeasy. The ligation reactions were transformed into DH5α competent cells and selected on LB agar supplemented with ampicillin 100mg/ml. Blue/white screening was utilised to select for positive clones. Clones were grown up in LB supplemented with ampicillin 100μg/ml. Plasmid DNA was extracted using Qiagen spin miniprep kit and sequenced. Primer sequences used to verify for each construct are shown (Table 7.1:11).

7.1.4 *Cloning into pGEX 4T*

The pGEMTeasy plasmids were digested with Bam HI and Sal I or Not I restriction enzymes (Figure 7.1:16). The resulting digest was run out on 1% agarose gel and the fragment extracted with Qiagen Spin gel extraction kit. The fragments were then cloned into the pGEX 4T containing an N-terminal glutathione-S-transferase sequence, then transformed into XL-1 blue competent cells and selected on LB agar supplemented with ampicillin 100mg/ml. Plasmids were purified using Qiagen maxiprep kit and checked by restriction digest (Figure 7.1:17) and sequenced.

7.1.5 *Talin Reconstitution and Protein Purification*

The talin FERM domain construct in pET15b (Figure 7.1:8) was reconstituted from filter paper as described (see Materials and Methods) and transformed into XL-1 Blue for maxiprep extraction. The plasmid was sequenced to confirm correct orientation using primers described in Table 7.1:11. The purified plasmid was transformed into BL21 electrocompetent cells and the protein purified using nickel coated magnetic beads.

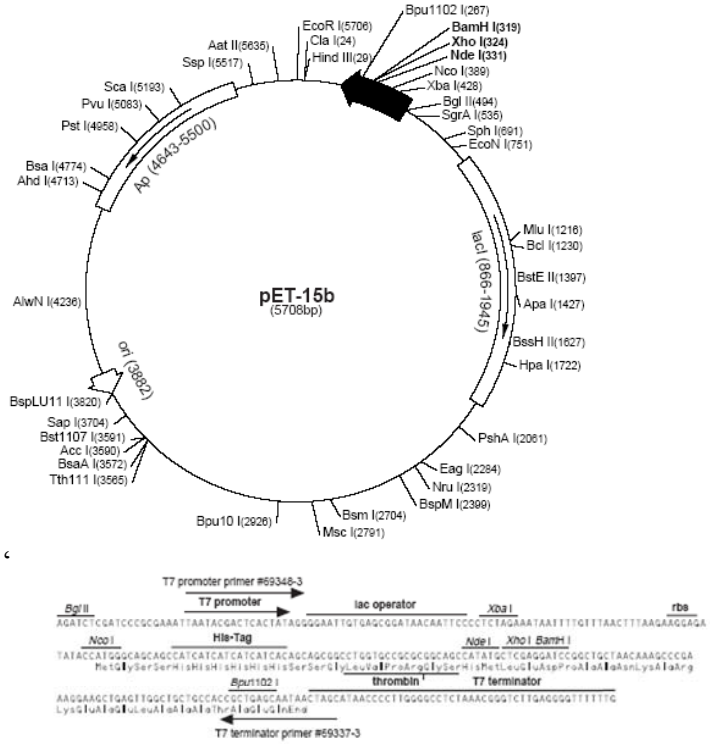

Figure 7.1:8. pET15b vector map with N-terminal his tag sequence, multiple cloning site (below) and thrombin cleavage site.

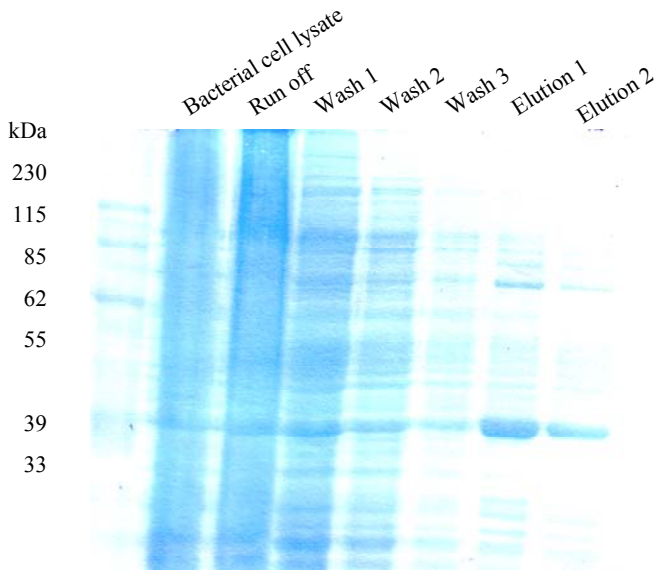

Figure 7.1:9. His tagged talin purified from BL21 bacteria (40kDa).

Construct	Primers	Restriction Sites	PCR Programme
CD31 wild type	Forward 5'-GATCGGATCCTGTTATTTTCTGAGGA-3'	BamHI and Sal I	94°C for 2 minutes 30 seconds twenty-two cycles of 94°C for 30 seconds 52°C for 30 seconds 72°C for 30 seconds then 72°C for 5 minutes.
	Reverse 5'-TATAGTCGACCTAAGTTCCATCAAGGGA-3'		
CD31 ITIM, 701 and QSA	Forward 5'-GATCGGATCCTGTTATTTTCTGAGGA-3'	Bam HI and Sal I	94°C for 2 minutes 30 seconds twenty-two cycles of 94°C for 30 seconds 52°C for 30 seconds 72°C for 30 seconds then 72°C for 5 minutes.
	Reverse 5'-TATAGTCGACCTAAGTTCCATCAAGGGA-3'		
CD31 CD31TM30Δ88	Forward 5'-GATCGGATCCTGTTATTTTCTGAGGA-3'	BamHI and Not I	94°C for 2 minutes 30 seconds twenty-two cycles of 94°C for 30 seconds 52°C for 30 seconds 72°C for 30 seconds then 72°C for 5 minutes.
	Reverse 5'-AGCGGCCGCAATGATCAAGAG-3'		
CD31TMΔ25,93	Forward 5-GCCGCCGGATCCCTTCTGAACTCCAACAACGAG-3'	BamHI and Sal I	94°C for 2 minutes 30 seconds twenty-two cycles of 94°C for 30 seconds 52°C for 30 seconds 72°C for 30 seconds then 72°C for 5 minutes.
	Reverse 5'-TATAGTCGACCTAAGTTCCATCAAGGGA-3'		

CD31TMΔ31,87	Forward 5'-GCATGGATCCATGTCAGATCCCAATATG-3' Reverse 5'-TATAGTCGACCTAAGTTCCATCAAGGGA-3'	BamHI and Sal I	94°C for 2 minutes 30 seconds twenty-two cycles of 94°C for 30 seconds 52°C for 30 seconds 72°C for 30 seconds then 72°C for 5 minutes.
CD31TMΔ50,68	Forward 5'-GACGGATCCCATGCAATGAAACCAATA-3' Reverse 5'-TATAGTCGACCTAAGTTCCATCAAGGGA-3'	BamHI and Sal I	94°C for 2 minutes 30 seconds twenty-two cycles of 94°C for 30 seconds 52°C for 30 seconds 72°C for 30 seconds then 72°C for 5 minutes.
CD31TM104,Δ14	Forward 5'-GATCGGATCCTGTTATTTTCTGAGGA-3' Reverse 5-CTAGCATTATAGCGGCCGCTAGGCATCAGGGACAGCTTT-3'	BamHI and Not I	94°C for 2 minutes 30 seconds twenty-two cycles of 94°C for 30 seconds 52°C for 30 seconds 72°C for 30 seconds then 72°C for 5 minutes.
Site Directed mutagenesis generation of super primer	**CD31N27A Forward** 5'-CTTCTGAACTCCGCCAACGAGAAAATG-3' **Reverse** 5'-CATTTTCTCGTTGGCGGAGTTCAGAAG-3' **CD31N27D Forward** 5'-CTTCTGAACTCCGACAACGAGAAAATG-3' **Reverse** 5'CATTTTCTCGTTGTCGGAGTTCAGAAG-3' **CD31E28A/K29A/M30A Forward** 5'-TGGCGGCCGCGTCAGAT	BamHI and Sal I	94˚ C for 2 minutes and 30 seconds twenty two cycles of 94˚C for 30 seconds 53˚C for 40 seconds 72˚C for 40 seconds then 72˚C for 4 minutes

	CCCAATATGGA -3' **Reverse** 5'-ATAGCGGCCGCGTTGTTGGAGTTCAGAAG-3' **CD31 K54A Forward** 5'-AGAAACCATGCAATGGCTCCAATAAATGATAATAAA-3' **Reverse** 5'-TTTATTATCATTTATTGGAGCCATTGCATGGTTTCT-3' **CD31 K85A/K86A Forward** 5'-AAAGATCTAGGAGCTGACACAGAGACA-3' **Reverse** 5'-TGTCTCTGTGTCAGCAGCTCCTAGATCTTT-3'		
Site directed mutagenesis PCR with super primer to generate mutant pcDNA3 plasmid	Primer as super primer	Bam HI and Sal I	94˚C for 2 minutes and 30 seconds sixteen cycles of 94˚C for 1 minute 53˚C for 45 seconds 68˚C for 10 minutes then 68˚C for 20 minutes
CD31N27A, CD31N27D, CD31 K54A, CD31 K85A/K86A cytoplasmic domain amplification from mutant pcDNA3 plasmid	Forward 5'-GATCGGATCCTGTTATTTTCTGAGGA-3' Reverse 5'-TATAGTCGACCTAAGTTCCATCAAGGGA-3'	BamHI and Sal I	94°C for 2 minutes 30 seconds twenty-two cycles of 94°C for 30 seconds 52°C for 30 seconds 72°C for 30 seconds then 72°C for 5 minutes.
CD31TMΔ37,81	Reverse 5'-TATAGTCGACCTAAGTTCCATCAAGGGA-3' Forward 5'-	BamHI and Sal I	94°C for 2 minutes 30 seconds twenty-two cycles of 94°C for 30 seconds 52°C for 30 seconds

	TGGATCCATGGAAGCTAACAGTCAT-3’		72°C for 30 seconds then 72°C for 5 minutes.
CD31TMΔ41,77	Reverse 5’-TATAGTCGACCTAAGTTCCATCAAGGGA-3’ Forward 5’-TGGATCCAGTCATTACGGTCACAAT-3’	BamHI and Sal I	94°C for 2 minutes 30 seconds twenty-two cycles of 94°C for 30 seconds 52°C for 30 seconds 72°C for 30 seconds then 72°C for 5 minutes.
CD31TM19,Δ109	Reverse 5’-TATAGTCGACCTAAGTTCCATCAAGGGA-3’ Forward 5’-GATCGGATCCTGTTATTTTCTGAGGA-3’ Forward 5’-CACCATGACATCGCGGAGATGGC-3’	Bam HI Sal I	94°C for 2 minutes 30 seconds twenty-two cycles of 94°C for 30 seconds 52°C for 30 seconds 72°C for 30 seconds then 72°C for 5 minutes.

Table 7.1:10. Primers, restriction sites and PCR programme included in PCR of CD31 cytoplasmic domain and SHP-2 constructs.

Construct	Primer Sequence
CD31 pGEMTeasy	Forward 5'-TAATACGACTCACTATAGGG-3'
	Reverse 5'- CATTTAGGTGACACTATAG-3'
CD31 pGEX	Forward 5'- AACGTATTGAAGGCTATC-3'
	Reverse 5'-CATCCGCTTACAGACA-3'
SHP-2 eGFP	Forward 5'CGTCGCCGTCCAGCTCGACCAG-3'
	Reverse 5-CATGCTCCTGCTGGAGTTCGTC-3'
SHP-2 pCMV hygromycin	Forward 5'AGGTCAGGGATGGTCCAGACA-3'
	Reverse 5' TTCTGCTGTTGCATCAGGCCCAC-3'
Talin pET15b	Forward 5'-TAATACGACTCACTATAGGG-3'
	Reverse 5'-CTAGTTATTGCTCAGCGGT-3'

Table 7.1:11. Sequences of primers used in verifying constructs.

7.1.6 *Protein Induction*

Protein production was initiated by pGEX 4T1 plasmid transformation into BL21 electrocompetent bacteria, and protein production was induced by the addition of IPTG (Figure 7.1:18, Figure 7.1:19 and Figure 7.1:20). Protein was purified by GST affinity for glutathione on agarose beads (Figure 7.1:21, Figure 7.1:22 and Figure 7.1:23).

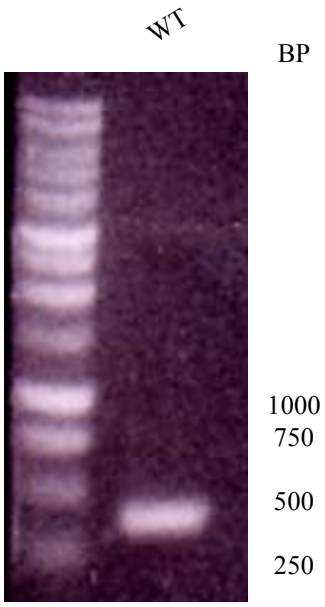

Figure 7.1:12. Wild-type CD31 PCR product at 400bp incorporating 5' Bam HI and 3'Sal I restriction sites.

Figure 7.1:13. PCR of tyrosine and serine mutant CD31 cytoplasmic domains. The fragments are approximately 400bp.

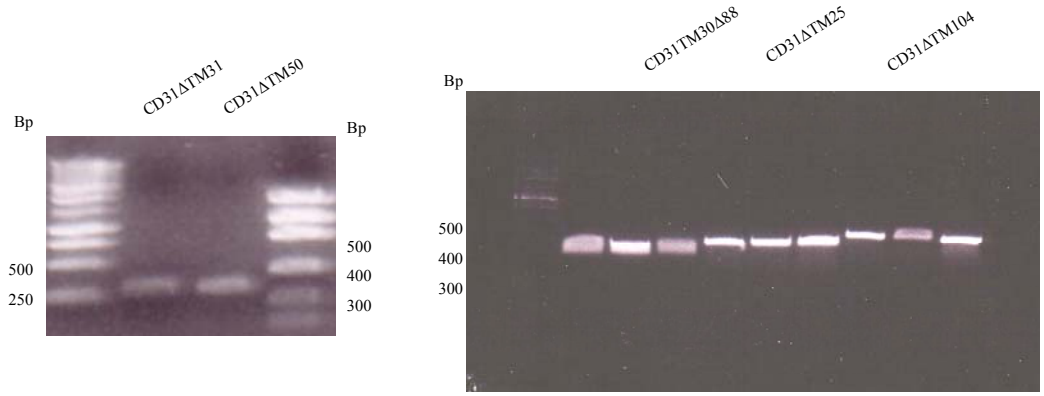

Figure 7.1:14. Truncated CD31 PCR fragments CD31TM30,Δ88 (100bp), CD31TMΔ25,93 (325bp), CD31TMΔ31,87 (310bp), CD31TMΔ50,68 (300bp), CD31TM104,Δ14 (355bp).

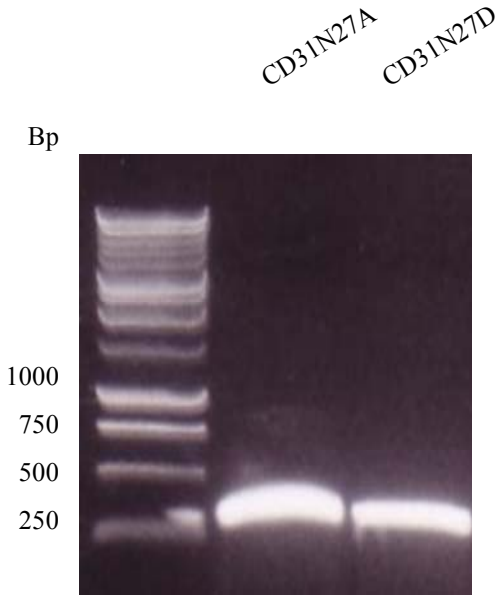

Figure 7.1:15. SNNEK mutant CD31 PCR (400bp).

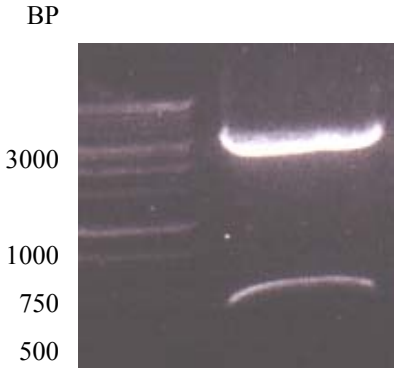

Figure 7.1:16. pGEMTeasy (3kb) digested with Bam HI and Sal I liberates the CD31 fragments (400bp) that now have 5' Bam HI and a 3' Sal I restriction ends.

Figure 7.1:17. pGEX (5kb) digested with Bam HI and Sal I to check correct orientation of CD31 fragment (400bp).

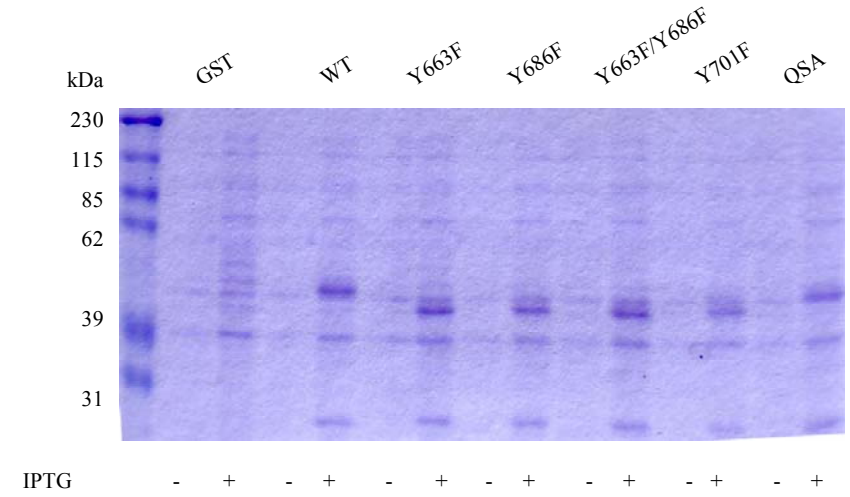

Figure 7.1:18. Bacterial lysates from each clone, production of recombinant protein (40kDa) was only initiated by the addition of IPTG, separated on 10% acrylamide and stained with Coomassie blue.

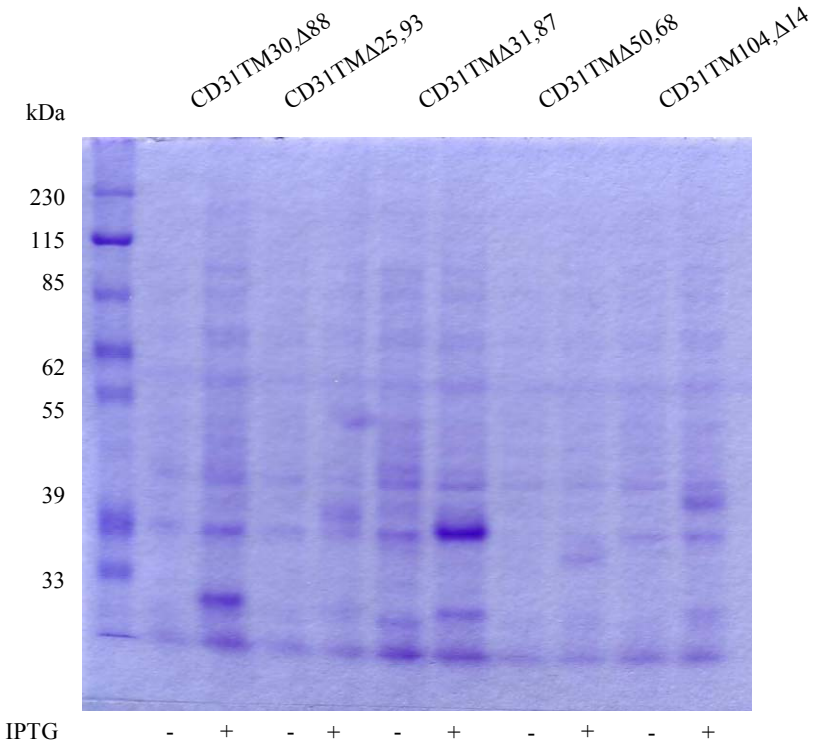

Figure 7.1:19. Truncated GST-CD31 recombinant proteins (CD31TM30Δ88 28kDa; CD31ΔTM25 37.5kDa; CD31ΔTM31 37kDa; CD31ΔTM50 34.5kDa; CD31ΔTM104 38.4kDa) showing IPTG induces protein production separated on 10% acrylamide and stained with Coomassie blue.

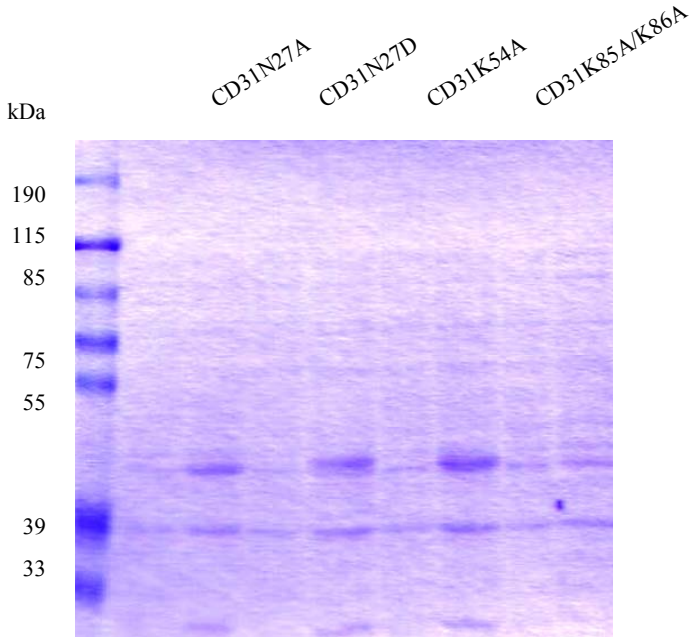

Figure 7.1:20. SNNEK and lysine mutant recombinant proteins (40kDa) showing induction by IPTG separated on 10% acrylamide and stained with Coomassie blue.

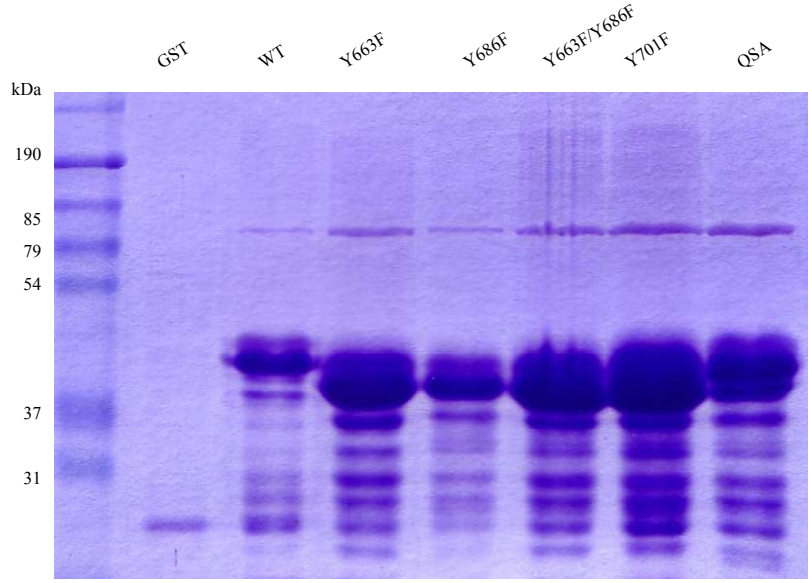

Figure 7.1:21. Purified GST (25kDa), wild-type and mutant CD31 proteins (40kDa) separated on a 10% acrylamide gel and stained with Coomassie blue.

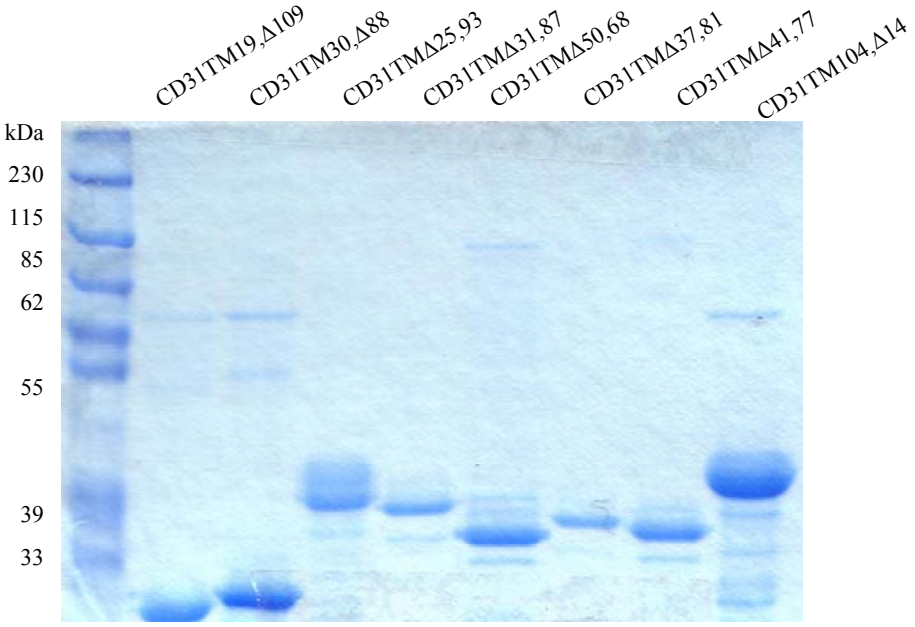

Figure 7.1:22. Truncated GST-CD31 constructs purified from bacteria. 10µl loaded onto 10% acrylamide and stained with Gelcode blue (Pierce).

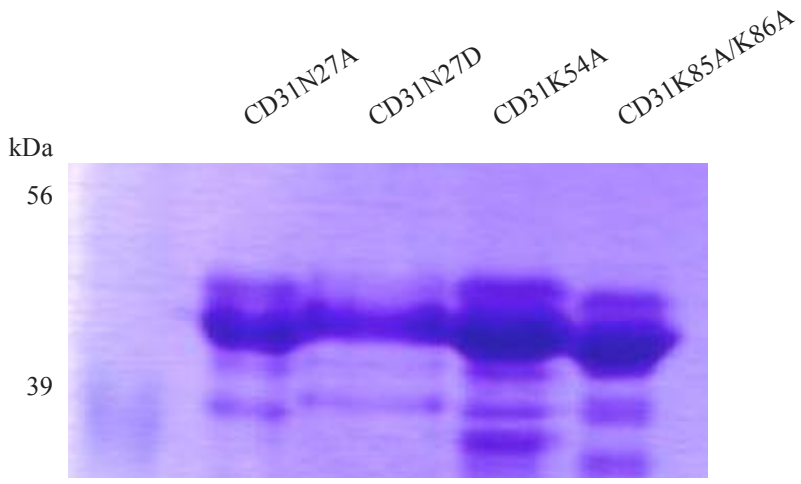

Figure 7.1:23. SNNEK and lysine mutant purified recombinant proteins (40kDa) separated on 10% acrylamide and stained with Coomassie blue.

7.2 Troubleshooting GST Pulldowns

This section outlines the methodology used to optimise the method for the GST pulldown work in Chapter 3.

The investigation originally started with GST pulldowns adapting the method from [60] for use with Jurkats. Briefly the method is cell lysis and clearance of supernatant, then recombinant protein was added, then glutathione-agarose beads. The beads were then washed in pulldown buffer (50mM Tris pH 7.4, 100mM NaCl, 0.5% Tween 20, 10mM β-mercaptoethanol), and then the recombinant proteins plus any bound proteins were eluted with 5mM glutathione buffer. When used with GST, wild-type, Y663F, Y686F, Y663F/Y686F, Y701F and QSA constructs and blotted for SHP-2 (binds to phosphorylated CD31 cytoplasmic domain), there was non-specific binding to the GST alone (Figure 7.2:1).

7.2.1 *Increasing Salt Concentration*

To attempt to eliminate non-specific binding the salt concentration was increased in the pulldown buffer that was used to wash the beads from 100mM to 500 and 750mM and blotted for SHP-2 and Hsp90 (see chapter 3 for study on CD31 and Hsp90 interactions). There was also non-specific binding to the GST (Figure 7.2:2). The lysate was precleared with either beads or GST before the pulldown, but this had no effect on non-specific binding (Figure 7.2:3).

The process was re-examined again, and the protocol changed slightly to accommodate extra wash steps. The cells were lysed as previously described and recombinant protein added. The beads were then washed in 10mM Tris pH8 and

100mM β-mercaptoethanol, to reduce the glutathione on the beads then in 10mM Tris pH8 to removes excess mercaptoethanol. The washed beads were then incubated with the protein/lysate as described. The beads were then washed in 20mM Tris pH8 and 200mM NaCl to remove weak i.e. non-specific interactions, then with 20mM Tris pH8 and 200mM NaI. NaI acts as a chaotropic agent to disrupt salt bridges and hydrophobic bonds. This may help to remove non-specific binding to the GST which may have been promoted by increasing the salt concentration. The pulldowns were then blotted for SHP-2 and Hsp90, however these conditions did not remove the non-specific binding (Figure 7.2:4).

The salt was removed from the system, and performed the GST pulldown again, collecting each wash fraction and blotting for SHP-2 and Hsp90. There was still non-specific binding to the GST and to the beads (Figure 7.2:5).

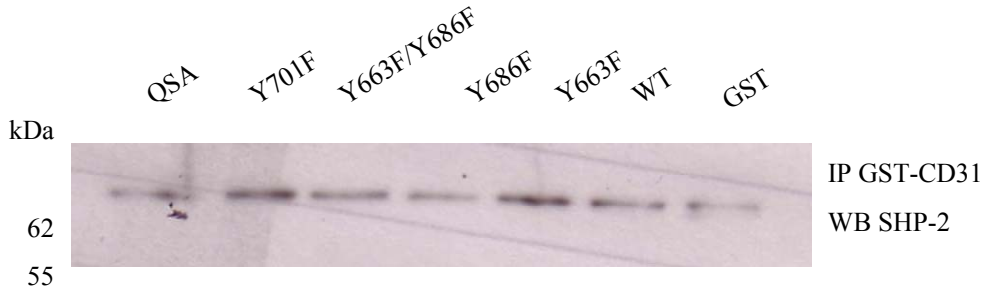

Figure 7.2:1. GST pulldown from CD31 negative Jurkat lysates showing non-specific binding of SHP-2 to the GST alone.

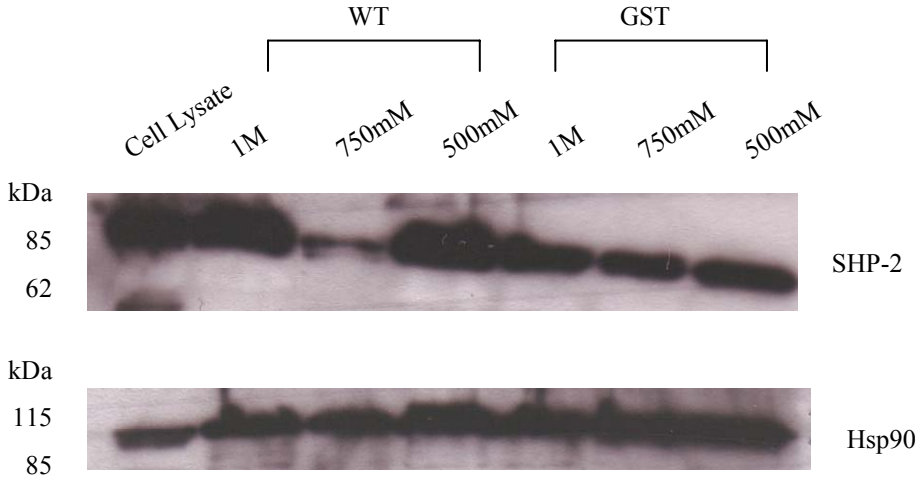

Figure 7.2:2. GST pulldown with GST or GST-CD31 with different salt concentrations in the pulldown buffer, showing non-specific binding to the GST.

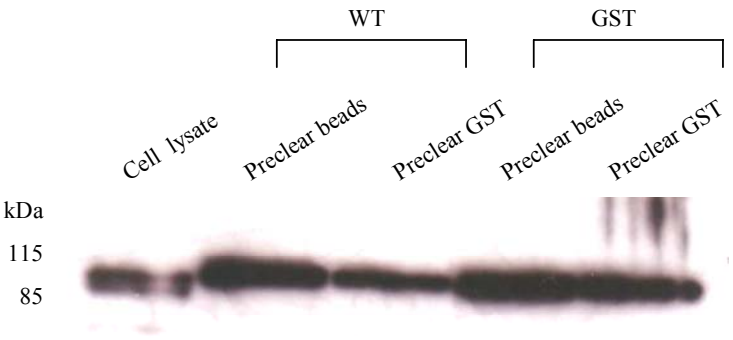

Figure 7.2:3. GST and CD31 pulldowns precleared with either GST alone or beads before performing pulldowns and blotted for Hsp90 showing non-specific binding to GST alone.

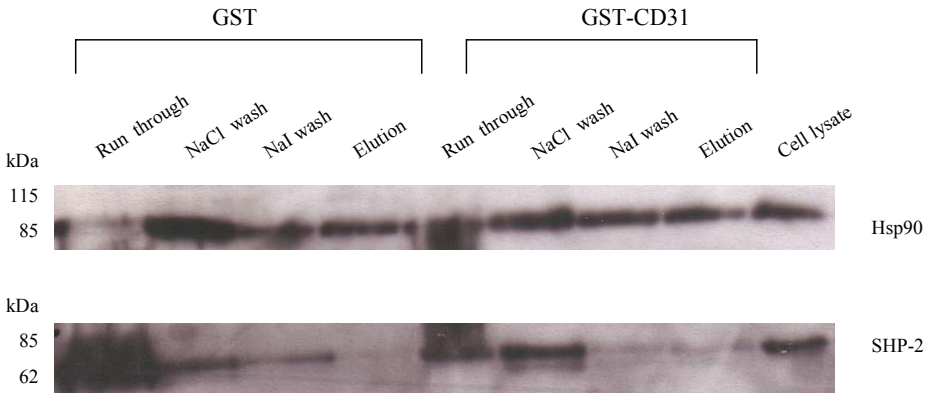

Figure 7.2:4. GST pulldowns blotted for SHP-2 and Hsp90 with a NaCl wash and a NaI wash showing non-specific binding to the GST.

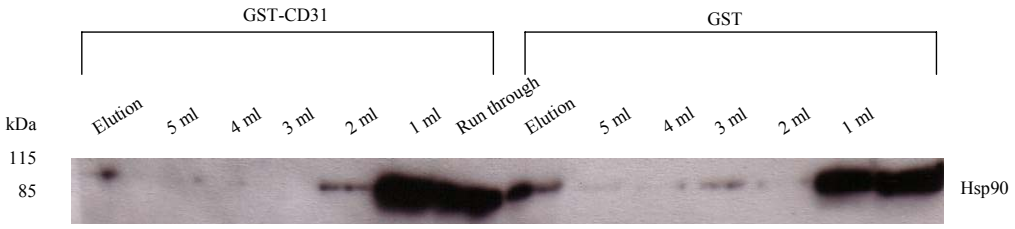

Figure 7.2:5. GST pulldowns with 5 X10^6 CD31 negative Jurkats, washed with 5ml cell lysis buffer (no salt) and each wash fraction collected and blotted for Hsp90 showing non-specific binding to the GST alone.

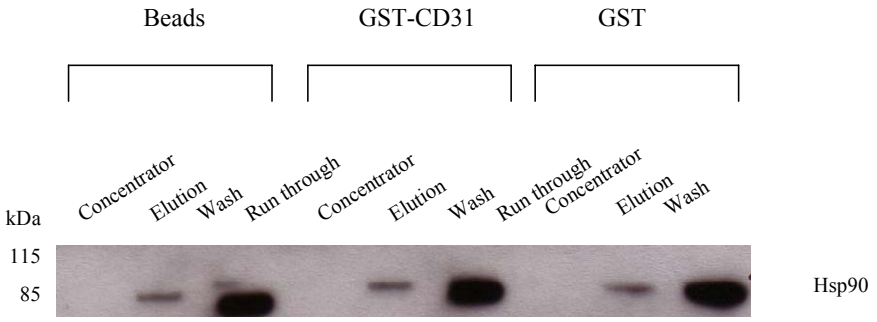

Figure 7.2:6. GST pulldowns with 5 X10^6 CD31 negative Jurkats, with the elution fraction passed through a concentrator column.

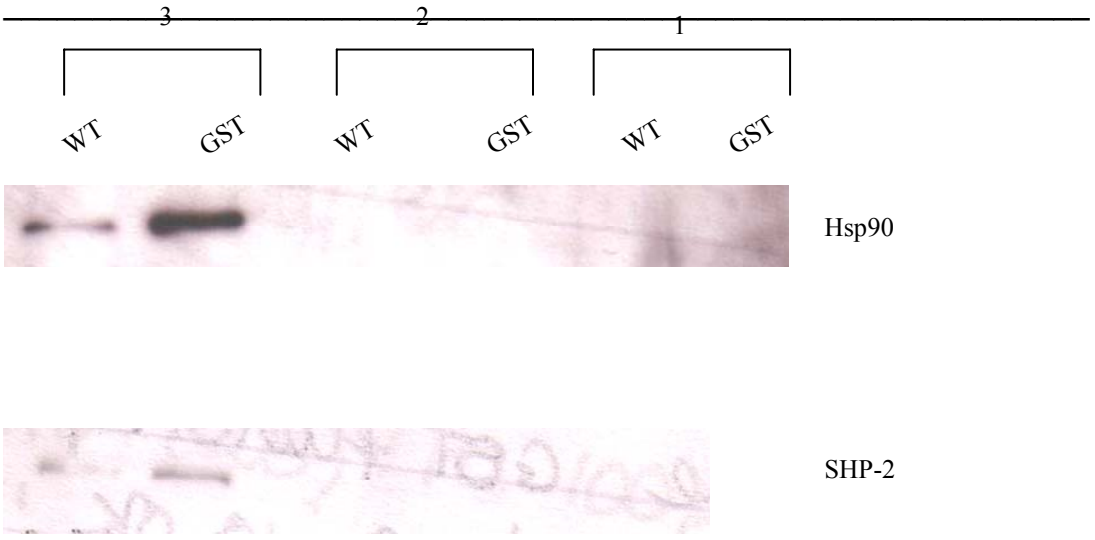

Figure 7.2:7. Three different methods of GST pulldown showing no binding of SHP-2 or Hsp90 to CD31 to methods 1 and 2, and non-specific binding to method 3.

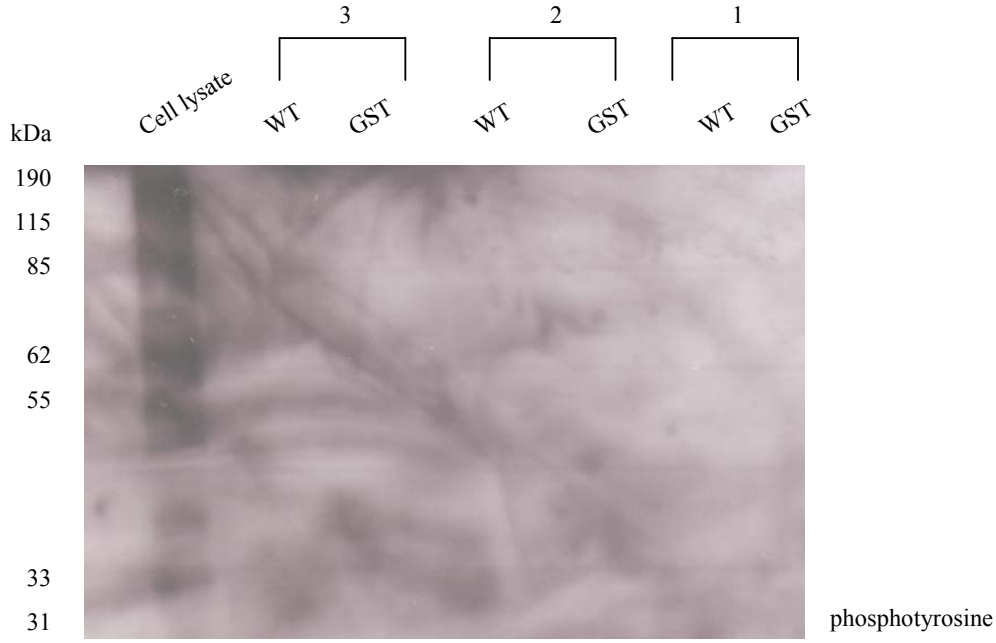

Figure 7.2:8. Three methods of GST pulldown blotted for tyrosine phosphorylated proteins, showing the GST-CD31 protein is not tyrosine phosphorylated.

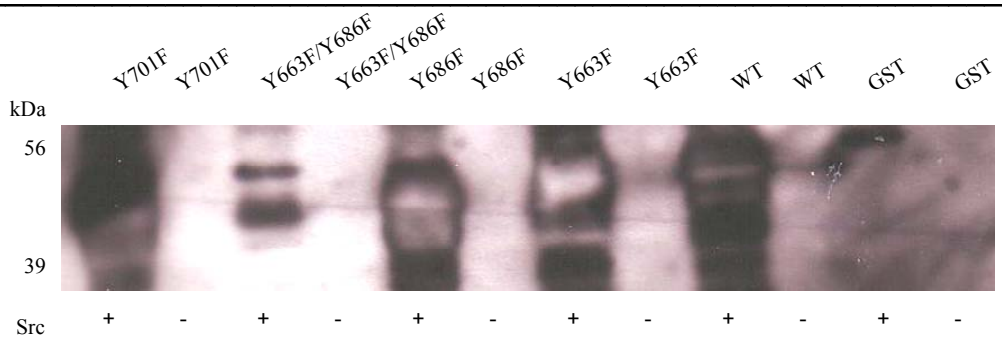

Figure 7.2:9. Recombinant proteins are tyrosine phosphorylated by recombinant src, construct Y663F/Y686F shows less overall phosphorylation.

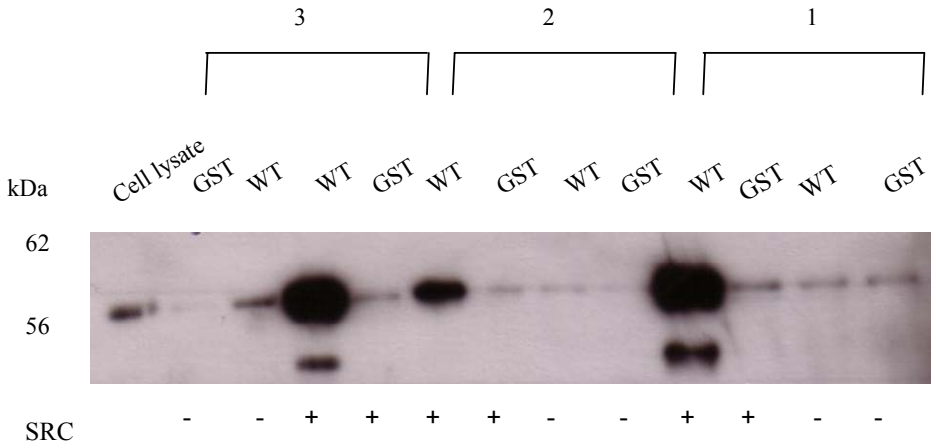

Figure 7.2:10. GST pulldowns with recombinant proteins phosphorylated with recombinant src by three different methods blotted for SHP-2 shows method 2 to provide the least amount of non-specific binding.

7.2.2 *Literature Search*

The whole approach was reconsidered and a literature search performed for GST pulldowns with leukocytes. Three methods were chosen, [182] used Jurkats, [183] used the same manufacturer of agarose beads and [184] are a group that works extensively on CD31. All lysis was carried out on ice for 20 minutes (checked by trypan blue exclusion), with lysis buffer at a concentration of 1ml per 10 million cells, before centrifugation at 20000g for 15 minutes. The methods are shown below (Table 7.2:1).

Method	Lysis buffer	Pulldown Method and Wash	Reference
1	20mM Tris pH7.4 1% Triton-X_{100} 2mM $MgCl_2$ 150mM NaCl 1mM NaF 1mM Na_3VO_4 1mM protease inhibitor cocktail	Beads combined with recombinant protein Add beads to lysate for 90 minutes Wash beads three times in lysis buffer Beads Resuspended in sample buffer	[182]
2	50mM Tris-HCl pH7.4 1% IPEGAL 40 250mM NaCl 1mM NaF 1mM Na_3VO_4 1mM protease inhibitor cocktail	Cell lysate precleared with agarose beads overnight Beads combined with recombinant protein Beads added to precleared lysate for 2 hours Beads washed three times in lysis buffer and once with PBS Beads resuspended in PBS and sample buffer	[183]
3	Lysis buffer: 50mM Tris pH7.4 1% IPEGAL 40 10% glycerol 150mM NaCl 1mM Na_3VO_4 1mM NaF 1mM protease inhibitors IP buffer: 50mM Tris pH7.4 1% Triton-X_{100} 150mM NaCl 5mM EDTA	Beads combined with recombinant protein Beads added to lysate for 2 hours IP buffer added for 2 hours Beads washed with IP buffer Beads resuspended in sample buffer	[184]

Table 7.2:1. Buffer ingredients and methodology for GST pulldown trialled.

7.2.3 *Requirement for Phosphorylation*

The three methods were blotted for SHP-2 and Hsp90 (Figure 7.2:7), but no SHP-2 was detected as binding to CD31. As it has been previously shown that SHP-2 binds to tyrosine phosphorylated cytoplasmic domain of CD31, phosphotyrosine was probed for. As expected there was no phosphorylation of recombinant proteins by virtue of them being in the cell lysate, or by being produced by the bacteria (Figure 7.2:8).

The recombinant proteins were phosphorylated with recombinant src kinase [56] (Figure 7.2:9) and used the phosphorylated protein in GST pulldowns with the three methods again. When blotting for SHP-2 (Figure 7.2:10), method 1 showed non-specific binding to the GST alone, and a strong band with wild-type CD31. Method 2 shows less non-specific binding with GST alone, and a good band with wild type CD31. Method 3 shows non-specific binding to the GST, and good binding to wild-type CD31. It was decided that method 2 provided the least amount of background binding, and was used in all subsequent GST pulldowns.

7.3 Troubleshooting Jurkat Transfection

7.3.1 *Amaxa Transfection*

To provide a positive control for transfection, the Amaxa electroporation protocol includes a GFP vector. Transfecting CD31 positive Jurkats with this vector should indicate the transfection efficiency, and several programmes are recommended for the Jurkat cell line, including a programme specifically for use with Jurkats that have previously been transfected, as is the case with the CD31 positive Jurkats. 2μg of

GFP vector was transfected into the Jurkats as per the manufacturer's instructions, and the cells harvested after 24hrs incubation, and analysed by flow cytometry (Figure 7.3:1and Figure 7.3:2). The number of GFP positive cells was very low, showing the transfection efficiency to be well below that which would allow testing the effects of silencing SHP-2 expressing using siRNA.

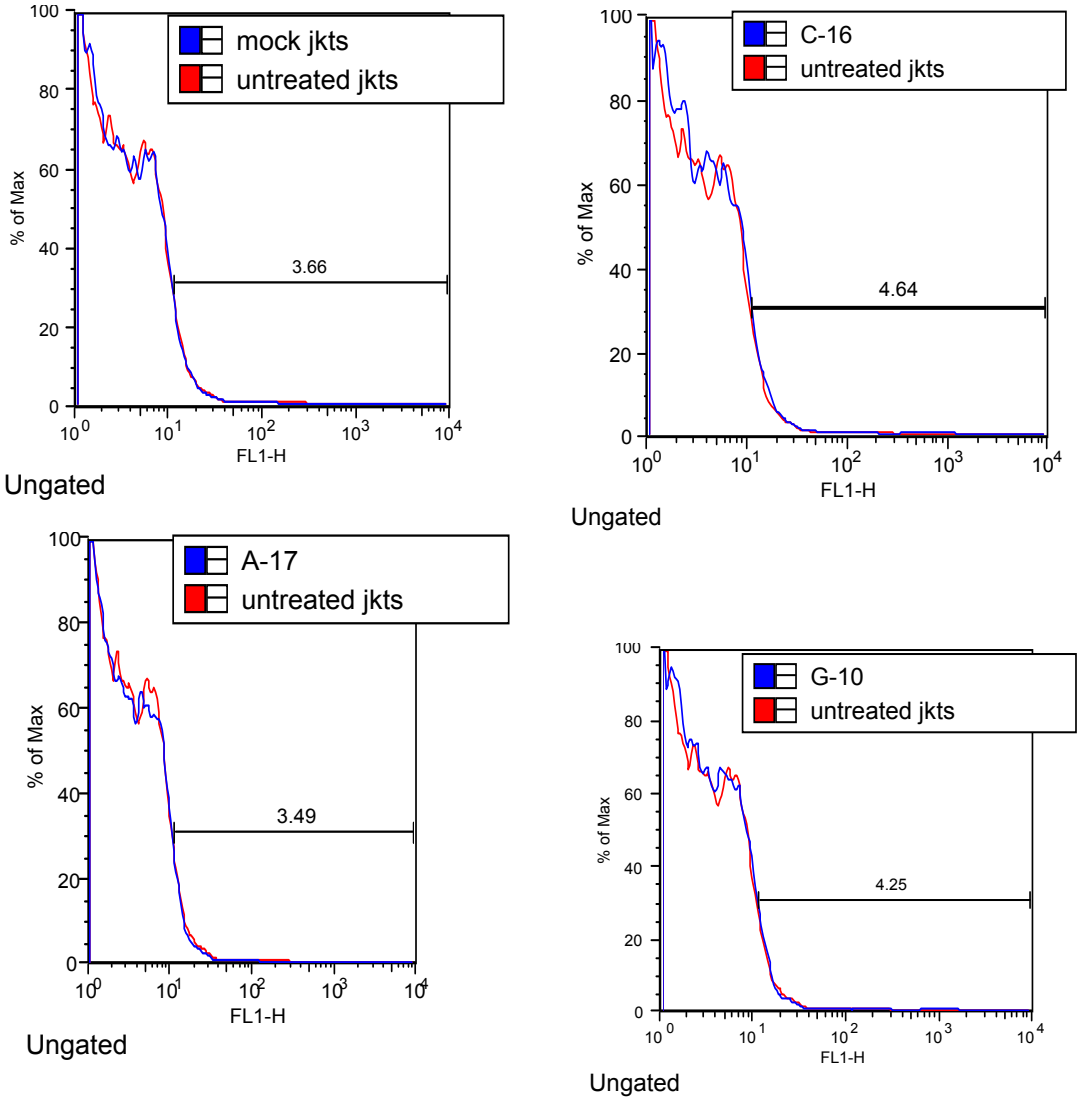

Figure 7.3:1. CD31 positive Jurkats transfected with GFPmax vector (Amaxa) or mock control using Amaxa protocol and transfection programmes A-17, C-16 and G-10 show low transfection efficiency. Marker indicates percentage GFP positive cells compared with mock transfected cells.

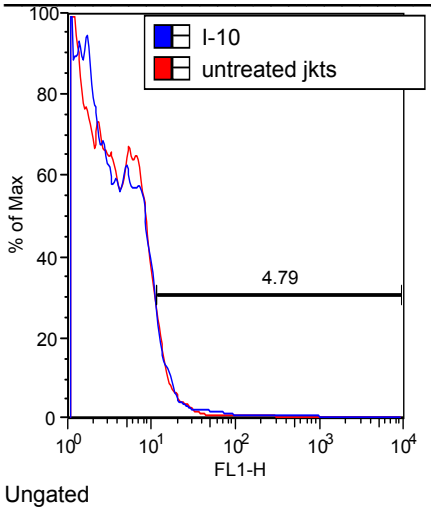

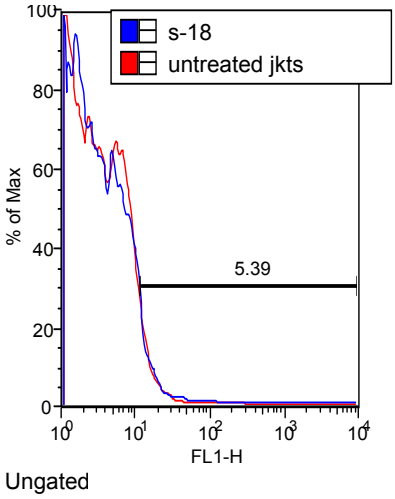

Figure 7.3:2. CD31 positive Jurkats transfected with GFPMax vector (Amaxa) using Amaxa protocol and transfection programmes I-10 (for previously transfected cells), and S-18 shows low transfection efficiency.

As MM6 cells also express both SHP-1 and SHP-2, attempts were made to transfect these cells initially with the GFP vector as a positive control. However, we were unable to demonstrate convincing transfection of MM6 with GFP (Figure 7.3:3); therefore the transfection of siRNA to knock-down SHP-2 was not attempted.

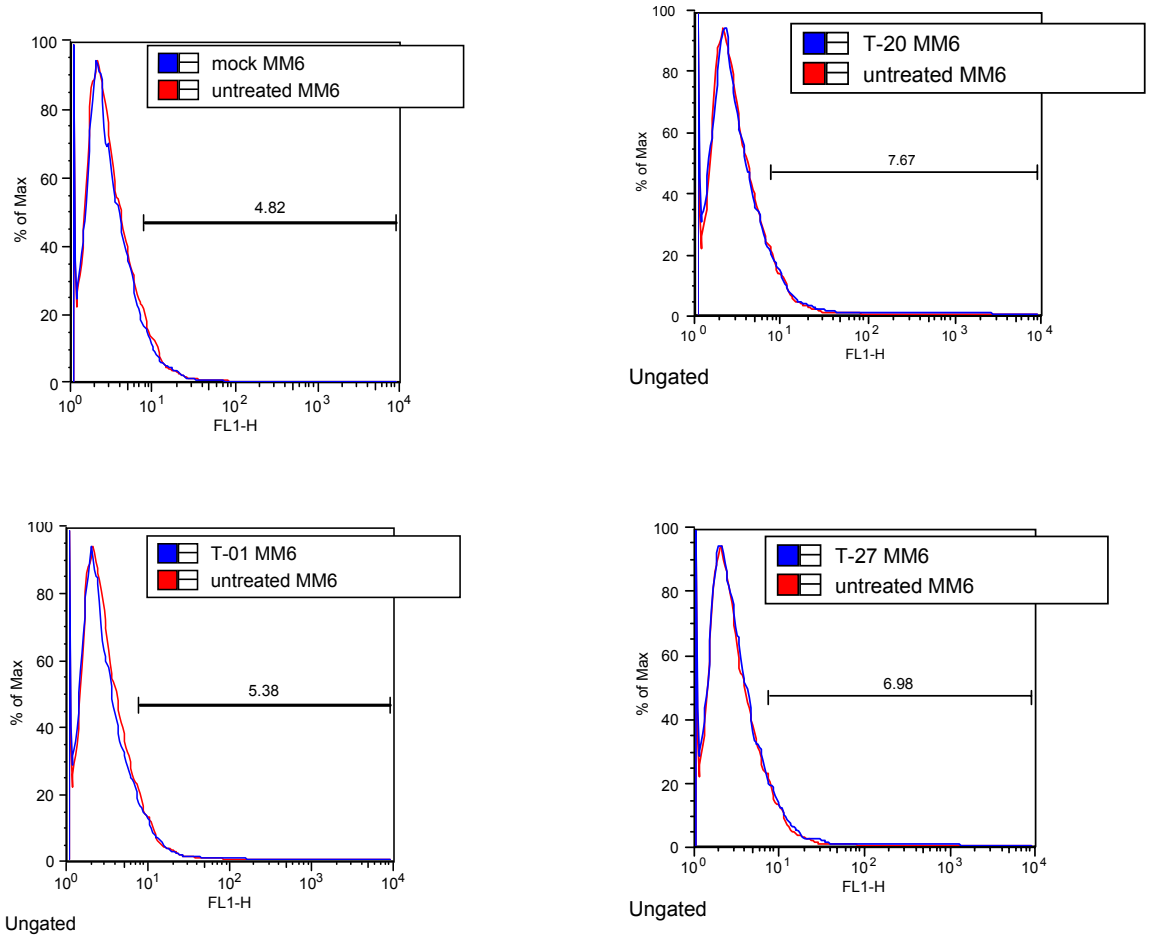

Figure 7.3:3. MM6 cells transfected with GFPMax vector and Amaxa programmes provided by Amaxa customer data show low transfection efficiency.

7.3.2 *SHP-2 siRNA Constructs*

A human SHP-2 sequence [185] was used to generate an siRNA construct. As a positive control of transduction and silencing, human lamin A/C [186] was also cloned, and a scrambled sequence [187] was used as a negative control (Figure 7.3:4). These constructs were to be cloned into a modified pLenti 6 plasmid vector for transcription. The modified vector contains the human H1 promoter, for transcription of short hairpin RNA in mammalian cells [188] and CMV-GFP promoter, so when packaged, the transduced cells produce GFP and can be sorted if desired. However, although time constraints did not permit this to occur, we would predict that knock-down of SHP-2 in CD31 positive Jurkats might impair their detachment from THP-1.

To produce the lentiviral vector for packaging the SHP-2 siRNA constructs, a modified pLenti vector would have been created that would express the constructs in mammalian cells under the H1 promoter. The original pLenti vector (Figure 7.3:5) was to be modified to remove the topoisomerase site and existing promoters via restriction digest with Cla I and Bcl I. A short oligo was then ligated into this region which contained a multiple cloning site with Cla I, Bam HI and Bcl I sites. The mammalian promoter H1 and the CMV-GFP promoter was amplified by PCR from a mammalian expression plasmid and inserted into the blunt TOPO vector (Figure 7.3:6) to give an intermediate vector into which the siRNA constructs could firstly be annealed to create double-stranded DNA then cloned via Sal I and Hind III. The entire region encoding the siRNA

construct, the H1 and CMV-GFP promoter could be cut out via Bgl II digestion and ligated into the modified pLenti vector via the Bam HI site. This ligation is possible due to Bgl II cutting at sequence **A** GATCT and Bam HI cutting at **G** GATCC, which leaves the same sticky end to anneal the fragments to (Figure 7.3:7 shows whole scheme). The plasmid could then be transfected into the packaging cell line and virus produced with which to transduce CD31 positive Jurkats and assay the effect upon detachment from THP-1.

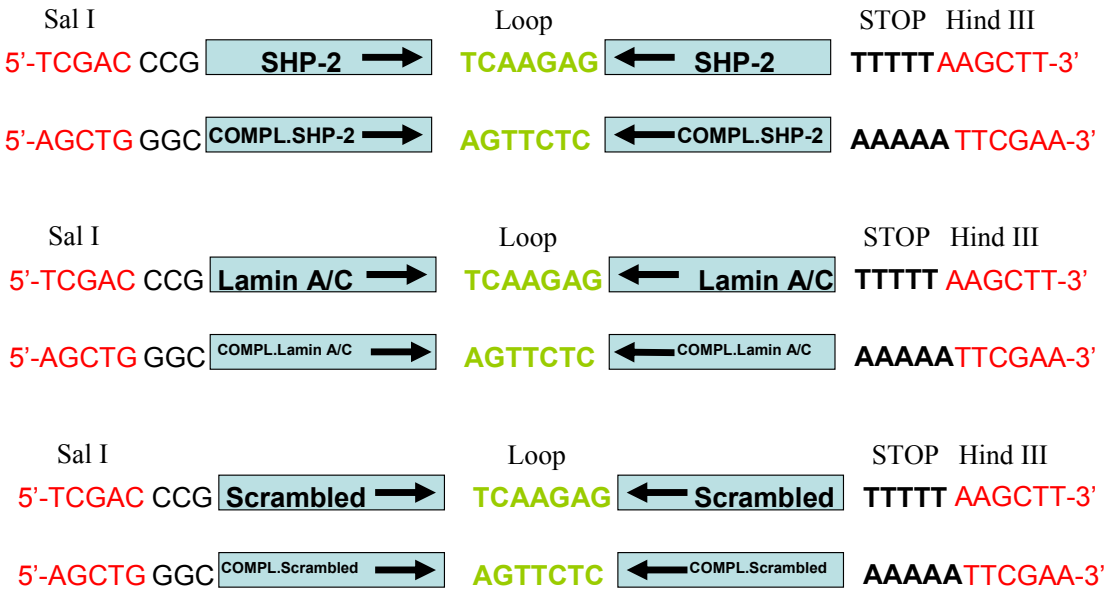

Figure 7.3:4. SHP-2, lamin A/C and scrambled siRNA hairpin constructs to be generated with Sal I and Hind III restriction sites and a loop for cloning into pLenti MCS-H1.CMV-GFP, which produces hairpin RNA for processing and RNA silencing and is also GFP tagged.

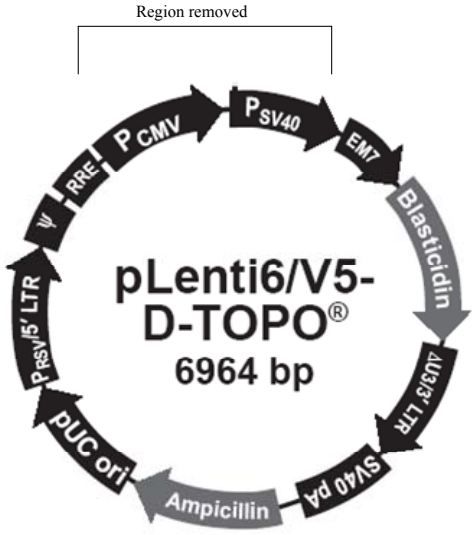

Figure 7.3:5. pLenti vector (Invitrogen) from which the topoisomerase sites and promoter region was to be removed by restriction digest and replaced with a short oligo containing a multiple cloning site with restriction sites Cla I, Bam HI and Bcl I.

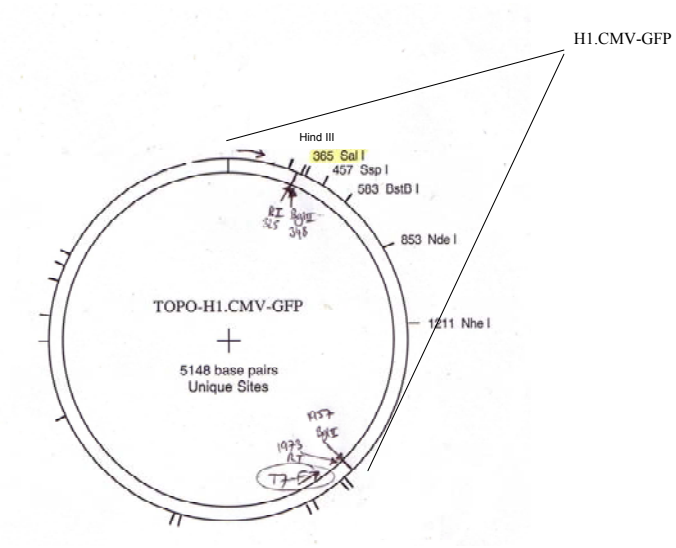

Figure 7.3:6. Blunt vector containing the mammalian H1 and CMV-GFP promoters which was to have the siRNA constructs ligated in and then cut from this vector and ligated into the pLenti vector.

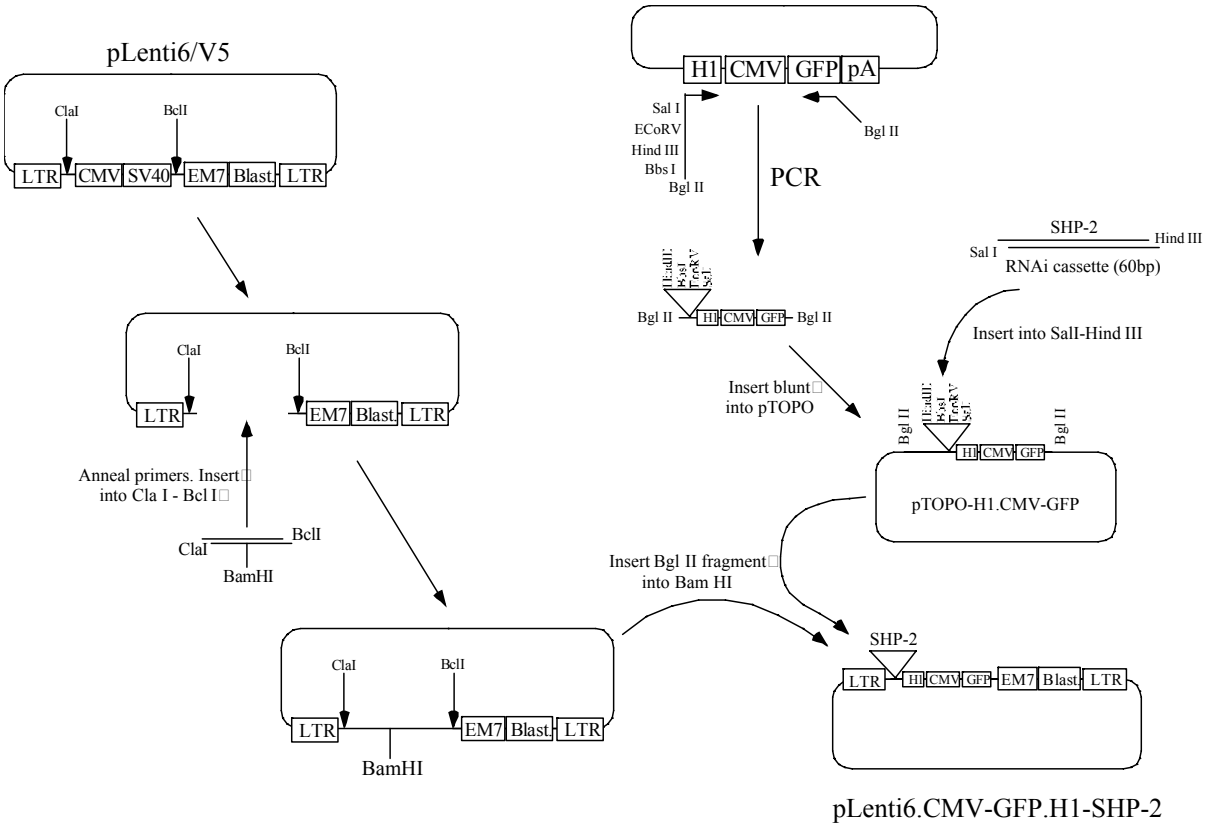

Figure 7.3:7. Schematic showing cloning strategy of siRNA constructs by annealing fragments, ligating into an intermediate blunt vector and then restriction digest to remove the siRNA sequence and H1 and CMV-GFP promoter, then finally ligating into the modified pLenti as described previously (Scheme courtesy of Dr Jason King, University of Edinburgh, UK).

8 References

1. Simon, S. I. & Green, C. E. Molecular mechanics and dynamics of leukocyte recruitment during inflammation. *Annu Rev Biomed Eng* **7**, 151-85 (2005).

2. Reedquist, K. A. et al. The small GTPase, Rap1, mediates CD31-induced integrin adhesion. *J Cell Biol* **148**, 1151-8 (2000).

3. Voermans, C., Rood, P. M., Hordijk, P. L., Gerritsen, W. R. & van der Schoot, C. E. Adhesion molecules involved in transendothelial migration of human hematopoietic progenitor cells. *Stem Cells* **18**, 435-43 (2000).

4. Tanaka, Y. et al. CD31 expressed on distinctive T cell subsets is a preferential amplifier of beta 1 integrin-mediated adhesion. *J Exp Med* **176**, 245-53 (1992).

5. Muller, W. A., Weigl, S. A., Deng, X. & Phillips, D. M. PECAM-1 is required for transendothelial migration of leukocytes. *J Exp Med* **178**, 449-60 (1993).

6. Dangerfield, J., Larbi, K. Y., Huang, M. T., Dewar, A. & Nourshargh, S. PECAM-1 (CD31) homophilic interaction up-regulates alpha6beta1 on transmigrated neutrophils in vivo and plays a functional role in the ability of alpha6 integrins to mediate leukocyte migration through the perivascular basement membrane. *J Exp Med* **196**, 1201-11 (2002).

7. Berman, M. E., Xie, Y. & Muller, W. A. Roles of platelet/endothelial cell adhesion molecule-1 (PECAM-1, CD31) in natural killer cell transendothelial migration and beta 2 integrin activation. *J Immunol* **156**, 1515-24 (1996).

8. Berman, M. E. & Muller, W. A. Ligation of platelet/endothelial cell adhesion molecule 1 (PECAM-1/CD31) on monocytes and neutrophils increases binding capacity of leukocyte CR3 (CD11b/CD18). *J Immunol* **154**, 299-307 (1995).

9. Buckley, C. D. et al. Identification of alpha v beta 3 as a heterotypic ligand for CD31/PECAM-1. *J Cell Sci* **109 (Pt 2)**, 437-45 (1996).

10. Gao, J. L., Lee, E. J. & Murphy, P. M. Impaired antibacterial host defense in mice lacking the N-formylpeptide receptor. *J Exp Med* **189**, 657-62 (1999).

11. Thompson, R. D. et al. Divergent effects of platelet-endothelial cell adhesion molecule-1 and beta 3 integrin blockade on leukocyte transmigration in vivo. *J Immunol* **165**, 426-34 (2000).

12. Chiba, R. et al. Ligation of CD31 (PECAM-1) on endothelial cells increases adhesive function of alphavbeta3 integrin and enhances beta1 integrin-mediated adhesion of eosinophils to endothelial cells. *Blood* **94**, 1319-29 (1999).

13. Mamdouh, Z., Chen, X., Pierini, L. M., Maxfield, F. R. & Muller, W. A. Targeted recycling of PECAM from endothelial surface-connected compartments during diapedesis. *Nature* **421**, 748-53 (2003).

14. Gergely, J., Pecht, I. & Sarmay, G. Immunoreceptor tyrosine-based inhibition motif-bearing receptors regulate the immunoreceptor tyrosine-based activation

motif-induced activation of immune competent cells. *Immunol Lett* **68**, 3-15 (1999).

15. Inagaki, K. et al. SHPS-1 regulates integrin-mediated cytoskeletal reorganization and cell motility. *Embo J* **19**, 6721-31 (2000).

16. Timms, J. F. et al. SHPS-1 is a scaffold for assembling distinct adhesion-regulated multi-protein complexes in macrophages. *Curr Biol* **9**, 927-30 (1999).

17. Latour, S. et al. Bidirectional negative regulation of human T and dendritic cells by CD47 and its cognate receptor signal-regulator protein-alpha: down-regulation of IL-12 responsiveness and inhibition of dendritic cell activation. *J Immunol* **167**, 2547-54 (2001).

18. Motegi, S. et al. Role of the CD47-SHPS-1 system in regulation of cell migration. *Embo J* **22**, 2634-44 (2003).

19. Backstrom, E., Kristensson, K. & Ljunggren, H. G. Activation of natural killer cells: underlying molecular mechanisms revealed. *Scand J Immunol* **60**, 14-22 (2004).

20. Blery, M., Olcese, L. & Vivier, E. Early signaling via inhibitory and activating NK receptors. *Hum Immunol* **61**, 51-64 (2000).

21. Burshtyn, D. N. et al. Conserved residues amino-terminal of cytoplasmic tyrosines contribute to the SHP-1-mediated inhibitory function of killer cell Ig-like receptors. *J Immunol* **162**, 897-902 (1999).

22. Stebbins, C. C. et al. Vav1 dephosphorylation by the tyrosine phosphatase SHP-1 as a mechanism for inhibition of cellular cytotoxicity. *Mol Cell Biol* **23**, 6291-9 (2003).

23. Bruhns, P., Marchetti, P., Fridman, W. H., Vivier, E. & Daeron, M. Differential roles of N- and C-terminal immunoreceptor tyrosine-based inhibition motifs during inhibition of cell activation by killer cell inhibitory receptors. *J Immunol* **162**, 3168-75 (1999).

24. Yusa, S. & Campbell, K. S. Src homology region 2-containing protein tyrosine phosphatase-2 (SHP-2) can play a direct role in the inhibitory function of killer cell Ig-like receptors in human NK cells. *J Immunol* **170**, 4539-47 (2003).

25. Ott, V. L., Tamir, I., Niki, M., Pandolfi, P. P. & Cambier, J. C. Downstream of kinase, p62(dok), is a mediator of Fc gamma IIB inhibition of Fc epsilon RI signaling. *J Immunol* **168**, 4430-9 (2002).

26. Phillips, N. E. & Parker, D. C. Cross-linking of B lymphocyte Fc gamma receptors and membrane immunoglobulin inhibits anti-immunoglobulin-induced blastogenesis. *J Immunol* **132**, 627-32 (1984).

27. Brauweiler, A. M. & Cambier, J. C. Autonomous SHIP-dependent FcgammaR signaling in pre-B cells leads to inhibition of cell migration and induction of cell death. *Immunol Lett* **92**, 75-81 (2004).

28. Lesourne, R., Fridman, W. H. & Daeron, M. Dynamic interactions of Fc gamma receptor IIB with filamin-bound SHIP1 amplify filamentous actin-dependent negative regulation of Fc epsilon receptor I signaling. *J Immunol* **174**, 1365-73 (2005).

29. Jensen, W. A., Marschner, S., Ott, V. L. & Cambier, J. C. FcgammaRIIB-mediated inhibition of T-cell receptor signal transduction involves the phosphorylation of SH2-containing inositol 5-phosphatase (SHIP), dephosphorylation of the linker of activated T-cells (LAT) and inhibition of calcium mobilization. *Biochem Soc Trans* **29**, 840-6 (2001).

30. Oda, T., Ohka, S. & Nomoto, A. Ligand stimulation of CD155alpha inhibits cell adhesion and enhances cell migration in fibroblasts. *Biochem Biophys Res Commun* **319**, 1253-64 (2004).

31. Kirschbaum, N. E., Gumina, R. J. & Newman, P. J. Organization of the gene for human platelet/endothelial cell adhesion molecule-1 shows alternatively spliced isoforms and a functionally complex cytoplasmic domain. *Blood* **84**, 4028-37 (1994).

32. Goldberger, A. et al. Biosynthesis and processing of the cell adhesion molecule PECAM-1 includes production of a soluble form. *J Biol Chem* **269**, 17183-91 (1994).

33. Baldwin, H. S. et al. Platelet endothelial cell adhesion molecule-1 (PECAM-1/CD31): alternatively spliced, functionally distinct isoforms expressed during mammalian cardiovascular development. *Development* **120**, 2539-53 (1994).

34. Sheibani, N., Sorenson, C. M. & Frazier, W. A. Differential modulation of cadherin-mediated cell-cell adhesion by platelet endothelial cell adhesion molecule-1 isoforms through activation of extracellular regulated kinases. *Mol Biol Cell* **11**, 2793-802 (2000).

35. Wang, Y., Su, X., Sorenson, C. M. & Sheibani, N. Tissue-specific distributions of alternatively spliced human PECAM-1 isoforms. *Am J Physiol Heart Circ Physiol* **284**, H1008-17 (2003).

36. Li, Z. J. et al. Kinetic expression of platelet endothelial cell adhesion molecule-1 (PECAM-1/CD31) during embryonic stem cell differentiation. *J Cell Biochem* **95**, 559-70 (2005).

37. Duncan, G. S. et al. Genetic Evidence for Functional Redundancy of Platelet/Endothelial Cell Adhesion Molecule-1 (PECAM-1): CD31-Deficient Mice Reveal PECAM-1-Dependent and PECAM-1-Independent Functions. *J Immunol* **162**, 3022-3030 (1999).

38. Schenkel, A. R., Chew, T. W. & Muller, W. A. Platelet endothelial cell adhesion molecule deficiency or blockade significantly reduces leukocyte emigration in a majority of mouse strains. *J Immunol* **173**, 6403-8 (2004).

39. Schenkel, A. R., Chew, T. W., Chlipala, E., Harbord, M. W. & Muller, W. A. Different susceptibilities of PECAM-deficient mouse strains to spontaneous idiopathic pneumonitis. *Exp Mol Pathol* (2006).

40. Wakelin, M. W. et al. An anti-platelet-endothelial cell adhesion molecule-1 antibody inhibits leukocyte extravasation from mesenteric microvessels in vivo by blocking the passage through the basement membrane. *J Exp Med* **184**, 229-39 (1996).

41. Wong, M. X., Roberts, D., Bartley, P. A. & Jackson, D. E. Absence of platelet endothelial cell adhesion molecule-1 (CD31) leads to increased severity of local and systemic IgE-mediated anaphylaxis and modulation of mast cell activation. *J Immunol* **168**, 6455-62 (2002).

42. Solowiej, A., Biswas, P., Graesser, D. & Madri, J. A. Lack of platelet endothelial cell adhesion molecule-1 attenuates foreign body inflammation because of decreased angiogenesis. *Am J Pathol* **162**, 953-62 (2003).

43. Wilkinson, R. et al. Platelet endothelial cell adhesion molecule-1 (PECAM-1/CD31) acts as a regulator of B-cell development, B-cell antigen receptor (BCR)-mediated activation, and autoimmune disease. *Blood* **100**, 184-93 (2002).

44. Carrithers, M. et al. Enhanced susceptibility to endotoxic shock and impaired STAT3 signaling in CD31-deficient mice. *Am J Pathol* **166**, 185-96 (2005).

45. Mendel, I., Kerlero de Rosbo, N. & Ben-Nun, A. A myelin oligodendrocyte glycoprotein peptide induces typical chronic experimental autoimmune encephalomyelitis in H-2b mice: fine specificity and T cell receptor V beta expression of encephalitogenic T cells. *Eur J Immunol* **25**, 1951-9 (1995).

46. Graesser, D. et al. Altered vascular permeability and early onset of experimental autoimmune encephalomyelitis in PECAM-1-deficient mice. *J. Clin. Invest.* **109**, 383-392 (2002).

47. Tada, Y. et al. Acceleration of the onset of collagen-induced arthritis by a deficiency of platelet endothelial cell adhesion molecule 1. *Arthritis Rheum* **48**, 3280-90 (2003).

48. Albelda, S. M. et al. Role for platelet-endothelial cell adhesion molecule-1 in macrophage Fcgamma receptor function. *Am J Respir Cell Mol Biol* **31**, 246-55 (2004).

49. Muller, W. A., Ratti, C. M., McDonnell, S. L. & Cohn, Z. A. A human endothelial cell-restricted, externally disposed plasmalemmal protein enriched in intercellular junctions. *J Exp Med* **170**, 399-414 (1989).

50. Sun, Q. H. et al. Individually distinct Ig homology domains in PECAM-1 regulate homophilic binding and modulate receptor affinity. *J Biol Chem* **271**, 11090-8 (1996).

51. Deaglio, S. et al. Human CD38 (ADP-ribosyl cyclase) is a counter-receptor of CD31, an Ig superfamily member. *J Immunol* **160**, 395-402 (1998).

52. Piali, L. et al. CD31/PECAM-1 is a ligand for alpha v beta 3 integrin involved in adhesion of leukocytes to endothelium. *J Cell Biol* **130**, 451-60 (1995).

53. Prager, E. et al. Interaction of CD31 with a heterophilic counterreceptor involved in downregulation of human T cell responses. *J Exp Med* **184**, 41-50 (1996).

54. Lu, T. T., Barreuther, M., Davis, S. & Madri, J. A. Platelet endothelial cell adhesion molecule-1 is phosphorylatable by c-Src, binds Src-Src homology 2 domain, and exhibits immunoreceptor tyrosine-based activation motif-like properties. *J Biol Chem* **272**, 14442-6 (1997).

55. Kogata, N. et al. Identification of Fer tyrosine kinase localized on microtubules as a platelet endothelial cell adhesion molecule-1 phosphorylating kinase in vascular endothelial cells. *Mol Biol Cell* **14**, 3553-64 (2003).

56. Cao, M. Y. et al. Regulation of mouse PECAM-1 tyrosine phosphorylation by the Src and Csk families of protein-tyrosine kinases. *J Biol Chem* **273**, 15765-72 (1998).

57. Hua, C. T., Gamble, J. R., Vadas, M. A. & Jackson, D. E. Recruitment and activation of SHP-1 protein-tyrosine phosphatase by human platelet endothelial cell adhesion molecule-1 (PECAM-1). Identification of immunoreceptor tyrosine-based inhibitory motif-like binding motifs and substrates. *J Biol Chem* **273**, 28332-40 (1998).

58. Newton-Nash, D. K. & Newman, P. J. A new role for platelet-endothelial cell adhesion molecule-1 (CD31): inhibition of TCR-mediated signal transduction. *J Immunol* **163**, 682-8 (1999).

59. O'Brien, C. D., Cao, G., Makrigiannakis, A. & DeLisser, H. M. Role of immunoreceptor tyrosine-based inhibitory motifs of PECAM-1 in PECAM-1-dependent cell migration. *Am J Physiol Cell Physiol* **287**, C1103-1113 (2004).

60. Gratzinger, D., Barreuther, M. & Madri, J. A. Platelet-endothelial cell adhesion molecule-1 modulates endothelial migration through its immunoreceptor tyrosine-based inhibitory motif. *Biochem Biophys Res Commun* **301**, 243-9 (2003).

61. Gratzinger, D., Canosa, S., Engelhardt, B. & Madri, J. A. Platelet endothelial cell adhesion molecule-1 modulates endothelial cell motility through the small G-protein Rho. *Faseb J* **17**, 1458-69 (2003).

62. Henshall, T. L., Jones, K. L., Wilkinson, R. & Jackson, D. E. Src homology 2 domain-containing protein-tyrosine phosphatases, SHP-1 and SHP-2, are required for platelet endothelial cell adhesion molecule-1/CD31-mediated inhibitory signaling. *J Immunol* **166**, 3098-106 (2001).

63. Pumphrey, N. J. et al. Differential association of cytoplasmic signalling molecules SHP-1, SHP-2, SHIP and phospholipase C-gamma1 with PECAM-1/CD31. *FEBS Lett* **450**, 77-83 (1999).

64. Biswas, P. et al. PECAM-1 promotes beta-catenin accumulation and stimulates endothelial cell proliferation. *Biochem Biophys Res Commun* **303**, 212-8 (2003).

65. Ilan, N., Mahooti, S., Rimm, D. L. & Madri, J. A. PECAM-1 (CD31) functions as a reservoir for and a modulator of tyrosine-phosphorylated beta-catenin. *J Cell Sci* **112 Pt 18**, 3005-14 (1999).

66. Ilan, N., Cheung, L., Pinter, E. & Madri, J. A. Platelet-endothelial cell adhesion molecule-1 (CD31), a scaffolding molecule for selected catenin family members whose binding is mediated by different tyrosine and serine/threonine phosphorylation. *J Biol Chem* **275**, 21435-43 (2000).

67. Isnardi, I., Bruhns, P., Bismuth, G., Fridman, W. H. & Daeron, M. The SH2 domain-containing inositol 5-phosphatase SHIP1 is recruited to the intracytoplasmic domain of human FcgammaRIIB and is mandatory for negative regulation of B cell activation. *Immunol Lett* (2005).

68. Ilan, N. et al. Pecam-1 is a modulator of stat family member phosphorylation and localization: lessons from a transgenic mouse. *Dev Biol* **232**, 219-32 (2001).

69. Buitenhuis, M., Coffer, P. J. & Koenderman, L. Signal transducer and activator of transcription 5 (STAT5). *Int J Biochem Cell Biol* **36**, 2120-4 (2004).

70. Wang, Y. & Sheibani, N. PECAM-1 isoform-specific activation of MAPK/ERKs and small GTPases: Implications in inflammation and angiogenesis. *J Cell Biochem* (2006).

71. Cunnick, J. M., Mei, L., Doupnik, C. A. & Wu, J. Phosphotyrosines 627 and 659 of Gab1 constitute a bisphosphoryl tyrosine-based activation motif (BTAM) conferring binding and activation of SHP2. *J Biol Chem* **276**, 24380-7 (2001).

72. Osawa, M., Masuda, M., Kusano, K. & Fujiwara, K. Evidence for a role of platelet endothelial cell adhesion molecule-1 in endothelial cell mechanosignal transduction: is it a mechanoresponsive molecule? *J Cell Biol* **158**, 773-85 (2002).

73. Wang, Z. & Moran, M. F. Phospholipase C-gamma1: a phospholipase and guanine nucleotide exchange factor. *Mol Interv* **2**, 352-5,338 (2002).

74. Pellegatta, F., Chierchia, S. L. & Zocchi, M. R. Functional association of platelet endothelial cell adhesion molecule-1 and phosphoinositide 3-kinase in human neutrophils. *J Biol Chem* **273**, 27768-71 (1998).

75. Calderwood, D. A. et al. The Talin head domain binds to integrin beta subunit cytoplasmic tails and regulates integrin activation. *J Biol Chem* **274**, 28071-4 (1999).

76. Lee, H. S. et al. Characterization of an actin-binding site within the talin FERM domain. *J Mol Biol* **343**, 771-84 (2004).

77. Priddle, H. et al. Disruption of the talin gene compromises focal adhesion assembly in undifferentiated but not differentiated embryonic stem cells. *J Cell Biol* **142**, 1121-33 (1998).

78. Giannone, G., Jiang, G., Sutton, D. H., Critchley, D. R. & Sheetz, M. P. Talin1 is critical for force-dependent reinforcement of initial integrin-cytoskeleton bonds but not tyrosine kinase activation. *J Cell Biol* **163**, 409-19 (2003).

79. Martel, V. et al. Conformation, localization, and integrin binding of talin depend on its interaction with phosphoinositides. *J Biol Chem* **276**, 21217-27 (2001).

80. Yan, B., Calderwood, D. A., Yaspan, B. & Ginsberg, M. H. Calpain cleavage promotes talin binding to the beta 3 integrin cytoplasmic domain. *J Biol Chem* **276**, 28164-70 (2001).

81. Moulder, G. L., Huang, M. M., Waterston, R. H. & Barstead, R. J. Talin requires beta-integrin, but not vinculin, for its assembly into focal adhesion-like structures in the nematode Caenorhabditis elegans. *Mol Biol Cell* **7**, 1181-93 (1996).

82. Cram, E. J., Clark, S. G. & Schwarzbauer, J. E. Talin loss-of-function uncovers roles in cell contractility and migration in C. elegans. *J Cell Sci* **116**, 3871-8 (2003).

83. Newman, P. J. & Newman, D. K. Signal transduction pathways mediated by PECAM-1: new roles for an old molecule in platelet and vascular cell biology. *Arterioscler Thromb Vasc Biol* **23**, 953-64 (2003).

84. Brown, S. et al. Apoptosis disables CD31-mediated cell detachment from phagocytes promoting binding and engulfment. *Nature* **418**, 200-3 (2002).

85. Dogusan, Z., Montecino-Rodriguez, E. & Dorshkind, K. Macrophages and stromal cells phagocytose apoptotic bone marrow-derived B lineage cells. *J Immunol* **172**, 4717-23 (2004).

86. Gardai, S. J. et al. Cell-surface calreticulin initiates clearance of viable or apoptotic cells through trans-activation of LRP on the phagocyte. *Cell* **123**, 321-34 (2005).

87. Ferrero, E. et al. Transendothelial migration leads to protection from starvation-induced apoptosis in CD34+CD14+ circulating precursors: evidence for PECAM-1 involvement through Akt/PKB activation. *Blood* **101**, 186-93 (2003).

88. Gao, C. et al. PECAM-1 functions as a specific and potent inhibitor of mitochondrial-dependent apoptosis. *Blood* **102**, 169-79 (2003).

89. Noble, K. E., Wickremasinghe, R. G., DeCornet, C., Panayiotidis, P. & Yong, K. L. Monocytes stimulate expression of the Bcl-2 family member, A1, in endothelial cells and confer protection against apoptosis. *J Immunol* **162**, 1376-83 (1999).

90. Bird, I. N. et al. Homophilic PECAM-1(CD31) interactions prevent endothelial cell apoptosis but do not support cell spreading or migration. *J Cell Sci* **112 (Pt 12)**, 1989-97 (1999).

91. Limaye, V. et al. Sphingosine kinase-1 enhances endothelial cell survival through a PECAM-1-dependent activation of PI-3K/Akt and regulation of Bcl-2 family members. *Blood* **105**, 3169-77 (2005).

92. Ilan, N., Mohsenin, A., Cheung, L. & Madri, J. A. PECAM-1 shedding during apoptosis generates a membrane-anchored truncated molecule with unique signaling characteristics. *Faseb J* **15**, 362-72 (2001).

93. Hart, S. P., Ross, J. A., Ross, K., Haslett, C. & Dransfield, I. Molecular characterization of the surface of apoptotic neutrophils: implications for functional downregulation and recognition by phagocytes. *Cell Death Differ* **7**, 493-503 (2000).

94. Shultz, L. D., Rajan, T. V. & Greiner, D. L. Severe defects in immunity and hematopoiesis caused by SHP-1 protein-tyrosine-phosphatase deficiency. *Trends Biotechnol* **15**, 302-7 (1997).

95. Roach, T. I. et al. The protein tyrosine phosphatase SHP-1 regulates integrin-mediated adhesion of macrophages. *Curr Biol* **8**, 1035-8 (1998).

96. Cyster, J. G. & Goodnow, C. C. Protein tyrosine phosphatase 1C negatively regulates antigen receptor signaling in B lymphocytes and determines thresholds for negative selection. *Immunity* **2**, 13-24 (1995).

97. Qu, C. K. et al. Biased suppression of hematopoiesis and multiple developmental defects in chimeric mice containing Shp-2 mutant cells. *Mol Cell Biol* **18**, 6075-82 (1998).

98. Qu, C. K., Nguyen, S., Chen, J. & Feng, G. S. Requirement of Shp-2 tyrosine phosphatase in lymphoid and hematopoietic cell development. *Blood* **97**, 911-4 (2001).

99. Saxton, T. M. et al. Abnormal mesoderm patterning in mouse embryos mutant for the SH2 tyrosine phosphatase Shp-2. *Embo J* **16**, 2352-64 (1997).

100. Bottcher, A. et al. Involvement of phosphatidylserine, alphavbeta3, CD14, CD36, and complement C1q in the phagocytosis of primary necrotic lymphocytes by macrophages. *Arthritis Rheum* **54**, 927-938 (2006).

101. Wright, S. D., Ramos, R. A., Tobias, P. S., Ulevitch, R. J. & Mathison, J. C. CD14, a receptor for complexes of lipopolysaccharide (LPS) and LPS binding protein. *Science* **249**, 1431-3 (1990).

102. Devitt, A. et al. Human CD14 mediates recognition and phagocytosis of apoptotic cells. *Nature* **392**, 505-9 (1998).

103. Devitt, A. et al. Persistence of apoptotic cells without autoimmune disease or inflammation in CD14-/- mice. *J Cell Biol* **167**, 1161-70 (2004).

104. Savill, J., Hogg, N., Ren, Y. & Haslett, C. Thrombospondin cooperates with CD36 and the vitronectin receptor in macrophage recognition of neutrophils undergoing apoptosis. *J Clin Invest* **90**, 1513-22 (1992).

105. Moodley, Y. et al. Macrophage recognition and phagocytosis of apoptotic fibroblasts is critically dependent on fibroblast-derived thrombospondin 1 and CD36. *Am J Pathol* **162**, 771-9 (2003).

106. Taylor, P. R. et al. A hierarchical role for classical pathway complement proteins in the clearance of apoptotic cells in vivo. *J Exp Med* **192**, 359-66 (2000).

107. Ogden, C. A. et al. C1q and mannose binding lectin engagement of cell surface calreticulin and CD91 initiates macropinocytosis and uptake of apoptotic cells. *J Exp Med* **194**, 781-95 (2001).

108. Fadok, V. A., de Cathelineau, A., Daleke, D. L., Henson, P. M. & Bratton, D. L. Loss of phospholipid asymmetry and surface exposure of phosphatidylserine is required for phagocytosis of apoptotic cells by macrophages and fibroblasts. *J Biol Chem* **276**, 1071-7 (2001).

109. Seigneuret, M. & Devaux, P. F. ATP-dependent asymmetric distribution of spin-labeled phospholipids in the erythrocyte membrane: relation to shape changes. *Proc Natl Acad Sci U S A* **81**, 3751-5 (1984).

110. Williamson, P. & Schlegel, R. A. Transbilayer phospholipid movement and the clearance of apoptotic cells. *Biochim Biophys Acta* **1585**, 53-63 (2002).

111. Hoffmann, P. R. et al. Phosphatidylserine (PS) induces PS receptor-mediated macropinocytosis and promotes clearance of apoptotic cells. *J Cell Biol* **155**, 649-59 (2001).

112. Hanayama, R. et al. Autoimmune disease and impaired uptake of apoptotic cells in MFG-E8-deficient mice. *Science* **304**, 1147-50 (2004).

113. Fadok, V. A. et al. A receptor for phosphatidylserine-specific clearance of apoptotic cells. *Nature* **405**, 85-90 (2000).

114. Li, M. O., Sarkisian, M. R., Mehal, W. Z., Rakic, P. & Flavell, R. A. Phosphatidylserine receptor is required for clearance of apoptotic cells. *Science* **302**, 1560-3 (2003).

115. Bose, J. et al. The phosphatidylserine receptor has essential functions during embryogenesis but not in apoptotic cell removal. *J Biol* **3**, 15 (2004).

116. Luciani, M. F. & Chimini, G. The ATP binding cassette transporter ABC1, is required for the engulfment of corpses generated by apoptotic cell death. *Embo J* **15**, 226-35 (1996).

117. Christiansen-Weber, T. A. et al. Functional loss of ABCA1 in mice causes severe placental malformation, aberrant lipid distribution, and kidney glomerulonephritis as well as high-density lipoprotein cholesterol deficiency. *Am J Pathol* **157**, 1017-29 (2000).

118. Murao, K. et al. Characterization of CLA-1, a human homologue of rodent scavenger receptor BI, as a receptor for high density lipoprotein and apoptotic thymocytes. *J Biol Chem* **272**, 17551-7 (1997).

119. Imachi, H. et al. Human scavenger receptor B1 is involved in recognition of apoptotic thymocytes by thymic nurse cells. *Lab Invest* **80**, 263-70 (2000).

120. Kawasaki, Y., Nakagawa, A., Nagaosa, K., Shiratsuchi, A. & Nakanishi, Y. Phosphatidylserine binding of class B scavenger receptor type I, a phagocytosis receptor of testicular sertoli cells. *J Biol Chem* **277**, 27559-66 (2002).

121. Luu, N. T., Rainger, G. E., Buckley, C. D. & Nash, G. B. CD31 regulates direction and rate of neutrophil migration over and under endothelial cells. *J Vasc Res* **40**, 467-79 (2003).

122. DeLisser, H. M. et al. Involvement of endothelial PECAM-1/CD31 in angiogenesis. *Am J Pathol* **151**, 671-7 (1997).

123. Schimmenti, L. A., Yan, H. C., Madri, J. A. & Albelda, S. M. Platelet endothelial cell adhesion molecule, PECAM-1, modulates cell migration. *J Cell Physiol* **153**, 417-28 (1992).

124. Savill, J., Dransfield, I., Gregory, C. & Haslett, C. A blast from the past: clearance of apoptotic cells regulates immune responses. *Nat Rev Immunol* **2**, 965-75 (2002).

125. Kohro, T. et al. A comparison of differences in the gene expression profiles of phorbol 12-myristate 13-acetate differentiated THP-1 cells and human monocyte-derived macrophage. *J Atheroscler Thromb* **11**, 88-97 (2004).

126. Hakansson, P. et al. Establishment and phenotypic characterization of human U937 cells with inducible P210 BCR/ABL expression reveals upregulation of CEACAM1 (CD66a). *Leukemia* **18**, 538-47 (2004).

127. Fischer, D., Pike, M., Koren, H. & Snyderman, R. Chemotactically responsive and nonresposive forms of a continuous human monocyte cell line. *J Immunol* **125**, 463-465 (1980).

128. Steube, K. G., Teepe, D., Meyer, C., Zaborski, M. & Drexler, H. G. A model system in haematology and immunology: the human monocytic cell line MONO-MAC-1. *Leuk Res* **21**, 327-35 (1997).

129. Koeffler, H. P. & Golde, D. W. Acute myelogenous leukemia: a human cell line responsive to colony-stimulating activity. *Science* **200**, 1153-4 (1978).

130. Jackson, D. E., Ward, C. M., Wang, R. & Newman, P. J. The protein-tyrosine phosphatase SHP-2 binds platelet/endothelial cell adhesion molecule-1 (PECAM-1) and forms a distinct signaling complex during platelet aggregation. Evidence for a mechanistic link between PECAM-1- and integrin-mediated cellular signaling. *J Biol Chem* **272**, 6986-93 (1997).

131. Pathak, M. K. & Yi, T. Sodium Stibogluconate Is a Potent Inhibitor of Protein Tyrosine Phosphatases and Augments Cytokine Responses in Hemopoietic Cell Lines. *J Immunol* **167**, 3391-3397 (2001).

132. Stegmeier, F., Hu, G., Rickles, R. J., Hannon, G. J. & Elledge, S. J. A lentiviral microRNA-based system for single-copy polymerase II-regulated RNA interference in mammalian cells. *Proc Natl Acad Sci U S A* **102**, 13212-7 (2005).

133. Wang, Q., Downey, G. P., Herrera-Abreu, M. T., Kapus, A. & McCulloch, C. A. SHP-2 modulates interleukin-1-induced Ca2+ flux and ERK activation via phosphorylation of phospholipase Cgamma1. *J Biol Chem* **280**, 8397-406 (2005).

134. Palu, G., Parolin, C., Takeuchi, Y. & Pizzato, M. Progress with retroviral gene vectors. *Rev Med Virol* **10**, 185-202 (2000).

135. Kafri, T., van Praag, H., Ouyang, L., Gage, F. H. & Verma, I. M. A packaging cell line for lentivirus vectors. *J Virol* **73**, 576-84 (1999).

136. Musso, T. et al. CD38 expression and functional activities are up-regulated by IFN-gamma on human monocytes and monocytic cell lines. *J Leukoc Biol* **69**, 605-12 (2001).

137. Hajas, G. et al. New phenotypic, functional and electrophysiological characteristics of KG-1 cells. *Immunol Lett* **92**, 97-106 (2004).

138. Iwata, S., Ohashi, Y., Kamiguchi, K. & Morimoto, C. Beta 1-integrin-mediated cell signaling in T lymphocytes. *J Dermatol Sci* **23**, 75-86 (2000).

139. Oh, E. S. et al. Regulation of early events in integrin signaling by protein tyrosine phosphatase SHP-2. *Mol Cell Biol* **19**, 3205-15 (1999).

140. Yu, D. H., Qu, C. K., Henegariu, O., Lu, X. & Feng, G. S. Protein-tyrosine phosphatase Shp-2 regulates cell spreading, migration, and focal adhesion. *J Biol Chem* **273**, 21125-31 (1998).

141. Manes, S. et al. Concerted activity of tyrosine phosphatase SHP-2 and focal adhesion kinase in regulation of cell motility. *Mol Cell Biol* **19**, 3125-35 (1999).

142. Inagaki, K. et al. Roles for the protein tyrosine phosphatase SHP-2 in cytoskeletal organization, cell adhesion and cell migration revealed by overexpression of a dominant negative mutant. *Oncogene* **19**, 75-84 (2000).

143. Maroun, C. R., Naujokas, M. A. & Park, M. Membrane targeting of Grb2-associated binder-1 (Gab1) scaffolding protein through Src myristoylation sequence substitutes for Gab1 pleckstrin homology domain and switches an epidermal growth factor response to an invasive morphogenic program. *Mol Biol Cell* **14**, 1691-708 (2003).

144. Lamorte, L., Rodrigues, S., Naujokas, M. & Park, M. Crk synergizes with epidermal growth factor for epithelial invasion and morphogenesis and is required for the met morphogenic program. *J Biol Chem* **277**, 37904-11 (2002).

145. Paddison, P. J., Caudy, A. A., Bernstein, E., Hannon, G. J. & Conklin, D. S. Short hairpin RNAs (shRNAs) induce sequence-specific silencing in mammalian cells. *Genes Dev* **16**, 948-58 (2002).

146. Nobes, C. D. & Hall, A. Rho GTPases control polarity, protrusion, and adhesion during cell movement. *J Cell Biol* **144**, 1235-44 (1999).

147. Enciso, J. M. et al. Elevated glucose inhibits VEGF-A-mediated endocardial cushion formation: modulation by PECAM-1 and MMP-2. *J Cell Biol* **160**, 605-15 (2003).

148. Yaffe, M. B. How do 14-3-3 proteins work?-- Gatekeeper phosphorylation and the molecular anvil hypothesis. *FEBS Lett* **513**, 53-7 (2002).

149. de Hoog, C. L., Foster, L. J. & Mann, M. RNA and RNA binding proteins participate in early stages of cell spreading through spreading initiation centers. *Cell* **117**, 649-62 (2004).

150. Fratelli, M. et al. Identification by redox proteomics of glutathionylated proteins in oxidatively stressed human T lymphocytes. *Proc Natl Acad Sci U S A* **99**, 3505-10 (2002).

151. Vincent, P. A., Xiao, K., Buckley, K. M. & Kowalczyk, A. P. VE-cadherin: adhesion at arm's length. *Am J Physiol Cell Physiol* **286**, C987-97 (2004).

152. Holgado-Madruga, M. & Wong, A. J. Role of the Grb2-associated binder 1/SHP-2 interaction in cell growth and transformation. *Cancer Res* **64**, 2007-15 (2004).

153. Lu, M. et al. A Steric-inhibition model for regulation of nucleotide exchange via the Dock180 family of GEFs. *Curr Biol* **15**, 371-7 (2005).

154. Roose, J. P., Mollenauer, M., Gupta, V. A., Stone, J. & Weiss, A. A diacylglycerol-protein kinase C-RasGRP1 pathway directs Ras activation upon antigen receptor stimulation of T cells. *Mol Cell Biol* **25**, 4426-41 (2005).

155. Evans, P. C., Taylor, E. R. & Kilshaw, P. J. Signaling through CD31 protects endothelial cells from apoptosis. *Transplantation* **71**, 457-60 (2001).

156. Buchner, J. Hsp90 & Co. - a holding for folding. *Trends Biochem Sci* **24**, 136-41 (1999).

157. Picard, D. Heat-shock protein 90, a chaperone for folding and regulation. *Cell Mol Life Sci* **59**, 1640-8 (2002).

158. Dittmar, K. D. & Pratt, W. B. Folding of the glucocorticoid receptor by the reconstituted Hsp90-based chaperone machinery. The initial hsp90.p60.hsp70-dependent step is sufficient for creating the steroid binding conformation. *J Biol Chem* **272**, 13047-54 (1997).

159. Schreiber, S. L. Chemistry and biology of the immunophilins and their immunosuppressive ligands. *Science* **251**, 283-7 (1991).

160. Pratt, W. B., Galigniana, M. D., Harrell, J. M. & DeFranco, D. B. Role of hsp90 and the hsp90-binding immunophilins in signalling protein movement. *Cell Signal* **16**, 857-72 (2004).

161. Pratt, W. B. & Toft, D. O. Regulation of signaling protein function and trafficking by the hsp90/hsp70-based chaperone machinery. *Exp Biol Med (Maywood)* **228**, 111-33 (2003).

162. Ning, Y. M. & Sanchez, E. R. Evidence for a functional interaction between calmodulin and the glucocorticoid receptor. *Biochem Biophys Res Commun* **208**, 48-54 (1995).

163. Wong, M. X. et al. Proteolytic cleavage of platelet endothelial cell adhesion molecule-1 (PECAM-1/CD31) is regulated by a calmodulin-binding motif. *FEBS Lett* **568**, 70-8 (2004).

164. Xu, Y. & Lindquist, S. Heat-shock protein hsp90 governs the activity of pp60v-src kinase. *Proc Natl Acad Sci U S A* **90**, 7074-8 (1993).

165. Bijlmakers, M. J. & Marsh, M. Hsp90 is essential for the synthesis and subsequent membrane association, but not the maintenance, of the Src-kinase p56(lck). *Mol Biol Cell* **11**, 1585-95 (2000).

166. Sikorski, R. S., Boguski, M. S., Goebl, M. & Hieter, P. A repeating amino acid motif in CDC23 defines a family of proteins and a new relationship among genes required for mitosis and RNA synthesis. *Cell* **60**, 307-17 (1990).

167. Lamb, J. R., Tugendreich, S. & Hieter, P. Tetratrico peptide repeat interactions: to TPR or not to TPR? *Trends Biochem Sci* **20**, 257-9 (1995).

168. Blatch, G. L. & Lassle, M. The tetratricopeptide repeat: a structural motif mediating protein-protein interactions. *Bioessays* **21**, 932-9 (1999).

169. Hirano, T., Kinoshita, N., Morikawa, K. & Yanagida, M. Snap helix with knob and hole: essential repeats in S. pombe nuclear protein nuc2+. *Cell* **60**, 319-28 (1990).

170. D'Andrea, L. D. & Regan, L. TPR proteins: the versatile helix. *Trends Biochem Sci* **28**, 655-62 (2003).

171. Scheufler, C. et al. Structure of TPR domain-peptide complexes: critical elements in the assembly of the Hsp70-Hsp90 multichaperone machine. *Cell* **101**, 199-210 (2000).

172. Pathak, M. K. & Yi, T. Sodium stibogluconate is a potent inhibitor of protein tyrosine phosphatases and augments cytokine responses in hemopoietic cell lines. *J Immunol* **167**, 3391-7 (2001).

173. Stein, B. N., Gamble, J. R., Pitson, S. M., Vadas, M. A. & Khew-Goodall, Y. Activation of endothelial extracellular signal-regulated kinase is essential for neutrophil transmigration: potential involvement of a soluble neutrophil factor in endothelial activation. *J Immunol* **171**, 6097-104 (2003).

174. Poggi, A., Panzeri, M. C., Moretta, L. & Zocchi, M. R. CD31-triggered rearrangement of the actin cytoskeleton in human natural killer cells. *Eur J Immunol* **26**, 817-24 (1996).

175. Ji, G. et al. PECAM-1 (CD31) regulates a hydrogen peroxide-activated nonselective cation channel in endothelial cells. *J Cell Biol* **157**, 173-84 (2002).

176. Kagan, A., Melman, Y. F., Krumerman, A. & McDonald, T. V. 14-3-3 amplifies and prolongs adrenergic stimulation of HERG K+ channel activity. *Embo J* **21**, 1889-98 (2002).

177. Cherubini, A. et al. Human ether-a-go-go-related gene 1 channels are physically linked to beta1 integrins and modulate adhesion-dependent signaling. *Mol Biol Cell* **16**, 2972-83 (2005).

178. Ficker, E., Dennis, A. T., Wang, L. & Brown, A. M. Role of the cytosolic chaperones Hsp70 and Hsp90 in maturation of the cardiac potassium channel HERG. *Circ Res* **92**, e87-100 (2003).

179. Fu, Y., Luo, N., Lopes-Virella, M. F. & Garvey, W. T. The adipocyte lipid binding protein (ALBP/aP2) gene facilitates foam cell formation in human THP-1 macrophages. *Atherosclerosis* **165**, 259-69 (2002).

180. Newman, P. J. et al. PECAM-1 (CD31) cloning and relation to adhesion molecules of the immunoglobulin gene superfamily. *Science* **247**, 1219-22 (1990).

181. Simmons, D. L., Walker, C., Power, C. & Pigott, R. Molecular cloning of CD31, a putative intercellular adhesion molecule closely related to carcinoembryonic antigen. *J Exp Med* **171**, 2147-52 (1990).

182. Alblas, J., Ulfman, L., Hordijk, P. & Koenderman, L. Activation of Rhoa and ROCK are essential for detachment of migrating leukocytes. *Mol Biol Cell* **12**, 2137-45 (2001).

183. Jin, S., Song, Y. C., Emili, A., Sherman, P. M. & Chan, V. L. JlpA of Campylobacter jejuni interacts with surface-exposed heat shock protein 90alpha and triggers signalling pathways leading to the activation of NF-kappaB and p38 MAP kinase in epithelial cells. *Cell Microbiol* **5**, 165-74 (2003).

184. Biswas, P. et al. Identification of the regions of PECAM-1 involved in beta- and gamma-catenin associations. *Biochem Biophys Res Commun* **329**, 1225-33 (2005).

185. Higashi, H. et al. Helicobacter pylori CagA induces Ras-independent morphogenetic response through SHP-2 recruitment and activation. *J Biol Chem* **279**, 17205-16 (2004).

186. Tang, S., Tao, M., McCoy, J. P. & Zheng, Z. M. Short-term induction and long-term suppression of HPV16 oncogene silencing by RNA interference in cervical cancer cells. *Oncogene* (2005).

187. Zou, G. M., Chan, R. J., Shelley, W. C. & Yoder, M. C. Reduction of Shp-2 expression by siRNA reduces murine embryonic stem cell-derived in vitro hematopoietic differentiation. *Stem Cells* (2005).

188. Myslinski, E., Ame, J. C., Krol, A. & Carbon, P. An unusually compact external promoter for RNA polymerase III transcription of the human H1RNA gene. *Nucleic Acids Res* **29**, 2502-9 (2001).